Proceedings of the 20th International Ship and Offshore Structures Congress (ISSC 2018) Volume II – M.L. Kaminski and P. Rigo (Eds.)

doi:10.3233/978-1-61499-864-8-73

COMMITTEE V.2

EXPERIMENTAL METHODS

COMMITTEE MANDATE

Concern for advances in structural model testing and full-scale experimentation and in-service monitoring and their role in the design, construction, inspection and maintenance of ship and offshore structures. This shall include new developments in:
1. Best practice and uncertainty analysis
2. Experimental techniques;
3. Full field imaging and sensor systems;
4. Big data applications for ship and offshore structures
5. Correlation between model, full-scale and numerical datasets

AUTHORS/COMMITTEE MEMBERS

Chairman: D. Dessi, *Italy*
F. Brennan, *UK*
M. Hoogeland, *The Netherlands*
XB. Li, *China*
C. Michailides, *Cyprus*
D. Pearson, *Canada*
J. Romanoff, *Finland*
XH. Shi, *China*
T. Sugimura, *Japan*
G. Wang, *USA*

KEYWORDS

Experimentation, Structural Testing, Laboratory Testing, Small and Large scale, Full-scale Test, Similarity Laws, Correlation, Big-Data, Sensors.

CONTENTS

1. INTRODUCTION 76

2. ACRONYMS & ABBREVIATIONS 76

3. LABORATORY EXPERIMENTATION 77
3.1 Scaled and small size 77
3.1.1 Ultimate strength 77
3.1.2 Fatigue 78
3.1.3 Cracking and fracture 79
3.1.4 Corrosion 83
3.1.5 Friction 83
3.2 Large scale experiment 84
3.2.1 Ultimate strength 84
3.2.2 Large scale fatigue testing 85
3.3 Impact & impulsive loading and response assessment 86
3.3.1 Ship Collisions and Grounding 86
3.3.2 Underwater explosion 89
3.3.3 Vibration 90
3.4 Fluid-structure interaction 92
3.4.1 Hydroelastic scaled tests 92
3.4.2 Slamming and water impact tests 94

4. FULL SCALE TESTS 95
4.1 Ships and offshore structures 95
4.1.1 Monitoring of loads and responses 95
4.1.2 Structural identification 97
4.2 Application of experimentation, inspection and monitoring 99
4.2.1 Design 99
4.2.2 Construction 99
4.2.3 Operation, Inspection, Monitoring and Maintenance 100

5. CORRELATION ISSUES BETWEEN SCALED (PHYSICAL) MODELS, FULL-SCALE STRUCTURES (SHIP AND OFFSHORE) AND NUMERICAL SIMULATIONS 101
5.1 Scaling laws 101
5.2 Model to full-scale investigation 102
5.3 Integration of experiments and numerical simulations 103

6. BEST PRACTICE AND GUIDELINES 105
6.1 Data uncertainty 105
6.2 Design of experiments 106
6.3 Quality standards 107

7. CONTEMPORARY AND EMERGING TECHNIQUES 107
7.1 Overview of current techniques 108
7.1.1 Displacement measurement 108
7.1.2 Strain/stress measurement 108
7.1.3 Force measurement 110
7.1.4 Pressure measurement 110
7.1.5 Acceleration measurement 111
7.1.6 Multi-variable measurements 111
7.2 Novel measurement Techniques 112

7.2.1 MEMS 112
7.2.2 WSN 115
7.2.3 Energy Harvesting Devices 118
7.3 Big-data analysis 119
7.3.1 Values of Big Data as a Technology 119
7.3.2 Recent Activities in the Maritime Industry 120
7.3.3 Status of Maritime Application of Big Data 121
7.3.4 Future Potentials of R&D 122
7.3.5 Conclusions 122

8. CONCLUSIONS AND RECOMMENDATIONS FOR FUTURE WORK 122

REFERENCES 123

1. INTRODUCTION

Experimental research has a long tradition in naval architecture and marine engineering, as the early establishment of the International Towing Tank Conference (ITTC) gives evidence. Due to its focus on hydrodynamics, structure-related experimentation has received little or no attention within ITTC. Until the present ISSC, experimental investigations have been considered by different committees depending on their specific mandate. Thus, for the first time in the history of ISSC activity, a committee has been established to perform a systematic review of experimental methods focusing on their use in the structural design and operation of ships and offshore structures.

The need to delimit the vast field of experimental methods was clear from the beginning of the committee's work. The following criteria have been initially set to select the topics: (i) specific consideration of experimental methods concerning structural testing, or aimed to improve the reliability of structural design in a broader sense; (ii) priority to experimental topics related to Technical Committees; (iii) available expertise among the committee members.

The report can be divided into two parts; the first is dedicated to a general review of methods and techniques, further sorted based on the distinction between laboratory experimentation (Section 3) and full-scale tests (Section 4); the second is focused on some cross-cutting themes, as detailed in the following. The fundamental issue of the correlation and synergic use of model-scale, full-scale and numerical data is considered in Section 5, also accounting for approaches in structural scaling. Best practice and guidelines, involving uncertainty analysis, optimal test design and quality standards, are reviewed in Sections 6. Finally, Section 7 is dedicated to the review of contemporary and emerging techniques, with a special attention to the Big Data problem and its implications in ocean engineering.

2. ACRONYMS & ABBREVIATIONS

Some general acronyms and abbreviations frequently used in the report:

ABS	American Bureau of Shipping
AE	Acoustic Emission
API	American Petroleum Institute
ASME	American Society of Mechanical Engineers
ASTM	American Society for Testing Materials
BV	Bureau Veritas
BS	The British Standard Institution
CCS	China Classification Society
Class NK	Nippon Kaiji Kyokai (Japanese Classification Society)
CFD	Computer Fluid Dynamics
DIC	Digital Image Correlation
DNV	Det Norske Veritas
DNV-GL	Det Norske Veritas - Germanischer Lloyd
FBG	Fiber Bragg Grating
FDS	Fatigue Damage Sensor
FE(A)	Finite Element (Analysis)
FSI	Fluid Structure Interaction
IEC	International Electrochimical Commission
IEEE	Institute of Electrical and Electronics Engineers
IMO	International Maritime Organization
IMU	Inertial Motion Unit
ISA	International Society of Automation
ISO	International Organization for Standardization
ITTC	International Towing Tank Conference

LR	Lloyd's Register
MEMS	Micro-Electro Mechanical Systems
RBI	Risk Based Inspection
RMS	Root Mean Square
SHM	Structural Health Monitoring
UKAS	United Kingdom Accreditation Services
WES	The Japan Welding Society
WSN	Wireless Sensor Network

3. LABORATORY EXPERIMENTATION

With respect to laboratory tests, one can make a rough distinction between tests to determine fundamental mechanical properties and the dynamic structural response in dry or wet conditions. Fundamental mechanical properties include; strength/stiffness (ultimate strength, fracture and blast for example), resistance to deterioration mechanisms (fatigue, corrosion, and wear) and other properties such as friction and damping. Structural dynamic responses in dry conditions refer to vibration / noise, grounding and collision. Examples of dynamic response to wet conditions, involve fluid-structure interaction (underwater explosion, slamming, etc.).

Experimental methods used to determine mechanical properties are linked with laboratory scale tests of materials and small components (Section 3.1). Information concerning the material or components can generally be acquired at relatively low cost and short lead time. Either for novel solutions or for verification of analysis methods, laboratory-scale tests can provide useful information. Large scale experiments (Section 3.2) utilize full-scale structures to determine proof loading and handling qualities. In this case, complete structures, sometimes scaled, or full-scale sections are exposed to experimental validation. Some response tests require the load development and loading process to be accounted for. The setup complexity of these response tests involves reproducing the interaction (*e.g.*, solid/solid as in collision and grounding) or the excitation (underwater explosion) (Section 3.3), as well as consistent scaling (hydroelastically scaled tests in water and ice) (Section 3.4).

3.1 Scaled and small size

3.1.1 Ultimate strength

For steel in particular and metals in general, ultimate strength at the coupon scale level is related to fracture. This section is concerned about fracture when no pre-existing notch or fatigue crack is assumed. Within this group, the stress intensities and levels of stress triaxiality are relatively modest, and the material typically fails in a ductile way. This group is best characterized by strains. Collision and grounding are some key examples. Historically, tensile tests have been used for deriving the strain limits; forming large databases of test data as the one provided by Paik *et al.* (2017) for metallic materials at different temperatures and strain rates.

As multi-axiality has a large influence on the strain criteria, including multi-axiality in the test set-up is a challenge. For this purpose, tests devised in the metal forming industry can be used. Banabic (2000) provides a good summary of experiments developed for the sheet metal industry; focusing on methods that involve deforming the material out of plane until it fails by membrane stretching. Hoogeland and Vredeveldt (2017) recently performed similar tests in dynamic conditions on full-thickness steel plates similar to those used in the maritime and offshore industries. Mohr and Marcadet (2015) provide a small series of tests intended for sheet metal application that may be scalable to plates. These experiments feature specimens that have different cutouts and are pulled in either tension or combined tension/shear. Although the techniques of Banabic (2000) and Mohr and Marcadet (2015) have indicated that multiple specimens are needed to obtain full multi-axiality, Voormeeren *et al.* (2014) provides theoretical evidence that only one specimen may be necessary under certain conditions. Haag *et al.* (2017)

give an example of a structural surrogate test with a drop experiment that simulates raking a pinnacle or iceberg.

3.1.2 Fatigue

Understanding of the fatigue phenomenon has been advanced through data accumulation during cyclic testing. S-N curves are used for the fatigue life evaluation by the Minor damage accumulation approach and are fundamentally obtained by cyclic testing until material failure. Regarding welded-structure such as ship and offshore structures, two sets of limit S-N curves are used. In the first set, joints are classified and grouped according to their geometry. The second set consists of S-N curves for straight material, either base, welded and/or exposed to corrosive environments, and the actual fatigue driving stresses are derived from stress concentration factors. The undisturbed, far field stress is the basis of the stress cycles ("S"). The S-N curves for fatigue design are provided, for instance, by Class society guidelines such as DNV-GL guideline (2015). Fatigue testing in sea water is mainly carried out in a corrosive atmosphere to capture the environmental effects. "Dry" fatigue testing can be done at frequencies up to 70 Hz and "wet" fatigue testing shall be limited to about 1 Hz to allow corrosion products to develop inside the crack. Fatigue tests are also particularly important to evaluate the effect of material coatings on fatigue performance.

Test specimen / Thickness effect

The welded joint specimen is of special interest for the fatigue performance of ship and offshore structures. There is no clear standard defining the size of the fatigue test specimen of welded joints. Usually, specimens representing hull structural details are of the same thickness and welded condition. Base material testing has led to a clear understanding of the thickness effect: increase in plate thickness causes a decrease in fatigue strength. For this reason, a correction coefficient is proposed by Class guidelines, *e.g.*, DNV-GL guideline (2015) and ABS guideline for offshore structures (2014). Yamamoto *et al.* (2012) investigated the dominating factors of the thickness effect considering different structural joint types or different loading patterns by fundamental experiment and FEA. It is confirmed that the thickness effect on fatigue strength is dominated by the stress concentration and the stress gradient at the weld toe that changes according to the shape of the joint. Moreover, the effect is clearly apparent for a variation of primary plate thickness when the thickness of the attached plate is proportionally increased, while the thickness variation effect is less obvious when the thickness of the attached plate is kept constant.

Load history / Variable loading

The fatigue life of ship and offshore structures is generally estimated by using S-N curves with constant amplitude loading. The fatigue crack propagation behavior, however, is especially influenced by variable loading related to the acceleration and delay phenomenon of a fatigue crack (a result of to over- and underload). This means that the experiment shall apply a variable load and record the crack growth simultaneously. The crack growth can be measured in several ways. Maljaars *et al.* (2015) describe the use of special crack gauges consisting of many equally spaced wires. The advancement of the crack is determined by the number of broken wires. Potential drop (either Alternating Current or Direct Current) allows the operator to measure the position of the crack front.

Fatigue test machine

Fatigue testing is usually carried out under tensile or bending loading conditions to get S-N curves. Many fatigue tests are suited for welded joints in ship and offshore structures. Alternatively, S-N curve development of exotic-materials may be acquired by the rotating bending fatigue test. As ISSC2015 III.2 (2015) indicates, many fatigue tests under multiaxial loading have been recently carried out. Moreover, Osawa *et al.* (2013) developed a low-cost fatigue test machine which allows for imposing variable loads according to given time-histories. Fatigue strength of out-of-plane gusset welded joints subject to springing and whipping superimposed

loads is examined by using Plate-Bending-Vibration type fatigue testing machines. The wave load is applied by using motors with eccentric mass. Springing vibration is superimposed by attaching an additional vibrator to the test specimen, and whipping vibration is superimposed by an intermittent hammering.

Measurement techniques for fatigue damage

There are some measurement techniques used to experimentally estimate the fatigue life. Acoustic emission (AE) is a method to record the fatigue crack growth characteristics of structural steel and welded connections. AE is the phenomena in which transient elastic waves are generated by the rapid release of energy from localized sources within a material as it undergoes deformation. Barsoum *et al.* (2009) showed AE graphs of cumulative absolute energy versus fatigue cycles capable of capturing the fatigue process. These characteristic curves track the fatigue crack growth with respect to time and can be used to see the severity of the AE activity associated with the crack growth process. Aggelis *et al.* (2011) investigated the AE behaviour of aluminium with V-notch and showed that certain characteristics undergo clearly measurable changes much earlier than final fatigue fracture. Additionally, this work demonstrated that the crack growth rate can be effectively monitored by using lock-in thermography under cyclic loading. The results obtained using this method were in agreement with the conventional compliance method. Kobayashi *et al.* (2016) developed the fatigue damage sensor with a notched test piece. Characteristics of Fatigue Damage Sensors (FDS) that are in use for fatigue life estimation of monitoring structural welding members in ship structures are discussed to improve the prediction accuracy of estimated fatigue life exposed to random wave loads such as storms under various loading conditions. Akai *et al.* (2015) developed dissipated energy measurement to estimate the crack initiation point. Fatigue limit estimation based on dissipated energy has been getting considerable attention. In this method, temperature change due to irreversible energy dissipation is measured by infrared thermography for various levels of stress amplitude. The dissipated energy measurement was also used to estimate the crack initiation point.

3.1.3 Cracking and fracture

In Section 3.1.1, the fracture of specimens without pre-existing notch or fatigue crack was discussed. This section is concerned with conditions in which a notch or fatigue crack is present at the onset of material failure. In this group, the notch or fatigue pre-crack increases the stress intensity and localized levels of stress triaxiality. This makes the failure mode much more localized. While the high local stress triaxialities can facilitate brittle fracture due to cleavage, this type of testing is also frequently done to determine ductile failure. It is assumed here that a fatigue crack or small welding/production defects can exist prior to the onset of fracture. Several basic material characteristics may be measured in this case, which are outlined below:

- Crack initiation: extension of a pre-existing notch or fatigue crack,
- Ductile tearing: continued stable extension of a crack once it has already initiated from a pre-existing notch of fatigue crack,
- Ductile crack arrestability: ability of a material to arrest a crack once it has started to propagate in an unstable, ductile failure mode,
- Brittle crack arrestability: ability of a material to arrest a crack once it has started to propagate in an unstable brittle failure mode, and
- Measuring the temperature at which the ductile to brittle transition temperature occurs.

The last parameter has many different forms, one common form is the temperature at which a J-integral test produces a critical stress intensity factor (K_{Jc}) equal to 100 MPa$\sqrt{m}$ when adjusted to an equivalent 25 mm thickness under quasi-static conditions.

Most testing methods fall into one or more of the above categories. The tests used to measure the main material characteristics fall into two major categories. The first category is quality control; summarized in Table 1. Quality control tests are generally designed to be extremely

low cost so that they can be performed routinely. Their main result is intended to give a qualitative idea of the safety of the material. The second category of tests are primarily designed to measure material characteristics used for quantitative analyses such as; structural design (container ship hatch coaming) or material development (high ductility high yield strength steels).

Charpy V notch testing is a quality control test that is intended to check whether or not the material fails in a brittle way at a given temperature. This test captures information about crack initiation, ductile tearing, and crack arrest. Because all the information is mixed together into a single measured value (the total impact energy), it can be difficult to extract the data on any one of the parameters specifically. However, many other uses have been found for Charpy tests, including the use of empirical correlations to estimate the fracture toughness in ductile, brittle, and transition conditions, depending on the failure mode the test featured. The Charpy V test has also been used to estimate the ductile to brittle transition temperature. These empirical relationships are outlined in BS 7910:2013+A1 (2015).

Instrumented Charpy V testing can be seen as a separate test from the standard "dumb" Charpy V testing. Instrumented Charpy V testing records the force time history of the impact. Together with the parameters of the test setup, the force time history can be translated to a force versus displacement signal. This method is standardized in ISO 14556:2015 (2015). Good results have been found correlating aspects of force versus displacement curves from instrumented Charpy V tests to various aspects of fracture initiation, tearing, propagation, and arrest. For example, Wallin *et al.* (2016) (amongst others) has shown that there is good correlation between the stress intensity of brittle crack arrest and T4kN, which can be measured from an instrumented Charpy V test.

Unlike Charpy-V testing (with or without instrumentation), most tests are designed to test one specific material parameter. There is a class of tests that are designed to measure the crack initiation of a material. These experiments are more sophisticated (and expensive) than Charpy V testing; however, they also produce values that can be used in design. Linear-elastic fracture toughness can be measured by the K_{Ic} of the material. This is standardized in ASTM E399, among other standards. However, most metallic materials are tough enough that satisfactory conditions for K_{Ic} testing is generally not possible. For those materials, elastic-plastic fracture parameters such as CTOD (Crack Tip Opening Displacement) or *J*-integral testing is recommended. Some standards that describe the measurement of CTOD or *J*-integral is, amongst others, ISO 12135 (2016). In most standards, the typical way of measuring CTOD or *J*-integral has been through either Single Edge Notched Bending (SENB) or Compact Tension (CT) tests. It has been shown that Single Edge Notched Tension (SENT) tests have a state of stress at the crack tip that is more representative of structures in which the primary stress is tension, especially in girth welds of pipes. SENT tests can be less conservative than the typically bending-dominated SENB and CT tests. Therefore, there has been a lot of effort to standardize a SENT test (Crintea and Moore, 2016; Moore and Hutchison, 2016; Hutchison *et al.*, 2015; Sarzosa *et al.*, 2015; Xue *et al.*, 2009), which has come to fruition in BS 8571:2014.

Some other developments in crack initiation testing, include; the reduction of cost of testing, transferring results between specimen geometries, and non-destructive fracture testing. For example, Walters and Van der Weijde (2013) proposed a method to reduce the cost of standard CTOD testing for steels that are at brittle or lower transitional temperatures. Coppejans and Walters (2017) have proposed a method of using damage mechanics to transfer results from a single ductile CTOD test to other specimen sizes. Finally, it is currently being investigated whether or not very small specimens (0.5 mm thick by 8 mm in diameter, which can presumably be sampled non-destructively from large structures) can be used to estimate brittle CTOD values (Walters *et al.*, 2017).

For ductile materials, the resistance to tearing increases after failure initiation. Therefore, taking only the "critical" fracture toughness of a ductile material is considered to be conservative. For

less conservative analyses, the benefit of the increased resistance to tearing is taken into account. The measurement of resistance curves (ASTM E1820 and BS 7448) requires the knowledge of the crack length at any given point in the force versus deflection curve, by multiple or single specimens. The study by Pussegoda *et al.* (2013) compared a multi specimen SENT (Single Edge Notched Tension) technique for finding resistance curves with a single-specimen technique.

In some situations, a ductile crack can arise and propagate for long distances. For instance, in the case of on-shore an off-shore pipelines, there is a lot of energy stored in the compressed gas and the propagating crack can advance faster than the gas decompression wave. In those situations, it is important to measure the ductile crack arrestability of the material. This is typically done with the Drop Weight Tear Test (DWTT) (ASTM E436). Hara and Fujishiro (2010) have correlated the Drop Weight Tear Test and Charpy V with full scale burst test.

Brittle crack arrest is another concern. Several tests are known to address the brittle crack arrest properties of steel. They share that a crack shall be initiated in colder and/or embrittled material which needs to halt at a certain point in the material and conditions of interest.

Table 1 Overview of fracture tests

Name of test	Typical specimen size	Remarks/ reference
Charpy V	10x10x55 mm	ISO 148, ASTM E23 (amongst others)
Instrumented Charpy V	10x10x55 mm	ISO 14556:2015
CTOD, *J*-integral	Full-thickness, proportional	ASTM E1820, BS 7448, ISO 12135
Drop weight tear test	250x77 mm by full thickness	ASTM E436
Pellini (Nil Ductility Transition Temperature)	Three sizes, not exceeding 100x100 mm	Puzak and Babecki, (1959), ASTM E208 (2012)
Double tension test	Not clear from reference, could be up to 1000 mm wide	WES 2815:2014
ESSO test	Large specimens, 1000 m wide and total 7 m long	WES 2815:2014
Transition temperature	Variable	ASTM E1921

Arrestability is an especially important parameter for the high yield, large thickness steel in hatch coamings of container ships. ESSO and Double-tension tests (WES 2815) are expensive tests that can be used to find crack arrest parameters for design analysis. The Compact Crack Arrest (CCA) (ASTM E1221) is another standardized test that also aims at finding crack arrestability analysis parameters. Otani *et al.* (2011), Sugimoto *et al.* (2012) described the use of ESSO tests to indicate crack arrest properties. Kubo *et al.* (2012) compared large scale crack arrest tests with full scale components of a container ship and found good agreement. Extensive efforts have been done to relate crack initiation with crack arrest. Ishikawa *et al.* (2012) investigated the applicability of small scale crack arrest tests with the large ESSO (wide plate) tests. Because of the very high cost of quantitative brittle crack arrestability testing, there is a special interest in establishing a quality control test that can be used to assure brittle crack arrestability without resorting to routine expensive testing. For this role, the Pellini test, standardized in ASTM E208 (2012), is proposed. However, the Pellini test does not have the same ductile to brittle transition temperature as larger-scale crack arrest testing so the test temperature would need to be adjusted from the service temperature. Hauge *et al.* (2015) have suggested the use

of Pellini testing with an offset temperature for verification of brittle crack arrestability of structures in the Arctic.

A final consideration is the Ductile to Brittle Transition Temperature (DBTT). This temperature is the temperature at which the failure mode changes from ductile to brittle, and it is worth noting that it is defined in several ways depending on the testing technique. For example, one parameter is the T_{27J}, which is the temperature at which the Charpy V impact energy is equal to 27 J, and similar definition applies also to T_{40J}. Another parameter, the Fracture Appearance Transition Temperature (FATT), is determined as the temperature at which 50% of the Charpy fracture surface failed in a cleavage mode, with the other half presumably failed in a ductile mode. A parameter that makes use of more rigorous fracture mechanics principles is the T_0 value; which is the temperature at which the fracture toughness K_{Jc} is equal to 100 MPa√m for a specimen thickness of 25 mm in quasi-static testing (ASTM E1921).

A common way of reducing conservatism is accounting for the effect of crack tip constraint. This concept is based on the observation that the state of stress in a typical laboratory fracture specimen is different than found in the actual ship structure. Perhaps the most straightforward way to account for this would be to choose a fracture specimen that has a similar level of constraint as the structure; which has motivated the aforementioned interest in developing the SENT specimen. Alternative methods for reducing conservatism are based on post-processing test data; however, additional information is often required, such as the Weibull shape parameter *m* required by ISO 27306 for unwelded structures. The advice of ISO 27306 is to find this parameter by the procedure of Gao *et al.* (1998); requiring ten repetitions of two different fracture toughness specimen types, for a total of 20 tests. Other, less expensive ways of experimentally determining *m* have been proposed in the literature, *e.g.*, Andrieu *et al.* (2012), Cao *et al.* (2011), and Qian *et al.* (2015), the latter based on the T_0 value. Coppejans and Walters (2018) are currently comparing between the most recent test methods and the widely recognized approach of Gao *et al.* (1998). To avoid limitations of ISO 27306, recent research has dealt with extending its achievements to welded structures (Minami *et al.*, 2013); however, that work is still under development. Likewise, BS 7910 Annex N offers methods of adjusting for constraints depending on whether ductile or brittle failure is considered. Not all the methods presented in BS 7910 Annex N require further testing; however, many do. Best results would likely be achieved with some combination of using multiple specimen geometries and multiple crack depths, though this would clearly be the most expensive.

Figure 1: Raking damage tests: Mild Steel specimen is subjected to a lateral impact load. Deformation is recorded with DIC (Haag *et al.*, 2017).

3.1.4 Corrosion

Corrosion comes in many forms. It is the intention of this section to discuss the testing methods and measurement techniques that exist to capture the phenomenon. Corrosion tests are performed in laboratory conditions and exposure sites; either offshore or in sea wind and sun battered locations. Experimentation can be concerned with uniform corrosion. Corrosion rate (based on mass loss) as well as microscopic evaluation was performed; both typical methods for exposure test evaluations. For uniform corrosion tests and analyses, several methods are generally accepted:

- Open circuit potential (OCP)
- Linearized Polarization Resistance (LPR)
- Electrochemical Impedance Spectroscopy (EIS)

The first system defines the potential of a material with respect to a given reference electrode; most often Silver-Silverchloride (Ag-AgCl). A material with a higher potential value is commonly called more noble and may be less prone to corrosive degradation. The second method measures the resistance of a specimen when exposed to a variation of potentials around the OCP. Lower resistance normally indicates higher corrosion rates. Corrosion layers may also exhibit capacitive, protective capabilities. The protective capabilities can be found by EIS. The resistance of a specimen is measured along a long range of frequencies. The measured response can be modelled by a system of resistance and capacitive elements; the associated values provide information on uniform corrosion rate. It is important to note that these methods are based on the assumption of uniform corrosion. When local corrosion takes place, local electrochemical circuits (cathode-anode combinations) develop and may not be picked up by the measurement system.

Corrosion is a deterioration mechanism that requires long exposure periods; especially for general or uniform corrosion. Accelerating corrosion is limitedly possible. Raising the temperature is the best-known option to accelerate corrosion. The other challenge is consistency; feasible by controlling the test conditions. Localized corrosion poses specific challenges to experimental validation. For instance, the effect of microbial induced corrosion (MIC) is a trending topic. The variety of bacteria is large and the combination of the various species also influences the behavior of a single species. For example, Sulphur reducing bacteria in combination with Sulphur producing bacteria, will develop a lively, corrosive culture. Several works have addressed MIC in general; however, addressing the specific combination of electrochemical and MIC corrosion is less frequent. Zhang *et al.* (2016) describe a methodology used to combine clean working conditions with electrochemical measurements, described the effect of MIC activities on the electrochemical measurements, and recorded surface morphology as well as the material structure. Hence, the material constitution could be related to the corrosion behavior; which is influenced by local electrochemical corrosion and MIC.

3.1.5 Friction

Friction is a marginally understood phenomenon when it comes to steel-steel interaction during collision. Several publications underline the importance of friction, while none give the proper way to model and experimentally measure friction. Haag *et al.* (2017) has addressed the issue of friction by performing tests to measure the friction coefficient and show the influence on mechanical behavior. The friction was tested in a dedicated set-up. Further, two series of drop tests were performed: with and without friction. The contribution of friction on energy dissipation was estimated.

Dragt *et al.* (2015) have reported Full-scale bearing tests. A sliding bearing was tested for wear under operational conditions. The axle was pushed in the bearing (radial loading), whilst being rotated oscillatory between two defined points. This combination of loads makes it a complex test to perform. Measurement of small wear was performed with DIC.

3.2 Large scale experiment

3.2.1 Ultimate strength

Ultimate strength is a traditional topic of ISSC; which is related to the limit state of the ship and offshore structures. During the past few decades, the research was focused on plate, stiffened panels or box shaped specimens during the design stage without damages or deterioration. Due to the increased attention to life-cycle management in maritime industry, damaged and aged structures have been recently studied. Several experiments concerning the ultimate strength of plates or stiffened panels with cracks or pit corrosion were performed to investigate the collapse of the structural components and are considered in the following.

Specimens

Specimens are taking the form of plates, stiffened plates, box type specimens or part of ship structures. Normally they are large scale (¼ or more). Typically, the ultimate strength, post buckling strength or strength after initial deformation are considered. In the latter, the imposed deformation is the result of construction or aging processes, or other kinds of damage. In Shi *et al.* (2017) a series of stiffened plates with initial distortions and artificial cracks along the transverse, longitudinal and inclined directions were subjected to in-plane compression until achieving their ultimate strength. A plate cut from an aged ship was tested to obtain the ultimate strength including corrosion damage (Zhang *et al.,*2017d). Other types of damaged plate structures include severely corroded stiffened plates (Gorbatov *et al.*, 2017), thin steel plates with a central elongated circular opening (Saad-Eldeen *et al.*, 2016a), stiffened panels with a large lightening opening (Saad-Eldeen *et al.*, 2017) and steel plates with a large circular opening accounting for corrosion degradation and cracks (Saad-Eldeen *et al.*, 2016b).

Loading process

Loading is generally applied progressively on the short edge of the tested plates. Axial compression was applied using displacement control at the velocity of 0.5 mm/s by Chen *et al.* (1997) and recently by Shi *et al.* (2017) to capture the post-ultimate strength response. An alternative way is to apply the compression load at a specified rate, as reported by Zhang *et al.* (2017d), with a load rate of 1 kN/s up to a compression load of 50 kN, and beyond this value with a decreased rate of 0.5 kN/s.

Experiment set-up

Large scale ultimate load testing requires dedicated experimental set-ups. The Tubular Testing System (TTS) was first introduced by Chen *et al.* (1997). The TTS has the capability of applying both axial (tensile and compressive) and lateral loads to the specimens and can be used for fatigue testing as well. The set-up consists of a universal testing frame and electro-hydraulic servo controlled actuators with end supports designed to provide “pinned” connections as shown in Fig. 2 (see also Shi *et al.* (2017) for further comments about end supports). In the past decades, test set-ups have been continuously upgraded and the so-called Universal Testing Machine (UTM) can afford for testing in Arctic, cryogenic and elevated temperatures conditions; an example is the UTM recently installed at Korean Ship and Offshore Research Institute (KOSORI).

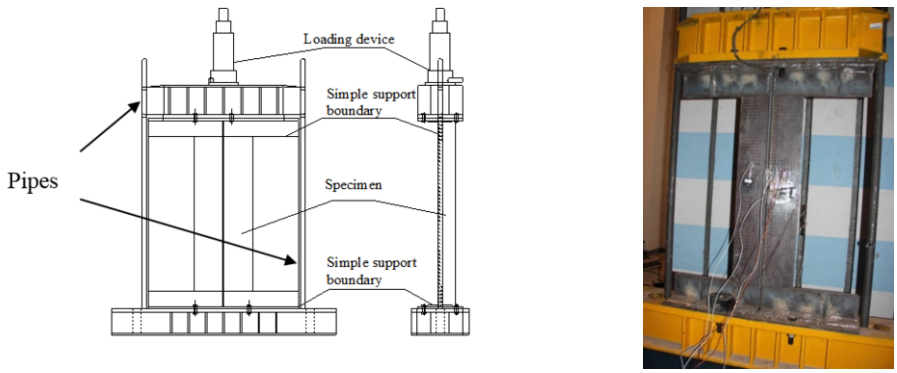

Figure 2: Test set-up (Shi *et al.*).

Boundary condition simulation

The boundary condition for an experiment is an idealization of the reality with the requirement to also be effective. One can choose pinned and/or fixed, and normally the cross section at the boundary remains unchanged during the experiment. Chen *et al.* (1997) described the end supports of TTS which were designed to provide "pinned" connections (see also Shi *et al.* (2017) for further comments). The design of the end supports allows the lateral displacement of the structure after ultimate point to simulate the post-buckling characteristics as well as rotations at the end. Instead of using a clamped support design, Zhang *et al.* (2017d) designed jigs to achieve a simple support boundary condition. Three types of the plate lateral edge support were also present in TTS, namely, (*i*) continuously supported edges, (*ii*) discretely support edges, (*iii*) free edges without any restraints. Finite element analyses showed that models with discretely supported edges have similar failure modes as the ones with continuously supported edges. The free edge boundary condition will have an effect on the failure mode of plate buckling. Models with discretely supported edges predicted multiple waves while the free edged model buckled in a single wave. These plate edge boundary conditions were also used in Shi *et al.* (2017) and the free edge in Zhang *et al.* (2017b) as the continuously supported edges.

Ship structures are normally exposed to a combination of loads; which, is difficult to simulate in a testing environment. Tanaka *et al.* (2015) described how the ultimate strength test of a hull girder with an open cross section could be analyzed regarding the ultimate strength under bending, warping and shear.

3.2.2 Large scale fatigue testing

To evaluate the fatigue strength of ship and offshore structures, large-scale model tests need to be performed under complex load and boundary conditions; consequently, different solutions have been adopted. Fricke and Paetzold (2010) carried out two types of full-scale tests: the first evaluated three models of web frame corners typical of ro/ro ships under constant amplitude loading and the second type tested five models representing the intersection between longitudinal and transverse web frames under constant and variable amplitude loading. All tests showed a relatively long crack propagation phase after crack initiation; calling for a reasonable failure criterion. The investigations provided good insight into the strength behaviour of complex welded structures and valuable information for validation of numerical codes.

Full scale fatigue tests of an aluminium ship structural detail were carried out by Tveiten *et al.* (2007) to obtain a design S-N curve. The test specimen consisted of a longitudinal stiffener and a transverse web plate. The fatigue test rig was designed to simulate the effect of lateral load transfer from a longitudinal stiffener into a transverse web. A total number of nine models were

tested at a constant load amplitude at a frequency of 2.5 Hz. Comparisons with the finite element method and recommendations on the procedure for fatigue assessment of aluminium ships (including S-N curve to be used) are provided.

Jang *et al.* (2010) investigated the fatigue crack propagation at the connection between a flat stiffener on a transverse web frame and the flange of a longitudinal stiffener on a bottom plate or inner bottom plate. Two typical types of web stiffeners were adopted; a straight end type and a softening end type. A test jig was designed to transfer the load from the actuator to the specimen along the line load at the centre of the specimen. Three different load levels and two types of specimens with load frequency of 5 Hz were tested. Two rolling supports were used to realize simple support boundary conditions. This paper proposes a set of formulas that are the most suitable for predicting a crack which starts from a welded joint of a top stiffener upon a longitudinal one and then grows into the bottom/side shell plate.

Yue *et al.* (2012) attempted to predict the fatigue life of a multi-planer tubular KK joint based on scaled model test and FEA. The specimen is welded by five hollow circular steel pipes. Although tubular KK joints among truss framed legs suffer a complex load combination, the axial load is usually predominant; it was also assumed dominant for the fatigue tests. A test rig was set up to fix the tubular joints subjected to axial loading and prescribed load application via the actuator. The FEA on both the real structure and the scaled model were performed to obtain their hot spot stress distributions. From the comparison and analysis of their hot spot stresses, the fatigue life of the real structure was provided based on the scaled model test result by use of the hot spot stress approach.

3.3 Impact & impulsive loading and response assessment

3.3.1 Ship Collisions and Grounding

Collisions and grounding are a major risk for maritime transport. Therefore, collision and grounding experiments have been carried out in full and model scales in order to investigate the collision mechanics of accidental events. In these experiments several effects can be included; however, simplifications are often required to narrow down the number of effects. Early experimental research dates back to the development of nuclear vessels (*e.g.*, Minorsky, 1959) and has been reviewed by Woisin (1979) with respect to internal mechanics with dry external mechanics. The heavily coupled internal and external mechanics are typically investigated separately to focus on some of the non-linear effects. Only a few actual collision or grounding event experiments were carried out in full scale (Vredeveldt and Wevers, 1992; Wevers and Vredeveldt, 1999; Lehmann and Peschmann, 2002; Wolf, 2003). Full scale experiments are expensive, difficult to perform and have provided limited validation data to give full understanding of the physics and uncertainties involved. As the data storage and the instrumentation capabilities increase, experiments based on extensive measurement techniques like Digital Image Correlation (DIC) are likely to improve our understanding of the coupled non-linear phenomena at full-scale. The following is a review of the different steps of the collision and grounding problem when experimental methods are utilised. Scaling issues are discussed in the following as well as in Section 5.1.

Collision and Grounding Event

Even if ship data in terms of production drawings, material certificates and surveying are well known, the collision or grounding event is often far less well-known. Sormunen *et al.* (2016a) investigated the influence of sea bottom shape idealisation with blunt cones in relation to the bathymetric big data (cloud of discrete points) measured from the Baltic Sea around the Finnish coast. It was shown that there are compensating effects when grounding damage is estimated with simplified models; for example, some errors can be made in the creation of "equivalent cones" for simulations or testing while the structural damage forms compensating effects. Further developments to form analytical models for simplified rock shapes are provided in Sormunen *et al.* (2016b) and Sormunen (2017). The analytical models can be used to simulate

true damages based on measured sea bottom shapes. Similarly, Roubos *et al.* (2017) investigated the berthing velocities at the port of Rotterdam with a portable laser system. Several measurements of relatively large seagoing container vessels were recorded and used as input for collision analysis; however, this kind of data generally allows for setting up more realistic grounding simulations as well. Numerical simulations involving internal and external mechanics are an increasingly accepted tool for design analysis (Moan *et al.*, 2017) of collision and grounding events. However, due to the strong non-linearities of the coupled problem, numerous challenges remain.

Experimental validation of analytical methods is of utmost importance due to their extensive use at the design stage. Zhang *et al.* (2017c) analysed 60 experimental results using analytical tools. A similar benchmark investigation was performed by Ehlers *et al.* (2008, 2012b) on full-scale experiments from the Netherlands. These benchmarks clearly demonstrated the gaps in modelling within the sub-problems of the coupled events. On the other hand, the experimental investigations at model scale by Tabri *et al.* (2008) focused on the coupled physics of ship motions, structural damage and sloshing in partial filled tanks. The scale ratio used by Tabri *et al.* (2008) was 35 and concluded that even though the similitude cannot be satisfied at the same time for all the influencing factors, the agreement between full- and model-scale experiments can be very good when proper values can be set. The study was later extended to include sloshing effects (Tabri *et al.,* 2009) and non-symmetric ship collisions in Tabri *et al.* (2010). Based on the above mentioned research, the full-scale results could be explained as well when all these phenomena were considered. Furthermore, the Froude-number based scaling is only partially effective as the different physical phenomena that affect the energy distribution in collision events do not scale in accordance with the same rules. In these experiments the structural response was simulated by homogenous foam to create the "equivalent" structural deformation in model and full-scale. This restriction was removed in the works of Calle *et al.* (2017b) who investigated the energy absorption of T cross-section beams and true ship structural topology in forced path on rigid wall as well as grounding and collision between two oil-tankers at 1:100 scale (scaled laser-welded metal structure). This work highlighted that as structures experience major non-linear deformations, the structural failure is difficult to predict. The difficulty is due to inapplicability of the usual material scaling as a result of necking formation and material characteristic microstructure (Calle and Alves, 2015). Thus, the scaling laws always neglect some aspects. The uncoupled approach remains a worthwhile simplification to gain insight into the physics of collision problem in addition to performing full and scaled tests as shown in the work of Cho *et al.* (2017). The coupling and scale effects remain unclear. On this side, Qiu *et al.* (2017) investigated the structural response and energy absorption of the simplified ship side under the impact of rigid indenters with different shapes and model scales.

Internal Mechanics

The key question relating to internal mechanics is the marine structure failure process and scaling of. Consequently, dynamic and quasi-static full-scale experiments are often employed to get new insights. Full and model-scale experiments of buffer bows are important for the validation of theoretical models as shown by Endo *et al.* (2002), Yamada and Endo (2005, 2007) and Yamada (2006). Quasi-static experiments were carried out to determine the interaction between the deformed colliding and collided ship structures (buffer-bow and double hull side structure) by Schöttelndreyer *et al.* (2011, 2013) and Tautz *et al.* (2013) who showed that the failure modes can be captured with theoretical models. Because of the complexity in modelling the complete scenario, further simplifications are frequently introduced in the experimental analysis by performing rigid indenter tests for the structural components. The panel experiments, complemented by material tests, by Rodd, (1996) Alsos (2008), Alsos and Amdahl (2009), Paik and Thambayalli (2003), Ehlers *et al.* (2012a), Liu *et al.* (2015b) indicate that the key question in the experiments is the failure process; which includes folding, buckling and fracture within the complex 3-dimensional shapes and welds. If the structure is designed ac-

cording to reliable design standards, it should not fail from the connections. The failure prediction then narrows down to the modelling of the failure strain of the base material; which requires proper material testing (*e.g.*, dog-bone specimen as prescribed by classification societies in their material certificates are often employed). The likeness of this test with respect to the failure mechanisms of 3D structures is limited because the strain path does not change as it does in real cases as shown by Benzerga and Leblond (2010) and Körgesaar *et al.* (2014). The problem becomes more complicated when temperature and strain-rate effects are included (Ehlers and Ostby, 2012; Park *et al.*, 2015).

Motivated by the full-scale experiments in The Netherlands, a sequence of structural strength tests on scaled structures have been carried out with Y and corrugated cores (Kitamura, 1997; Pedersen *et al.*, 2006; Rubino *et al.*, 2008a,b, 2009, 2010; St-Pierre *et al.*, 2015; Cao *et al.* 2017) as well as concrete structures (Niklas and Kozak, 2016; Woo *et al.*, 2015) reporting the experimental damage mechanisms of these crashworthy structures. More traditional marine structures have been investigated by Quinton *et al.* (2017) who showed that quasi-static assumptions of pressure patch for ice-induced load lead to unrealistic results due to neglected trailing edge effect by rigid rolling contact tests on plastically deforming steel plates. Gong *et al.* (2015) experimentally investigated the steel plate response and associated failure modes for different impactor shapes ranging from spheres to bulbs and rectangular sections. Liu *et al.* (2015a) investigated the dynamic response of impacted stiffened plates using traditional experimental techniques. Offshore structures response was investigated by Wang *et al.* (2016c) who performed experimental and numerical investigations on the T-joint of jack-up platform laterally punched by a knife edge indenter. A similar study was performed by Cerik *et al.* (2016).

The effects of cold environments on the physics of structural failures behind collision and grounding events have been experimentally investigated by many authors. Kim *et al.* (2016a) evaluated the effect of cold temperatures on the structural resistance of Arctic steel grades in terms of plates and stiffened plates. It was shown that during the room temperature tests the material remains ductile, however, the failure mode changes from ductile to brittle as a function of cold temperature. The investigations were extended in Ince *et al.* (2017) who performed impact experiments between steel plated structures and conical indenters made from steel and KOSORI fresh water ice, showing the possibility to numerically model the dynamic ice-structure-interaction.

Modern experimental techniques such as Digital Image Correlation (DIC) improves our understanding by measuring the strain fields on the specimen surface. One of the challenges in using DIC for collision and grounding tests is related to the adhesion of the speckle pattern used to identify the measurement facets when the fracture initiation and propagation is of concern. Gruben *et al.* (2017) and Körgesaar *et al.* (2017) applied DIC for the investigation of the fracture of stiffened panels under quasi-static and dynamic loading. Their study and the works of Hoogeland and Vredeveldt (2017) showed strain field data without adhesion issues; clearly demonstrating the potential of DIC in these highly challenging conditions. Another direction for future use of experimental investigations is provided by hybrid numerical-experimental methods (Getter *et al.*, 2015).

Consequences

Once collision or grounding has occurred, the consequence assessment becomes a coupled problem involving dynamic stability, progressive flooding and slowly varying loading on the ship (Bennet and Phillips, 2017). Jalonen *et al.* (2017) investigated the leakage and failure of non-watertight structures found in cruise ships in full scale. It was observed that the failure process is non-linear in terms of leakage as the structures start to collapse with large pressure heads increasing the gaps between frames and doors/classes. In Ruponen *et al.* (2013) the air compression effects inside a flooded tank of a damaged ship was studied through systematic full-scale tests with a decommissioned ship where the ventilation level of a flooded tank could be altered. Based on these ideas, Lee (2015b) predicted the capsize process of MV Sewol in

South Korea. Storheim *et al.* (2015) compared different state-of-the art failure criteria to predict the collision damage of the vessel Nils Holgersson collision.

3.3.2 Underwater explosion

Impact loading response of structures by underwater explosion has been investigated for many years. Experimentation has played an important role in understanding the underlying phenomena since the material characterization, loading description and associated responses are remarkably complex.

Test for material characterization

In order to understand the failure mechanisms under impact loading and perform numerical studies, a thorough understanding of the material properties is required. It is well known that the damage model under impact loading on metallic structures is related to the stress status. Some experiments were specifically carried out to test the dynamic mechanical behavior of materials for high-strength or high-temperature applications. Zhang and Suo (2017b) proposed a new experimental method for measuring the dynamic behavior of materials at high temperatures. The experimental set-up includes a classical split Hopkinson pressure bar and a MoSi2 heating source for achieving high temperatures. Experiments were successfully conducted on TC4 alloy with temperatures ranging from 20° to 1400° at the strain rate of 2000 s^{-1}, and on SiC at temperatures in the range 20°-1600° at the strain-rate of 250 s^{-1}. Fracture experiments of some high-strength steel were carried out by Fras *et al.* (2017), Li *et al.* (2014) and Li *et al.* (2015a). Fracture testing of sheet metal was investigated by Roth *et al.* (2015, 2016).

Loading

The pressure load produced by underwater explosion consists of a shock wave and bubble pulsation. After the detonation, there will be a shock wave propagating radially outwards, followed by a large oscillating bubble. The shock wave has the first damaging effect followed by successive bubble collapse and a high-speed jet.

Lee (2017) performed underwater explosion experiments using a small amount of shell-free Pentolite to observe the behavior of the generated gas bubble as well as measure the shock wave. Moon *et al.* (2017) measured the maximum pressure of the shock wave of an underwater explosion relying on underwater pressure sensors. To assess the measured signals, experiments were repeated five times under the same conditions. Small-scale underwater explosion experiments were carried out with two types of media at the bottom and different water depths in quasi-shallow water by Wang *et al.* (2015b). An analysis of measured data from different media at the bottom revealed that the peak pressure of shock waves in a water basin with a bottom of soft mud and rocks is about 1.33 times that of the case where the bottom material is only soft mud. Yanuka *et al.* (2015) conducted underwater experiments with wall boundaries having a parabolic cross section. This study showed that shock waves converge faster and the pressure near the line of convergence is larger. Zhang *et al.* (2015c) proposed a minus error approaching method to get the position of the explosion source using 4 effective pressure measurement points. Xie *et al.* (2015, 2016) have studied the time-frequency shock wave characteristics with underwater explosions in the free-field and near a ship hull. It revealed that more than 90% of the energy of the shock wave pressure signals condenses in the band lower than 8 kHz in the free-field and more than 80% of the hull pressure signals are mainly concentrated in a range of 20 kHz. Kostenko and Kryukov (2016) developed a technique to identify the explosion pulse based on the calculation and normalization of the mirror derivative of the received signal. In this way, the weak direct signals are amplified while the reflected ones can be suppressed.

The dynamics of underwater explosion bubbles has also received considerable attention with a particular focus on its dependence on the physical properties of boundaries adjacent to the bubble. Several experiments of a spark-generated bubble oscillating near a free surface and a rigid plate with a circular opening were conducted by Liu *et al.* (2017). Li *et al.* (2015b, 2017) studied the interaction between a violently oscillating bubble and a movable sphere with comparable size

near a rigid wall. Zhang *et al.* (2017a) investigated the interaction between an underwater explosion bubble and an elastic-plastic structure using small-scale experiments. Similar experiments were performed by Cui *et al.* (2016) to investigate bubbles subjected to gravity and various boundary conditions, including; single boundary, combined boundaries of free surface and solid wall, solid wall boundaries with a circular opening, and resilient wall boundaries. Ouyang *et al.* (2016) revealed that with an increase in charge density of each 100kg/m^3, the volume of the bubbles, acceleration and sound pressure level average increased by 1.78 times, 2.28 times and 1.15 times respectively. Zhang *et al.* (2015a) investigated the dynamics of large bubbles subject to various strengths of buoyancy effects.

Response

Underwater explosion is a severe threat to nearby ocean structures such as underwater construction, commercial and naval vessels. The latter requiring an assessment of their capability to withstand shock through expensive and lengthy tests. Scaled model experiments provide an opportunity to quantify the response associated with impact loading. Heshmati *et al.* (2017) designed a conical shock tube to investigate the underwater explosion phenomenon and its effects on nearby structures. Similar tests were conducted on a steel-plate (Park *et al.*, 2016) and clamped thin panel (Ren *et al.*, 2017). The influence of solid rubber coating on the transient response of floating structure to underwater shock wave was experimentally studied by Chen *et al.* (2016). It was shown that solid rubber coating can change the incident pressure on the wet surface as well as the dynamic characteristics of the coated structure. The high density and viscosity coating reduces the local deformation and global response when compared to high-stiffness low-compressibility coatings. A similar study was also carried out by Zhang *et al.* (2017a). Ming *et al.* (2016) experimentally recorded the damage process of ship structures subjected to underwater contact explosions. Zhang *et al.* (2015d) and Cheng *et al.* (2016) tested both a hull-girder model and a scaled ship model for dynamic response assessment to underwater explosion. The results show that the acceleration response and damage grade increase with shock factor and the local response is related to the vibration mode.

3.3.3 Vibration

Vibration and on-board noise measurements are related to distinct and often physically correlated phenomena for which sensors and experimental procedures are well consolidated for basic applications. For vibration and internal noise problems which depend strongly on the excitation and geometry of the structure, concerns at component level are limited to the estimation of structural damping or noise transmission coefficients. In the case of realistic configurations, the focus is on the response level related to comfort or fatigue and on the analysis of vibration and noise sources, transmission paths and influencing modal parameters (see Section 4.1.2).

Dry vibration testing

Vibration measurements require different levels of accuracy, bandwidth, spatial resolution and tolerance of insertion effects depending on the application. Vibration testing is used to estimate damping of structural components like a stiffened panel or more complicate configurations to improve the modeling of response at resonance. The structural damping is typically determined by evaluating the frequency response function with experimental modal analysis techniques during laboratory tests. The input force is applied and measured with instrumented hammers (impulsive force) or shakers (harmonic, sweep or stochastic load) and the vibratory response is recorded with modal accelerometers or strain gages. Soft-spring suspension is preferred when no specific boundary conditions are prescribed to facilitate FE model updating. When avoiding contact or insertion effect is desired, the laser Doppler vibrometry provides precise non-contact displacement measurements as required, for instance, to record the shaft vibrations induced by the propeller through the trust bearing (Pan *et al.*, 2002). Fiber Brag Grating (FBG) has also

been used for dynamic strain measurements (Jensen *et al.* 2000); who conducted wet-deck slamming tests with FRP sandwich panel using a network of 16 fiber optic Bragg grating strain sensors including comparison with the strain gage data.

Wet vibration testing

Dedicated experimental setups are required when the measurement of realistic vibration levels is the objective; as was done by Halswell *et al.* (2016) who dealt with the daily exposure limits to vibrations for the crew of high speed crafts. The core of the experimental campaign was based on 3D drop tests of rafts where three triaxial accelerometers were installed in place of the crew members. The measured acceleration time-histories provided peak values, RMS and weighted values from which the vibration dosage in the frequency range of 2-20Hz was obtained to verify the acceptance of regulations. The test matrix comprised of different drop heights and pitch angles to investigate the vibration exposure dependency on these factors. An important issue in complex set-ups is the cabling of sensor arrays. A solution was proposed by Bennet *et al.* (2014) who tested a wireless measurement system mounted on a floating elastic model excited by waves. The system consisted of three Shimmer 9DOFs wireless sensor nodes (triaxial accelerometer, gyroscope and magnetometer) equipped with SD card logger and Bluetooth connection. The triggering of the node acquisition and the post-test data downloading was obtained with an in-house MATLAB code. Good comparison was obtained in terms of heave and pitch response amplitudes (after proper processing of the node outputs) with the tethered system potentiometers. There is no direct comparison at the wireless nodes for elastic deformations, however, the node outputs are mixed with strain-gage information to provide the elastic line deformation. Among the few example of contactless measurements, Carrol (2006) estimated the radiated acoustic power of an underwater vibrating surface by measuring the response with a laser vibrometer and then compared the propagated noise inside the reverberant tank with hydrophone measurements. Kwon *et al.* (2013) applied digital image correlation to investigate the vibrational characteristics of composite beams immersed in water by collecting information about the added mass without the need to embed sensors potentially altering the structural properties or the interface with the surrounding fluid. Recently, the use of FBG for dynamic strain measurements in oscillating water intake risers is considered in the complex laboratory testing conducted by Wang *et al.* (2016d). The large deformations as well as the requirement of providing multiple measurement points along the entire riser length (up to 40 m, almost entirely and vertically immersed in the water pool) were driving factors for the choice of FBGs. There are 16 measuring stations in total along the riser. At each measuring station, there are four sensors around the circumference of the section: two for the in-plane responses, and the other two for the out-of-plane responses. The collected data allows for the determination of RMS of in-plane motion, out-of-plane motion and the separation of mode contributions to the overall deformation characterized by frequencies below 1 Hz.

Vibroacoustics

One of the main issues related to vibration and structure-borne noise onboard ships (this concept may be extended to offshore structures as well) mainly concerns the definition and fulfillment of (non-mandatory) habitability criteria, however, some mandatory rules apply to critical mechanical components like the propeller shaft. The ISO standards 6954-1984/2000 and 2631-1/2, as well as the optional class notations from classifications societies prescribe the significant physical parameters, acceptable exposure limits depending on ship areas, and experimental procedures for vibration level assessments (ISO 8041). The assessment of noise levels follows similar standards (IMO resolution MSC.337(91) for example) that indicate the procedures for the measurement of structure-borne noise. Therefore, the vibration and noise measurement sensor (accelerometers, velocity gauges, proximity probes, strain-gages and sound level meters) filter set, calibration and other requirements (sensor collocation, etc.) are prescribed to some extent. For this reason, relatively few accounts of experimental measurements appear in scientific literature while experimental procedures are periodically updated in technical papers issued by classification societies.

One of the most extensive experimental campaigns related to vibrations and noise has been carried out within the EU-FP7 project SILENV (2012). The main project objective involved the revision of the noise and vibration exposure requirements for crew and passengers of different ship categories; for which present and previously collected data were processed. New experimental procedures for vibration and noise measurements were defined and implemented by Turan *et al.* (2011) and Badino *et al.* (2012). Borelli *et al.* (2015) carried out full-scale noise level measurements in various compartments (living and working spaces) of a Ro-Pax ferry during navigation and maneuvers. The instrumentation was composed by two IEC 61672 Class 1 compliant sound level meters equipped with random incidence microphones and calibrated with IEC 60942 Class 1 compliant calibrators. When taking measurements in outdoor spaces, a windscreen was used along with proper correction factors. The measured levels were compared with recommended exposure limits to verify the compliance of the acoustic climate with regulations extensively reviewed in the paper.

3.4 Fluid-structure interaction

3.4.1 Hydroelastic scaled tests

Fluid-structure interaction (FSI) concerns all physical problems where rigid or elastic motion depends on, or are two-way coupled with, the nearby flow. The interaction between a rigid-body and the surrounding fluid is typically considered by ITTC (*e.g.*, seakeeping or propeller revolution). Here, the extent of FSI is restricted to the case of bodies subjected to deformations. Structural scaling allows for fitting the test setup into the laboratory space and preserving the basic features of the investigated phenomena in terms of elastic (and rigid) motions and fluid loads. To be effective, especially if getting new physical insights is the main objective, structural scaling requires consistent similarity laws as well as reducing in most cases the structural complexity of the full-scale problem. If the test purpose is extended or limited to the validation of FSI numerical codes, the reduction of uncertainties on the structural model can be attained by assessing the experimental setup through dedicated structural tests.

Ships

Segmented and elastically scaled models of ships have been used since the fifties (Mc Goldrick and Russo, 1956) for different aims (hydrodynamic load or vibratory response measurement) with their applications increasing in the last few decades. Apart from a few unsuccessful attempts with the so-called “continuous” models (Tasai, 1974; Hashimoto *et al*. 1978), elastic scaling has always implied a segmented hull layout achieved by an elastic backbone (Achtarides, 1979) or local springs (Jullumstrø and Aarsnes, 1993). The proper design of the metallic backbone (aluminum or steel) is a key factor in correctly accounting for the ship global deformations. The slenderness of backbones with hollow sections limits the correct frequency spacing of the bending modes due to lack of shear flexibility, however, the rotary inertia of the hull segments may partially recover shear flexibility up to the 3-node mode (Dessi *et al.*, 2008). Large open beam sections best fit the shear stiffness distribution while targeting torsional modes required for testing of containerships in oblique waves. To investigate the springing and whipping of ULCSs, Hong *et al.* used H-sections (2011,2012) and U-sections (2014). U-Section were capable of correctly replicating the first bending and torsional modes of a 10,000 TEU containership with a 6-segment model. To scale the stiffness of a 9000 TEU containership, Maron and Kapsenberg (2014) designed a box shaped backbone with openings on the top of the beam and a variation of the beam slope at the bow. Generally, the connection between the segments and the backbone must avoid relative rotations between the connecting parts especially for hull segments undergoing slamming; single bottom leg or double-side legs are exploited in most cases, however, more complicated arrangements can also be found as in Maron and Kapsenberg (2014). A special design of the structural layout allowed Jiao *et al.* (2015) to equip the segmented model with a self-propulsion system. The variable cross sections of the backbone matched the structural stiffness distribution while different solutions were adopted to link the backbone to the fiber-glass segments. Pressure was recorded at several points in the

bow along with vertical bending moments from calibrated strain measurements, thus accounting for the slamming loads and induced whipping response.

Scaled experiments with catamarans require a different arrangement of the backspline connecting the demihulls and supporting the deck. The first example was given by Hermundstad *et al.* (1994) who built a self-propelled flexible catamaran by using longitudinal and transversal connections (elastic hinges) between the demihull segments. The shear forces along the vertical axis and bending moments along the hinge axis were measured at each hinge by force transducers. The deck was divided into three parts and instrumented with small slamming panels to measure the impact forces which in turn provide the mean hydrodynamic pressure. The backbone layout was first exploited by Kyyro and Hakala (1997) for model tests in the towing tank and by Cheng (1997) in open water towing tests. The most systematic series of experiments has been carried out since 2006 with respect to fast catamarans exhibiting a centre-bow (Lavroff *et al.*, 2007; Thomas *et al.*, 2011). The segmented model is a hinge-type model with flexible connections between the 3 segments of each demihull and stiff bars connecting the segments from side to side; which also support the fore deck part with four load cells. Several pressure transducers were also installed on the centre-bow to map the slamming pressure field. The stiffness of the elastic links was adjusted to scale the vertical bending modes. The link deformations were measured with calibrated strain-gages to directly provide the bending moments. A different approach for the design of a flexible catamaran with a flat wetdeck (Figure 3) was followed by Dessi *et al.* (2016, 2017a). To reproduce the frequencies of the split and 2-node bending modes, a structural optimization procedure was employed for the design of the aluminum backspline connecting the hull portions (4+4 demihull segments and 2 wetdeck portions). The optimization procedure was also utilized to determine the distribution of structural mass and ballast required to match the rigid-body mass properties. The fore section of the flat wetdeck was suspended on two hinged bars affixed with piezo load cells and pressure caps to measure the global and local slamming load. The strains were measured on the aluminum truss at 36 points to provide bending moment and shear force distributions as well as the demihull segment forces.

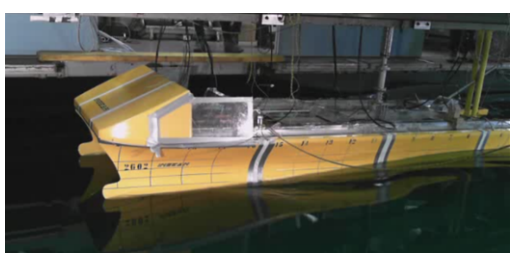

Figure 3: Flexible catamaran with elastic backspline (Dessi *et al.*, 2016)

Figure 4: Scaled test of the float-over concept with flexible topside (Dessi *et al.*, 2017b)

Offshore structures

FSI testing involving offshore structures have exhibited a wide range of study cases without a systematic classification over time. Thus, only some novel experimental applications are herein reported, and the reader has to refer to the reports of other Specialist Committees for a more extensive coverage. FSI testing on risers provides the ultimate step for verifying the effectiveness of vortex induced vibration (VIV) suppression devices as numerical modelling presents some issues for complex configurations. Gao *et al.* (2016) conducted experimental investigations on a flexible riser with and without helical strakes to assess the fatigue damage. The VIV were induced by towing a pretensioned riser model at constant speed. Up to 88 strain gages were applied on different riser sections to record the elastic response of in-line and cross-flow

vibration. The strain gauges provided sufficient data to compare the fatigue damage along the two directions with and without the suppression devices. Another example of unusual setups is the testing of float-over systems for the transportation and deployment of offshore structures. In Dessi *et al.* (2017b) the transported topside used to link two barges in a catamaran arrangement (Figure 4) was elastically scaled to investigate the relative rotations between the barges as well as the torsional and bending loads acting on the topside connections recorded with an optical system and a strain-gage array, respectively. A series of model tests with a realistic configuration of the vessel, carried topside and jacket were also performed by Kwon *et al.* (2017) and Kim *et al.* (2017) to investigate the performance of docking and mating operations in float-over installations. During the tests, the vessel motion, line tensions, fender forces and loads on LMUs (Leg Mating Unit) and DSUs (Deck Support Unit) were measured under various wave heading and amplitudes using special measuring devices.

Sloshing

Sloshing is another example of FSI for which the structural scaling of the tank elasticity affects the results. In Lugni *et al.* (2014) tank structural scaling was pursued by elastically scaling the first natural mode of a structural panel of Mark-III tank. The scaled instrumented elastic panel is clamped on the opposite top and bottom edges and sealed with silicon on the vertical sides. A static calibration of the strain gages applied on the plate was carried out under a uniform pressure load and their dynamical responses were verified by comparison with acceleration signals. The estimated structural damping was used in the plate FE model loaded with the measured pressures in a hybrid approach. The comparison of rigid and elastic (not-scaled) plate response for assessing the mitigation of the impulsive sloshing loads was carried out by Jiang *et al.* (2014), whereas Wei *et al.* (2015) considered inner structural details of the full-scale sloshing tank to experimentally identify the optimal value of the slat-screen solidity ratio to reduce the slamming loads. A challenging FSI investigation has been carried out by Lee *et al.* (2015a) who carried out a hydroelastic analysis of three elastic barges partially filled with water to validate numerical simulations. Using four cameras pointing to onboard infrared markers, they detected the relative torsional motion between the opposite sections of the flexible barges (made with Plexiglas) indicative of the hydroelastic response excited by oblique waves.

Ice

Testing in ice basins has received growing attention as long as artic routes become more affordable as a result of climate change. Dynamic ice-structure interaction has been subject to extensive research during the last decades to determine the ice-induced vibration fatigue. The goal of this research to consider ice-induced vibration fatigue at the design stage. Ziemer and Evers (2014) tested a compliant cylindrical structure (a lighthouse scaled by a factor of 8.7) under different ice conditions to investigate ice induced vibrations under laboratory conditions. Ice drift speed and thickness were varied to study the dependence of occurring vibrations on ice properties. The structural response was monitored by lasers as well as an inertia measurement unit to measure the acceleration and inclination of the structure. Ice loads were registered by two 6-component scales connecting the cylindrical structure to the mounting carriage. An open issue for ice tests is about the physical scaling of the ice sheet. These aspects were addressed by von Bock und Polach (2013, 2015) who presented a novel experimental technique to measure the model-scale ice property including grain size, elastic strain-modulus, compressive and tensile specimen tests. The model-scale ice thickness and the bending strength were also determined to classify the ice properties.

3.4.2 Slamming and water impact tests

Stenius *et al.* (2013) designed a new setup to experimentally investigate the consequences of slamming loads on impacting structures. Some representative high-speed craft hull bottom panels including; a glass-fiber reinforced single skin panel, foam-cored sandwich panel with glass fiber reinforced face sheets, and very stiff carbon-fiber sandwich panel were tested. Suàrez *et*

al. (2016) employed an experimental apparatus able to reproduce a cyclic slamming-like load in pre-impregnated and cured glass-fiber reinforced polymer panels. With respect to more realistic tests, the controlled environment allows for a precise correlation between the applied load and the damage propagation. High-speed velocity impact experiments were performed using the SHPB (split Hopkinson pressure bar) by Zhang *et al.* (2017b) to study the material properties under water impulsive loads. The specimen can be tested at high or low temperatures. A large impact facility to test metallic panels for ship and aeronautical applications has been recently developed for the EU project SARA (Figure 5). SARA enables the investigation of both elastic and plastic deformations at full-scale impacting speeds (Iafrati *et al.*, 2015, 2016). The specimen can be a panel or a portion of a real structure (Figure 6).

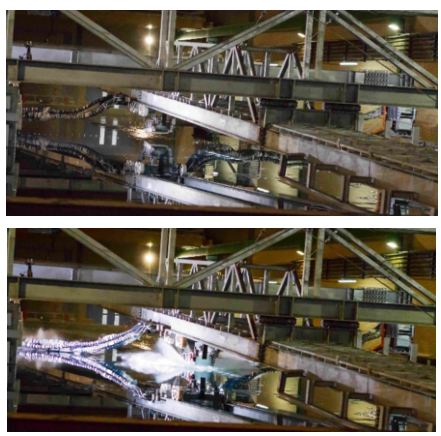

Figure 5: Large facility for high-speed impact testing.

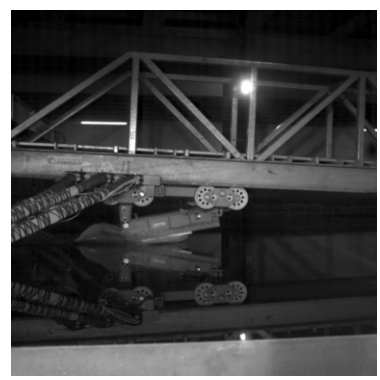

Figure 6: Detail of the carriage carrying the specimen.

4. FULL SCALE TESTS

4.1 Ships and offshore structures

4.1.1 Monitoring of loads and responses

This section reviews technologies for monitoring, environments, loads and responses of ships and offshore structures at sea.

(1) *Wave Measurement*
The WAMOS project (Hessner *et al.*, 2014) used the X-band radar for measuring waves from a sailing ship. The system gives the wave statistics values, such as the significant wave height and the directional spectrum, in real time. Koo *et al.* (2011) applied an onboard wave monitoring system (Wave Finder) to a large container ship. Using a marine X-band radar wave, parameters such as direction, period and height were acquired as done in the WAMOS project.

(2) *Load Measurement*
Schiere *et al.* (2017) developed a novel approach, or mode-based method, to derive load effects along the length of a vessel. In comparison, traditional approaches derive the sectional loads by processing strain gauge data in the section itself. The authors compared full scale trials and model tests along with numerical simulations and concluded that their mode-based method provide better results with less scatter than the traditional approach. Suominen *et al.* (2017a,b) discussed extensively the uncertainty related to measuring techniques related to ice loads. Historically, ice loads measurements onboard a ship were based on shear gauges placed side frames which are assumed to not deform plastically. This type of measuring system is very good for actual

operations as it is simple, robust and can be used both in short and long term. However, a major issue of this approach is that the ice load distribution was assumed beforehand. If this assumption is not accurate, the results will be too. If the strain measurement points in an instrumented panel can be increased significantly (by an order of magnitude or even more), the extension of the contact shape gets known far better. Digital Image Correlation (DIC) systems with computational inverse methods are potential future methods for this type of measurements.

Table 2: Notations for vessels with hull stress monitoring systems from major classification societies

Classification Society	HSMS Classification Notation Rules
DNV GL	HMON(A): where within the brackets is a better of A,C,D,E,G,H,L,M,N,O,P,S,T,W which denotes different sensors and data communications.
Bureau Veritas (BV)	MON-HULL
American Bureau of Shipping (ABS)	HM1:Motion Monitoring HM2:Stress Monitoring HM3:Voyage Data Recording for later evaluation
Lloyd's Register of Shipping (LRS)	ShipRight-SEA(Hss-n,optional extension) The extension –n signifies the number of strain gauges connected to the system. VDR An interface with the ship's voyage data recorder system to enable the recording of hull stress, ship motion and hull pressure information.
Korean Register of Shipping (KR)	Rules for Classification of Steel Ships(2008), Pt.9:Additional Installations, Ch.6:Hull Monitoring Systems
Nippon Kaiji Kyokai (NK)	Rules for Hull Monitoring Systems (valid at the date 07/2008)

Table 3: Sensors for monitoring ship hull structure of FPSO unit

Sensor Type	Monitoring Type	Maturity in Maritime
Strain Gauges (short and long baseline strain gauge)	Strain	Proven
Accelerometers	Acceleration	Proven
3D Laser Scannig	Optical	Proven
Photogrammetry	Optical	Proven
Fibre Optic	Optical	Proven
Pressure Sensors	Pressure	Proven
Conventional Ultrasonic Testing(UT)	Sound	Proven
Acoustic Resonance Testing(ART)	Sound	Un-Proven
Acoustic Emission Testing(AET)	Sound	Un-Proven
Guided Wave Testing(GWT)	Sound	Un-Proven
Remotely Operated Vehicle	Optical,Electrical, Sound	Un-Proven
Thermography	Temperature	Un-Proven
Sensor Networks (including Wireless Sensor Network)	Varies	Un-Proven
MEMS Accelerometers	Acceleration	State-of-the-art
MEMS Pressure Sensors	Pressure	State-of-the-art
Ice Accretion Sensor	Sound,Capacitance	State-of-the-art
Smart Coating	Color	State-of-the-art
Smart Dust	Electrical	State-of-the-art

(3) *Ship/Vessel Monitoring*

Fatigue damage assessment based on full scale monitoring of a large container carrier was reported by Koo *et al.* (2011). The full-scale monitoring system consists of a hull stress monitoring system (HSMS) and an onboard wave monitoring system (Wave Finder). The number of sensors in the midship region is four at each section. The HSMS provides an interactive user interface to display the bending moment, torsional moment, bottom slam occurrence, cumulative fatigue cycle count and real-time sensor display. The fatigue damage due to the high frequency components like springing/whipping was identified and found to be greater than what was expected. Guan (2015) reviewed commercially available HSMS and summarized notations for equipped vessels from major classification societies (see Tables 2 and 3). The author recommended that, for every FPSO vessel, at least one HSMS should be installed in compliance with regulation from the IMO. Additionally, he reviewed sixteen types of sensing technologies and categorized them into three groups: Proven, Un-Proven and State-of–the-art, according to the matureness and readiness for application in marine structures. He concluded that multiple sensing technologies should be systematically combined to provide more accurate information, and proposed the integration of proper wireless sensor network technology and Bayesian Network modelling as the future direction of FPSO hull monitoring system. Structural integrity

during operation is often ensured via monitoring the difference in loads in comparison with design loads. For example, in JIP MONITAS (Tammer *et al.*, 2014), prediction of soundness is tackled through monitoring of hull load.

(4) *Offshore structure monitoring*
Regarding riser structures, many real-time monitoring systems were proposed. Frazer *et al.* (2011) investigated the phenomenon known as Wake Induced Oscillation (WIO) of top tension risers (TTR) by monitoring the system in real time. To determine the riser motion amplitude, 3-DoF acceleration and 2-axis angular rate sensors are secured in a corrosion resistant Remotely Operated Vehicle (ROV) deployable canister. The selection of motion sensors is based on results from FEA conducted on the production TTRs. The strain sensors are mounted over critical welds above and below the upper centralizer to capture the strain response of fatigue critical areas on the TTR. Through the combination of motion and strain sensors a better understanding of WIO and its effects on fatigue can be gained. Using environmental data gathered from the vessel monitoring system and comparing it to the measured riser response future analytical models can be developed. Fibre optic sensors have gained increasing use in monitoring offshore structures, such as risers flowlines, umbilicals, wells, Tension Leg Platform (TLP) tendons, production and drilling risers, and mooring lines. Fiber optic sensors are capable of monitoring strain, temperature, pressure, and vibration. Eaton *et al.* (2015) details the plausibility of using pressure measurements from post-installed fiber Bragg grating (FBG) sensors with Model Predictive Control (MPC) to suppress severe slugging in subsea risers. Prior control schemes demonstrate that slugging is mitigated using a topside choke valve. The most effective methods use a pressure measurement immediately upstream of the touchdown zone of the riser; however, the majority of production risers do not have pressure sensing at that location. With advances in subsea clamp design and bonding it is now possible to install a non-penetrating FBG sensor to monitor pressure near the touchdown zone without shutting down production. Stabilizing the two-phase flow both reduces vibration-induced fatigue and has the potential to allow for increased throughput with relaxed topside processing constraints. The performance of the controller in reducing disturbances is influenced by sensor location, choke valve response time, and riser geometry. This study demonstrates that severe riser slugging is effectively controlled with MPC and a post-installed, non-penetrating FBG sensor.

In the subsea field, the efficiency of IRM (inspection, repair and maintenance) systems is progressing by development of communication technology with the sensor. The non-insertion type inspection of pipelines based on X-rays has been developed by Ledezma *et al.* (2015) as alternative of the pipeline inspection pig (a device inserted in the pipeline to perform various maintenance operations). In project 'Cage' (Kellner, 2015) General Electric (GE) exploits a smart platform for connecting a large e number of British Petroleum (BP) subsea wells to get information about vibrations, temperature, pressure. The implemented monitoring system is aimed to detect real-time abnormalities and to provide big data for improving performances and production.

4.1.2 Structural identification

Structural identification aims to validate or update mathematical models of structures using measurement results obtained from tests or full-scale trials. In daily practice structural identification involves also the assessment of test rigs and typically identification techniques are first verified at model-scale before being applied at full-scale. A related topic is structural health monitoring (SHM), which is also covered in the report of Committee V.7 (Structural Longevity).

Material properties
A FEM analysis of collision or grounding requires proper modelling of the material behaviour. The metal exhibits complex behaviour during a collision or grounding, involving triaxiality and "elemental" volume changes. Because there are very few studies on the influences of triaxiality

as traditionally, the strain-stress relationship of a metal is often defined based on uni-axial tensile tests. Many authors believe that strain rate, temperature and triaxiality have major influences on the simulation of collision or grounding events. Tests were conducted to steels (2W50, EH36, DH36) to various strain rates (0.001/s-200/s), at different temperatures (-40°C to +180°C) (Choung *et al.*, 2013), or at different triaxialities (Choung *et al.*, 2012). Recommendations were then made to change the Cowper-Symonds parameters. Kubiczek *et al.* (2017) used a high-speed camera to "measure" the strain field in the metal. They converted the measured load-end shortening curve into the stress-strain relationship with the assistance of a FEM analysis. Calle *et al.* (2017a) also adopted this hybrid experimental-numerical method in obtaining the stress-strain curves from experimentally obtained strain data. They tested different shell elements with a premise that the best element types would have the minimal differences between the calculated stress-strain curves and the measured force displacement curves.
Many FEM analyses treat ice as a unique material whose characteristics are defined based on either model tests or field measurements. Von Bock und Pollach and Ehlers (2017) developed an experimental technique to assess the material properties of the ice sheet in an ice basin. It is well acknowledged that scaling ice made in an ice basin to reproduce winter sea ice (see Section 3.4 for further details) remains a major technical challenge.

Dynamical structural properties
Structural identification of dynamical systems in engineering practice narrows the broader scope of system identification which aims to build mathematical models based on measured data. First attempts to use Fourier analysis, Auto-regressive Moving Average (ARMA), Maximum Entrophy Method (MEM) and Random Decrement Technique (RDT) for system identification of offshore platforms dated back to the seventies and eighties, in parallel to similar applications in civil engineering. From the nineties onwards, the system identification of ship and offshore structures benefited of the development of output-only methods for modal analysis which avoid the measurement of excitation.

Coppotelli *et al.* (2008) carried out a systematic identification of `wet' mode shapes and related modal parameters (frequency and damping) of a scaled ship model. They analysed the acceleration data using Frequency Domain Decomposition. Later, Mariani and Dessi (2012) used a tailored version of the Proper Orthogonal Decomposition on both acceleration and strain data. In both cases the required broadband excitation in the frequency range of interest was provided by the continuous wave loads. In Kim *et al.* (2016c) the identification of mode shapes is extended from bending to torsional modes using rosette type strain-gage measurements in five sections along the backbone of a 6-segments scaled model of a 10,000 TEU containership. The implemented POD technique for mode extraction follows that developed by Mariani and Dessi (2012) whilst the damping estimation is based on the linear decrement technique applied on a decay curve obtained from the random decrement technique. It is worth to recall that for a floating structure the concept of linear damping is an abstraction hard to verify in real-life, structural damping coexists with hydrodynamic damping, and relevant uncertainties on the results are present as shown also in Dessi *et al.* (2016, 2017a) for floating structures. The use of turbulent boundary layer excitation for extracting the modal parameters on plates wetted on one side was considered in Dessi and Faiella (2015) where specific attention was devoted to the possible change of the modal properties (frequency, damping and consequently added mass) with respect to the flow velocity. The plate was mounted on the bottom of a rigid ship model that underwent captive tests in the towing-tank. The adequate numerical representation of the real boundary conditions was one key issue in profitably comparing with theory and interpreting the experimental data, as also shown in the case of a similar full-scale application for the SILENV project. A method specifically developed for the identification of less excited modes in high-level, noisy, measured data from offshore structures is presented in Liu *et al.* (2016) and its effectiveness is compared with similar approaches like the Eigensystem Realization Algo-

rithm (ERA) and the Stochastic Subspace Identification (SSI) methods with respect to numerical cases. Its application to real cases has concerned two distinct offshore platforms under different excitations provided by ice and waves, respectively. At full-scale, using the FDD technique, Swartz *et al.* (2012) identified the low-frequency wet modes (along with the relative frequency and damping) of the Sea-Fighter catamaran with acceleration measurements collected from wireless sensor nodes. These mode shapes were used as reference for the design of the hydroelastically scaled model of the same catamaran in Dessi *et al.* (2017a), who applied input/output and output-only modal identification techniques along with DIC measurements to verify the effectiveness of the structural scaling of the catamaran.

4.2 Application of experimentation, inspection and monitoring

4.2.1 Design

An effective design is required to ensure the structural integrity of marine structures. Continuous monitoring and periodic inspections may contribute to improve the design accuracy by reducing the uncertainties on the expected loads and on the structural strength of the real structure. Storhaug and Haraide (2013) showed the results relative to hull monitoring measurements for a large containership. The owner/operator observed wave-induced vibrations (whipping/springing) via the hull monitoring system installed on-board. After a few years of measurements, the data was sent to DNV for assessment of the effect of vibrations and then to learn lessons about the design. The collected data show that the vessel was trading in more demanding areas than those (North Atlantic) assumed in design. The measured fatigue life based on a stress concentration factor of 2.0 was estimated to be well above the design life, implying that special attention to cracks should be seriously considered for future vessel operations even if no cracks had been identified so far during inspection. The vessel experienced two severe storms exceeding the rule of thumb value of 20% increase of loading level due to whipping. The measured wave bending moment (excluding whipping) also exceeded the long-term value specified by IACS URS11. The ultimate hull girder strength was calculated and compared with the combination of measured wave-induced bending moment and allowable (maximum) still water bending moment. If the maximum whipping moment is assumed, the safety margin of the hull girder bending strength is found to be below 1.0 for the original design, but keeps above for the strengthened vessel.
Drummen *et al.* (2008) carried out an experimental and numerical study of wave-induced fatigue damage in a containership which advances at a constant forward speed in irregular head waves. The model tests showed that the damage due to wave-induced vibrations made up approximately 40% of the total damage, and that this percentage slightly increased from bow to stern. The high-frequency contribution could be slightly smaller at full scale due to a larger damping. The main contribution to the high-frequency damage came from the two-node mode of hull vibration, while the other modes contributed less than 5% of the damage. The damage in the fore hull sections was negligible compared with the damage in the midships sections, while the damage in the aft sections was about 25% of this value. The largest contribution to the fatigue damage occurred in sea states with a peak period of around 14 s and a significant wave height of 5 m or above. Relatively to the investigated sea states, the experimental results indicated that the nonlinear effects on the wave frequency stress were mainly important in the forward cut, while they affected the high-frequency stress in all three cuts.

4.2.2 Construction

Since ship and offshore structures are huge welded structures, quality control of the assembling process under construction is very important. In recent years, 3D measurement technology has been applied to verify the final accuracy of the welded structures under construction and is more specifically introduced in Section 7.1. In this section some applications of 3D measurement are illustrated. The first one concerns the measurement method of welding deformation/strain to calculate the weld-induced residual stress. Shibahara (2012) used DIC technique developed

measuring both in-plane and out-of-plane deformations induced by weld. The stereo imaging method using two digital cameras has a high measurement accuracy and does not require calibration of the errors caused by the out-of-plane displacement. He demonstrated the measurement accuracy through a bead-on-plate welding test. The proposed method can measure transverse shrinkage and angular distortion with a high accuracy. This inherent strain data was then used as input for the simulation of welding deformation of large structure. The second application is aimed to assist the plate bending process. Sun and Hiekata (2014a,b) evaluated the accuracy of laser scanners in measuring the plate bending work. The evaluation process of the construction accuracy for curved shells and plates suffers from the lack of quantitative criteria, and heavily depends on implicit knowledge, that is, the skill and expertise of the workers. The shape of the objects is represented as cloud data points. In this system, cloud data points and design data are registered and displacement errors and evaluated and visualized by colour maps and histograms. In addition, Hiekata *et al.* (2016) visualized the result of evaluation by using the projection mapping. The output of the system was collectively projected on the curved shell and the difference with CAD shape was visualized. Matsuo *et al.* (2015) developed AR (Augmented Reality) application system to support shell metal forming by pressing or heating. The former AR application guide workers where and how to perform press work or gas heating work for getting the intended shape.

4.2.3 Operation, Inspection, Monitoring and Maintenance

The offshore oil and gas industry has accepted Risk-Based Inspection (RBI) as a rational way to carry out inspection, maintenance and repair for hull, topside, morning systems. Guidance on best practice of RBI has been published by API (2016a,b), ABS (2003), DNV (2010), LR (2010), and is covered by other ISSC committees.

Most of RBI programs relies on traditional means of inspection, mostly via human eyes. Some progressive operators/owners apply structural health monitoring techniques in some areas. Monitoring is considered viable especially for areas difficult or costly to access. The FPSO Joint Industrial Project (JIP) on Life Cycle Management Hull attempted to layout a framework for incorporating health monitoring into a FPSO's RBI scheme. This JIP (LMS, 2015) has a focus on monitoring corrosion and fatigue cracking, assessing their risks to the life-time structural integrity of FPSO, and planning and implementing inspection, repair, and maintenance accordingly. There is an apparent technological shift in industry, leveraging real-time monitoring to help owners and operators better understand the health of their assets and guide their maintenance and repair decisions.

A notable industrial project on health monitoring is MONITAS (Aalberts *et al.*, 2010), which has been extensively covered by ISSC over time. Tammer and Kaminski (2013) reviewed the methodology of the Risk Based Inspection (RBI) scheme and its application for safeguarding hull integrity of offshore floating structures, with fatigue as a primary degradation mechanism. The work has a distinct focus on the opportunities that RBI offers in combination with Structural Health Monitoring. To provide a clear picture of the state of the art knowledge, the current practices and regulations are briefly discussed after which the RBI methodology is introduced, the differences in guidelines and applications discussed and an 8-step approach is proposed. Subsequently, the methodology is outlined as an instrument for determining the residual fatigue life with the alternative inspection scope and schedule was discussed and within a framework specified in an Advisory Hull Monitoring System.

Increasingly, industrial guidance has become available to guide applying monitoring technologies. An example is the recently published *ABS Guidance Notes on Structural Monitoring Using Acoustic Emissions* (ABS, 2016). This guidance presents best practices for planning and executing Acoustic Emission Testing (AET), and has been built upon a series of at-sea tests on board tankers and containerships. Another example is the CCS Rules on Autonomous ship guidance (CCS (2015)). These Rules clearly include structural health monitoring a crucial part

of the future smart/intelligent shipping, and has specified in great details about how to plan hull monitoring, what frequency must be used for sensors, and how to interact with regulatory bodies. Generally, it is believed that we will see increased interest in R&D and application of health monitoring together with the supporting technologies such as sensoring, communication, data processing and decision-making (smart functions).

5. CORRELATION ISSUES BETWEEN SCALED (PHYSICAL) MODELS, FULL-SCALE STRUCTURES (SHIP AND OFFSHORE) AND NUMERICAL SIMULATIONS

5.1 Scaling laws

Scaling laws have been used in naval architecture since the foundation of dedicated experimental facilities like towing-tanks. Reynolds and Froude similarities have typically allowed for predicting the resistance and seakeeping behaviour of ships at full-scale. Later on hydroelastic scaling for ship structures have been based on an extended application of the Froude similarity; the ratio between the ship and the model scale values of several physical parameters (frequency, bending stiffness, shear area...) is expressed in terms of powers or fractional powers of the scale factor. A more cumbersome hydroelastic scaling with respect to vortex-induced vibration (VIV) tests where the investigation of the lock-in phenomenon implies that the structural frequency of the bluff-body oscillations falls close to the Strouhal frequency, which in turn depends also on the Reynolds number.

Recently, new advancements in the definition of scaling laws with respect to some specific structural problems, including; fatigue, collision and grounding, already mentioned in the specific sections. Kong *et al.* (2017) investigated the strain-rate effect of blast loaded plates by using dimensional analysis and analytical equations with emphasis on engineering calculations which need to be fast and robust. In addition, an empirical formula was developed to assess the equivalent stand-off distance, mass of TNT and impulse per unit area. A fundamental contribution concerning the scaling issues of ship collision and grounding, an extremely nonlinear phenomenon, is given by Pedersen and Zhang (2000) who reviewed the ship-size effect in relation to resulting damages. Although the focus in this research was on the ships with similar order of magnitude in size, the equations derived in the paper serve as background information for the scaling rules in ship grounding and collisions. However, when the level of fidelity is increased to account structural details, strain rate and plate thickness effects, the scaling issues become very complex; as discussed separately under the collision and grounding section. In this respect, the work of Oshiro *et al.* (2017) shows that traditionally used LMT-scaling (length, mass, time) should be replaced by VSG-m-scaling (velocity, stress, impact mass) when dynamic problems of ship collisions are concerned. This recommendation was based on tests on dry models where effects of moving cargo and hydrodynamics are neglected, and the focus is purely on structural responses. It is also highlighted that even though geometrical similitude could be kept, the nominally identical materials do not give the same results when the scale is changed. This is due to processing of the steel sheets and the fact that the similar microstructure through the thickness is very difficult to keep as it is within distortion tolerances after manufacturing. The recent review on structural testing by Coutinho *et al.* (2016) gives a comprehensive overview of needed viewpoints when new similarities are to be formed. The review covers dimensional analysis, differential equations and their combinations as well as the use of energetic methods. It also reviews the major areas of current research in the structural mechanics community including impacting structures, rapid prototyping and size effects on brittle, quasi-brittle and ductile materials.

In terms of motions and related loads, the paper by Lupton and Langley (2017) discusses the importance of the platform size on slow drift motion. It is claimed that the fact that in some

cases the second-order slow drift response is smaller than the first order motion; while in another case this is larger due to scale effects of the floating structures. An expression is derived which approximates the scaling of slow drift motion, platform size and wave conditions. The investigation by Lau and Kelso (2016) presented a scaling law for the time-averaged thrust on submerged heaving and pitching fish-inspired hydrofoils. The Strouhal number *St* was used as a scaling parameter and successfully validated the scaling law by varying several experimental parameters, including; the non-dimensional heave amplitude (0.1,1), the pitch amplitude (0°, 45°), the Strouhal number (0.1, 0.95) and the Reynolds number in the range 1500-12500. In cases where the non-dimensional heave amplitude is large in relation to the pitch amplitude, the experimental results deviate from the scaling law.

5.2 Model to full-scale investigation

The scaling laws considered in Section 5.1 address the problem of correlating model and full-scale tests. For instance, the full-scale correlation of the ship resistance measured over a physical model in the towing-tank has been traditionally one of the main problems addressed and continuously revised by ITTC to set precisely the required onboard power for a target speed. When more complex measurements like those related to structural variables are considered, the correlation between model and full-scale is not only a matter of similitude because of the physical objects, the test conditions and the measuring techniques may significantly differ. Here some illustrative examples of correlation efforts are reported.

The problem of extrapolating model-test data to full-scale for new ship designs (which lacks proven procedures) was considered in the Ship Structure Committee report in 1972 in relation to the S.S. Volverine State and S.S. California Bears. The main objective was the prediction of the bending moment long-term distribution based on model-test data and ocean wave spectra. A detailed analysis of acceptable comparison factors to be checked was carried out and a procedure for estimating the full-scale trends from model test was successfully established. In general, it appeared that predictions of long-term trends are satisfactory when adequate ocean wave data in spectral form are available for model tests. In Dessi *et al*. (2009) the correlation of the vertical bending moment (VBM) between full-scale trials and scaled-model tests was carried out in terms of the response amplitude operator (RAO) at approximately one quarter length from the ship bow. If the ship response is almost in the linear regime (up to a certain wave elevation), the comparison in terms of the RAO allows for accepting similar but not identical encountered wave spectra with the same relative wave direction. An analysis of possible error sources was carried out to explain differences in some frequency ranges. The correlation between model and full-scale measurements becomes elaborate when nonlinear phenomena such as springing and whipping occur. In Storhaug *et al.* (2009) the focus was on estimating the effect of whipping on extreme loading to verify the IACS UR S11 rule which turned out in revising the rule and increasing the requirements.

An interesting correlation study concerning cargo sloshing of LNG tanker tanks was carried out in the frame of a Joint Industry Project (JIP) with BW Gas, Teekay, DSME, Lloyd's Register, DNV, Light Structures and GTT (Pasquier and Berthon, 2012). A first comparison of sloshing impact recordings at full-scale and at model-scale was performed. For the model tests, the actual ship motions recorded at sea have been used as inputs for the simulation platform. This allows a direct comparison of full scale and model tests results without the bias induced by the use of numerical sea-keeping analysis to produce tank motions. The results of the model tests at 1:40 scale have shown a good correlation with full-scale measurements. The trend in terms of impact frequency over several days of navigation has been found fairly consistent. A comparison between the measurements in both instrumented tank corners was also found to be fairly consistent. This tends to confirm that experimental simulations of LNG sloshing at the small scale provides a correct representation of the global flow inside tanks; as expected according to theory.

5.3 Integration of experiments and numerical simulations

Individual research advances in the last decade such as high-fidelity numerical models utilizing high-performance computing, large-scale laboratory experimentation, field testing and real-time monitoring have undoubtedly increased our level of understanding of the behaviour of ships and offshore structures. In some cases, these advances are effectively harnessed in a manner that leverages all relevant developments and translates them into predictive tools that can be directly used by stakeholders that mean to improve the performance of ships and offshore structures.

Three main categories of analysis methods of ships and offshore structures exist, namely, (a) computational models (numerical simulations) based on a specific method (*e.g.,* Finite Element Method, Computational Fluid Dynamics, Smoothed-Particles Hydrodynamics, analytical, mathematical), (b) physical models that are built in a specific scale and are tested in basins, flumes or real sea, and (c) measured data analysis for the estimation of the 'health' of a structure as well as for the prediction of the future status of it. The combined use and integration of the three main categories can result in cost-effective design and construction of modern ships and offshore structures, improvement of existing ships and offshore structures as well as proactive management during their life-cycle. The required integration should focus on emphasizing the strengths and balancing their individual drawbacks. Different approach types (*e.g.*, straightforward or in-loop) for the integration are met for ships and offshore structures.

Regarding methods for prediction of future responses based on a structural health monitoring (SHM) system, Kvåle and Øiseth (2017) present a monitoring system that is designed and installed on the Ber gsøysund Bridge; measurements are used for the numerical estimation of extreme response of the offshore structure. Mondoro *et al.* (2016) present a methodology for using the Structural Health Monitoring (SHM) data recorded in observed operational cells to predict the structural response of ship hulls in unobserved cells. The approach integrates SHM data from sea keeping trials and numerical simulation in order to quantify and reduce uncertainties in the prediction of structural response. The proposed methodology fits SHM data with generalized fitting functions and then estimates the response in unobserved cells (*i.e.*, different operating conditions). The approach predicts the power spectral density (PSD) and the time domain response in unobserved cells and is capable of developing a full set of data to enable spectral and time-based fatigue life estimation approaches. Wang *et al.* (2014) propose a novel method of sub structural identification and genetic algorithms that can be applied to jack-up platforms. With this method, system identification of offshore structures with unknown wave loading, initial conditions and foundation conditions, is achieved. The proposed method is validated with numerical simulations and experimental data. Decò and Frangopol (2015) develop a risk-informed approach for ship structures that integrates SHM information for estimating real-time optimal short-range routing of ships. Risk is based on the reliability analysis of the midship section of a hull and on its associated failure consequences. Based on monitored time series, a numerical approach named Modified Endurance Wave Analysis (MEWA) is presented by Diznab *et al.* (2014) for accurate estimation of the structural performance of an offshore jacket considering the random and probabilistic nature of wave loading and utilizing optimal time duration. With regard to damage identification, Hosseinlou and Mojtahedi (2016) develop a robust simplified method for structural integrity monitoring of offshore platform structures. They provide a useful damage diagnosis process by introducing the pseudo simplified (PS) model technique and successfully acquired damage indicators by using PS baseline FE model based on monitored data. Moreover, the sensitivity of the damage diagnosis algorithm resulting from the removal of some available sensors is examined.

With regard to structural model updating based on SHM data, Wang *et al.* (2015) summarize a new approach and experimentally validate this approach on a small-scale platform model when only a few lower-order spatially incomplete modes are measured. To handle the spatially incomplete mode shapes, an interpolation mode expansion technique based on the optimal fitting

method is used. With this mode expansion method, the number of sensors, the measurement of degrees of freedom, has no distinct effect on the structural model updating of the deck mass. For the completion of missing measured monitored data (both of structural responses of a floating structure and environmental data) of a SHM system, Panapakidis *et al.* (2016, 2017) integrated clustering techniques and data analysis to establish a system identification scheme. With regards to control methods Kandasamy *et al.* (2016) provide information about hybrid vibration control methods that use monitored data and numerical analysis methods. They emphasize that hybrid vibration control methods provide more practical approaches for implementation.

SHM systems can be used for the uncertainty assessment integrated with numerical models. Aldous *et al.* (2015) propose and describe the development of a rigorous and robust method for assessing the uncertainty in ship performance quantifications. The method has been employed to understand the uncertainty in estimated trends of ship performance resulting in the use of different types of data (continuous monitoring) and different ways in which that data is collected and processed. Wu *et al.* (2016) presented an integrated monitoring system of FPSOs with soft yoke mooring systems capable for a safety assessment of the offshore structure.

A complete integration between numerical simulations, physical model tests and monitored data is presented by Yi (2016); a local damage detection approach for jacket-type offshore structures by principal component analysis (PCA) and linear adaptive filter (LAF) techniques using FBG sensors is proposed based on a statistical approach. In addition, environmental effects due to variations in temperature and external loading were investigated. The technical feasibility of the proposed method for damage detection and localization is experimentally validated against physical model tests. Apart from the integration of the analysis methods, integration can be applied for the numerical simulation of wave transformation in the nearshore. Integration between real measurements and numerical analysis may lead to decrease of scale effects.

It is common that new design tools are validated against experimental data with some recent examples mentioned in the following. Azcona *et al.* (2017) developed a code for the analysis of mooring lines that was validated against experimental data for static and dynamic conditions. Lugni *et al.* (2015) developed a combined experimental and numerical investigation on the occurrence of parametric roll and water on deck in bow-sea regular waves close to head sea for an FPSO ship, with a focus on the roll instability phenomenon. Very common linear and nonlinear damping coefficients of different rigid body motions are calculated with the use of experiments and used in integrated numerical analysis models (Irkal *et al.*, (2016); Nematbakhsh *et al.*, 2015). Zhao *et al.* (2014) proposed an integrated simulation model of a side-by-side moored Floating Liquefied Natural Gas and Liquefied Natural Gas carrier system that is calibrated with physical model tests for offloading operation.

Wave tank testing of scaled models is standard practice mainly for the validation of the dynamics of conceptual designs. For some types of offshore structures and ships, Froude-Reynolds scaling laws conflict when they are applied simultaneously (*e.g.* for the testing of offshore wind turbines). Also, for some types of structures or ships, the effect and the induced loads of mechanical mechanisms (*e.g.*, rotor nacelle assembly) that are part of the overall structure should be accounted for during the implementation of the tests. Sauder *et al.* (2016) presented a method for performing Real-Time Hybrid Model testing (ReaTHM testing) of a floating wind turbine. In ReaTHM testing, one part of the system is modelled physically, while the other part, whose behaviour is assumed to be well described theoretically, is modelled numerically. Both physical and numerical substructures interact in real-time through a network of sensors and actuators. As a result, the testing of the floating wind turbine is permitted in a basin without a real wind generation system. Azcona *et al.* (2014) proposed a new methodology for the scaling of aerodynamic loading during combined wave and wind scaled tests at a wave tank with the use of a

ducted fan governed by a real-time computation of the full rotor coupled with the platform motions during the test. The methodology has been applied to the test of a 6MW semisubmersible floating wind turbine. Bracco *et al.* (2015) developed a test rig for dry testing on the ISWEC to reproduce the rated conditions of the 1:8 ISWEC prototype. The test rig was designed to reproduce the pitching angle given a time history recorded in the wave tank tests (Feed-Through mode). A Hardware-In-the-Loop simulation is achieved since the configuration of the Power Take-Off of the ISWEC has been manufactured and mounted on a test rig that is able to simulate the wave actions on the hull of ISWEC.

6. BEST PRACTICE AND GUIDELINES

Engineering stress and structural analysis is fundamentally based on material and other structural parameters (*e.g.* stiffness) which are measured either in a laboratory or in the field *e.g.,* structural health monitoring. Clearly, there is no such thing as a one hundred percent accurate measurement as every measurement is subject to some uncertainty. Measurement uncertainties associated with material and structural test results account for the material safety factors applied in structural analysis and design (Bristow and Irving (2007)). Material test uncertainties complicate both the analysis of experimental data and their subsequent use for structural applications. Materials and structural data are imperative for all structural calculations meaning that structural design and integrity assessment of ships and offshore structures are founded upon empirical science. Contemporary structural design methods involve probabilistic risk- / reliability-based methods which in themselves are extremely powerful but also present certain concerns (UK HSE, 2001). These are identified as *"confusion which arises from vague language, ill-defined and inconsistent terminology, and misinterpretation often present in published material on the topic. This is perhaps the main reason for misuse in some applications of the methods."* Therefore, the aim of this section is to address uncertainty in mechanical test measurements and those taken in the field so that materials and structural data can be appropriately reported. An excellent starting point for understanding uncertainty in mechanical testing can be found in Kandil (2000a), Kandil (2000b) and Bell (2001). This begins with the fundamental principal that *"in general no measurement or test is perfect and the imperfections give rise to an error of measurement in the result. Consequently, the result of a measurement is only an approximation to the value of the measurand and is only complete when accompanied by a statement of the uncertainty of that approximation. Indeed, because of measurement uncertainty, a 'true value' can never be known*." The UNCERT series of publications referred to by Kandil (2000a) is an invaluable and detailed resource for this subject area and recommended for further reading. The following sections address developments in Data Uncertainty, Design of Experiments and Quality Standards as relevant to the ship and offshore structures community.

6.1 Data uncertainty

Data can be acquired from a variety of sources but for the purposes here, we will consider data produced from laboratory tests and from measurements/monitored structures and components in the field. The latter is an extremely active area for research with Structural Health Monitoring (SHM) becoming prominent for ships and in particular for new offshore wind structures and the challenge here often can be managing extremely large amounts of data generated (Brennan and de Leeuw, 2008). This study sought to provide a Structural Integrity Monitoring Index or SIMDex which related the "accuracy" or acceptable uncertainty to the manner in which the data would be used, *e.g.*, for low- or high-cycle fatigue.

With respect to uncertainty of measurement, the object of measurement is to determine the value of the measurand, *i.e.*, the specific quantity subject to measurement. A measurement begins with an appropriate specification of the measurand, the generic method of measurement and the specific detailed measurement procedure. The result of a measurement is only an

estimate of the value of the measurand and is only complete when accompanied by a statement of the uncertainty of that estimation. Uncertainty is a quantification of the doubt about the measurement results and it is a good practice in any measurement to evaluate and report the uncertainty associated with test results. There are two categories of uncertainty evaluations (UKAS, 2016):

I. Type A evaluation is made by calculation from a series of repeated observations using statistical methods;

II. Type B evaluation is done using data from calibration certificates, previous measurement data, experience with the behaviour of the measurements, manufacturers' specifications and all other relevant information.

There are many possible sources of uncertainty in testing, which can come from the test instrument, the item being tested, the test procedure, the test environment, the operator skill and the sampling issues (ASTM E8/E8M-16a, 2016). These sources are not necessarily independent as unrecognised systematic effects may exist that cannot be considered but contribute to error. The existence of such effects may sometimes be evident from a re-examination of the results of an inter-laboratory comparison programme. Therefore, the sources can be further elaborated as follows (Salah *et al.*, 2015; UKAS, 2016):

I. Incomplete definition of the test; the requirement is not clearly described, *e.g.* temperature may be given at room temperature;
II. Imperfect realisations of the test procedure; even when the test conditions are clearly defined it may not be possible to produce the required conditions;
III. Sampling – the sample may not be fully repetitive;
IV. Inadequate knowledge of the effects of measurement of environmental conditions of the measurement process; or imperfect measurement of environmental conditions;
V. Personal bias in reading analogue instruments;
VI. Instrument resolution or discrimination threshold, or errors in graduation of a scale;
VII. Values of constants and other parameters used in data evaluations;
VIII. Values assigned to measurement standards (both reference and working) and reference materials;
IX. Changes in the characteristics of or performance of a measuring instrument since the last calibration;
X. Approximations and assumptions incorporated in the measurement method and procedure;
XI. Variations in repeated observations of a measurement value made under apparently identical conditions – such random effects may be caused by, for example, short term fluctuations in the local environment*, e.g.*, temperature, humidity and air pressure, variability in the performance of the tester.

In addition, computer models for post processing and analyzing measurement data are also prone to producing errors and a method proposed by Bayarri *et al.* (2017) is worth examination to ensure computer models are properly validated.

6.2 Design of experiments

Experiments and measurements made can rely upon standard methods. However, for example for offshore structures, non-standard parameters might be investigated using experimental methods. For example, Adedipe *et al.* (2015, 2016) developed an experimental procedure for investigation of cyclic fatigue load frequency on the corrosion fatigue of offshore structural steels. In this example standard compact tension specimens were tested following the relevant

ASTM standard however, no method existed to measure crack length for a specimen in seawater. A compliance method using an electrical resistance strain gauge was devised; the method calibrated against a known approach and an error analysis established.

Roessle and Fatemi (2000) examined strain-controlled fatigue properties of steels and the sensitivity or otherwise with approximations made and Salah *et al.* (2015) reported on uncertainty estimation of mechanical testing properties using sensitivity analysis and stochastic modelling. Sankararaman *et al.* (2011) detailed an uncertainty quantification and model validation of fatigue crack growth prediction.

Experiments can be designed in addition to support design methods. For example, Grell and Laz (2010) applied a probabilistic fatigue life prediction using AFGROW (Air Force GROW, a life prediction software) and accounting for material variability.

Numerous similar examples exist however the increasing development of SHM of real structures in the field have led to renewed interest in the uncertainty of measurements as often sensors and transducers are installed in the field under non-ideal conditions with sometimes the expectation of gaining "laboratory standard" precision. A number of authors have studied various aspect of this issue including Farrar and Warden (2013) proposing a machine learning approach, Guzman and Cheng (2016) sharing experience of the use of statistical date from a monitoring programme on Alpha Ventus (an offshore wind farm in the German sector) and Scheu *et al.* (2017) who examined the influence of statistical uncertainty of component reliability estimations on offshore wind farm availability.

6.3 Quality standards

Standards for testing materials and structural parameters are abundant, however frequently uncertainty is not specified nor quantified. Some useful standards are: ASTM (2016) which describes uncertainty measurement in standard test methods for tension testing of metallic materials; ASTM (2015) which is the Standard Practice for Statistical Analysis of Linear or Linearized Stress-Life (S-N) and Strain-Life (E-N) Fatigue Data; JCGM Standard (2012) which is an evaluation of measurement data setting out the role of measurement uncertainty in conformity assessment.

SHM is a developing practice, Buren *et al.* (2017) published a paper concerning guaranteeing robustness of structural condition monitoring to environmental variability which is concerned with the practical implementation of transducers in a hostile offshore environment. A whole host of offshore wind SHM papers and the uses of measured data have recently emerged. Some of these are: Ioannou *et al.* (2017a, 2017b), Kaufer and Cheng (2014) and a very useful review by Van des Bas and Sanderse (2017) of uncertainty quantification for wind energy applications.

Finally, Hafele *et al.* (2017) describe the efficient fatigue limit state design load sets for jacket substructures considering probability distributions of environmental states, Kim *et al.* (2016) the probabilistic fatigue integrity assessment in multiple crack growth analysis associated with equivalent initial flaw and material variability and Larsen *et al.* (2013) on reducing uncertainty in fatigue life limits of turbine engine alloys.

7. CONTEMPORARY AND EMERGING TECHNIQUES

An important aspect of experimental tests are the measurement techniques used to record the particular data of interest. Each experiment is challenged by the test unit loading, size, sample rate, physical location and test scope. For each test challenge there are existing and emerging technologies to address them. The following sections summarize current and emerging techniques to meet experimental test requirements and address test challenges. An interesting development over the past few years is the reduced sensor size, increased data sample rate and multi-faceted test scopes. When combined, these factors are conceptualized as 'Big Data'; however, one must understand the criteria required before an experimental test can be considered 'Big Data'. The

concept of Big Data has been a buzz word in many industries. A review of 'Big Data' as it applies to marine and offshore structures is provided.

7.1 Overview of current techniques

There are various physical quantity measurement sensing technologies currently developed and applied to structures for different experimental test scales and data measurement requirements. This section summarizes current measurement techniques used to measure displacements (7.1.1), stress & strain (7.1.2), force (7.1.3), pressure (7.1.4), acceleration (7.1.5) and multi-variable measurements, including fibre-optics measurement and digital image correlation (7.1.6).

Table 4: Features of specimen level displacement sensors

Contents	Contact sensor	Non-contact sensor			
		Optical	Eddy current	Ultrasonic	Laser
Measurement object	Solid	Almost all	Metal	Almost all	Almost all
Measurement distance	Short	Normal	Short	Long	Short
Measurement accuracy	High	High	High	Low	High

Table 5: 3D measurement methods (Shinoda and Nagata, 2015)

Type	Method	Accuracy	Work Size	Characteristic	Application Examples
Laser Radiation	Pattern projection method	~ 0.05 mm	Several meters	High precision measurement	Assembly improvement
	Light-section method	~ 0.08 mm	Dozens of meters	Portable measurement	Process improvement of manufacture
	Time-of-flight method	~ 2.00 mm	Several meters	Wide range measurement	Measurement in a house
Digital Photograph	Photometric-stereo method	~0.085mm	Several meters	Inline point measurement	Calibration of construction equipment
	Structure from motion (SfM)	~0.025mm	Several meters	Easy point measurement	Measurement of flatness of sheet-metal
	SfM & MVS (multi-view stereo)	~ 10.00 mm	Several hundred meters	Camera + software Cheap & wide range	Large scale measurement

7.1.1 Displacement measurement

Displacement measurement can be divided into the high accuracy measurement generally used at the specimen level and large-scale level used for monitoring. At the specimen level, displacements are measured using contact and noncontact systems, as reported in Table 4.

At the large-scale level, three dimensional (3D) measuring devices are well suited for measuring displacements. Measurement systems can be classified into the laser irradiation and camera photographing types shown in Table 5 following Shinoda and Nagata (2015); employed to determine the construction position for large structural projects, 3D shape measurement, etc.

7.1.2 Strain/stress measurement

Strain measurement is commonly acquired using electrical resistance strain-gauges and optical methods such as the photoelastic method. In addition to electrical resistance and optical methods, there are various measurement methods applied in accordance with specific test purposes. These are divided into point measurement (point-by-point local measurement) and full field measurement relative to a finite area size. Each feature is summarized in Table 6 and 7.

Table 6: Point strain measurement methods

Method	Measured value	Conversion to Strain/Stress	Measurement Range
Electrical resistance strain gauges	Gauge metal electrical resistance change. Resistance change is converted to voltage using a Wheatstone bridge circuit.	Point Strain By using change of electrical resistance and gauge factor.	Normal type: +/- 2% ε Post yield type: +/- 20% ε (-20 ~ 80 °C)
Displacement meter Contact type Non-contact (laser) type	Change of gauge length.	Point Strain = (change of gauge length) / (gauge length)	Dependent on the resolution of the displacement-meter.
X-ray stress measurement	Change of distance between lattice planes based on crystal diffraction.	Point Stress/Strain using the angle between normal line of lattice plane and that of specimen surface, and the diffraction angle.	Elastic-Plastic stress can be measured.
Neutron diffraction measurement	Change between lattice planes based on crystal diffraction.	Point Stress/Strain. Measures the stress at a deeper location than X-Rays.	Elastic-Plastic stress can be measured.

Table 7: Field strain/stress measurement methods

Method	Measured value	Conversion to Strain/Stress	Measurement Range
Photo-elastic	Stress distribution by the double reflex of polymer material.	Stress distribution (principal stress difference).	It is dependent on the model size.
Moire	Distance between Moire pattern. The grid which were attached to the object surface and reference grid are superimposed optically, and the Moire pattern arises due to deformation of the object.	Strain distribution ε = p / d p: pitch of reference grid d: distance between Moire pattern	Surface of object attached grid; • Geometric Moire = 0.025 ~ 0.05 mm • Moire Interferometry = .001 ~ 0.01 mm
Holographic	Diffracted light field scattered from the object.	Strain distribution (out-of-plane displacement)	Measuring range is small (< several cm Accuracy < 0.1 μm)
Speckle	Movement of the speckle pattern which arises laser beam interference.	Strain distribution	Accuracy < 10 με Measurement time < 10ms
Thermo-elastic	Temperature change accompanying elastic deformation.	Stress distribution Cyclic loading is required.	Dependent on the resolution of the Thermo-viewer.
Stress Paint	State of paint crack on surface of objects: Number and direction of crack.	Maximum strain distribution (principle stress).	Sensitivity is low (700 - 800 με)
Image Correlation	Distance between dots on material surface.	Stress distribution on the surface of object.	It is dependent on the resolution of the CCD camera.

Residual stress can also be measured using some of the techniques listed in Tables 3 and 4. Ficquet *et al.* (2013) presented a classification of various measurement methods for residual stresses based on the measurement depth and the depth of removed material. High accuracy in the residual stress measurement is important for the evaluation of fatigue and buckling strength. Kleiman *et al.* (2012, 2013) developed an ultrasonic computerized complex for the measurement of residual stresses. The average through thickness stresses can be measured using the acoustic-elasticity effect; according to which the velocity of elastic wave propagation in solids is dependent on the mechanical stress. Examples of non-destructive evaluation of stresses are shown in this paper as well as the verification of the method effectiveness. Sotoudeh *et al.* (2013) investigated residual stresses in steel-to-nickel dissimilar joints by using Neutron Diffraction Technique.

7.1.3 Force measurement

There are basically two kinds of load cells to measure forces:

- Strain-gauge (SG) type
- Piezo-electric (piezo) type

The SG-type load cell consists of a transducer element, deformed by the applied force, on which the strain gages are attached. The voltage output signal from the strain gages is related to the applied force. A piezo-electric sensor (crystal piezo electricity sensor) consists of two sets of quartz plates and an electrode foil in the middle. Since the crystal generates an electric charge proportional to the load applied along a specific crystal direction, the strain can be measured via the piezo-electric effect. Using a charge amplifier, the electric charge is converted into a voltage signal related to the applied load. The strain-gauge type sensor has little data drift and is therefore well suited for long-term monitoring applications. On the contrary, the piezo-electric type sensor presents a small amount of drift requiring zeroing before measurements and dedicated processing. In comparison with the strain-gauge type sensor, the piezo crystal element generates an electric charge only when the applied force is changed and the piezo-electric sensor itself has a higher natural frequency; making it well suited for dynamic motion and time-varying force measurement.

7.1.4 Pressure measurement

There are various kinds of pressure sensors used for different measurement conditions, pressure range and sensing material. Due to the bending deformation of the sensor diaphragm in contact with the fluid, pressure can be convertible into other physical quantities such as deformation. In turn, this deformation is transduced into an electrical output like voltage or current depending on the device. Pressure can then be calculated based upon the area of the loaded diaphragm. The most common types of pressure transducers are reported below.

(*i*) *Wheatstone bridge*
The strain-gages connected to a Wheatstone bridge configuration is the most common pressure sensor. This type of sensor can meet the demand of various accuracy, size, strong nature, and cost testing requirements. The bridge base sensor can measure absolute pressure, gauge pressure, and differential pressure in high or low voltage applications. The strain gauges are used for detection of deformation of the pressured diaphragm.

(*ii*) *Electrical capacitance*
The electrical capacitance pressure sensor utilizes the capacitance change between a metal diaphragm and a fixed metal plate. The capacitance between the two metal plates changes with the distance between metal plates resulting from the applied pressure.

(*iii*) *Piezoelectric*
The piezoelectric type sensor uses only the electrical property of the crystal oscillator. The crystal generates an electric charge when deformation takes place. This charge is then converted to a proportional output voltage with the aid of an amplifier. The applied pressure is measured by output voltage. Piezoelectric sensors are sensitive to the influence of shock and vibration.

(*iv*) *Optical fibre*
Optical fibre type sensors can also be used to measure pressure. Wakahara *et al.* (2008) developed the affix-type multipoint pressure sensor by using Fibre Bragg Grating (FBG) technology. In this study, the FBG pressure sensor was affixed to the fore and aft-body surfaces of a model ship during resistance tests. The optical fibre sensor allowed for the measurement of multi-point pressure on curved surfaces of a ship with temperature compensation. The measured pressures were compared with the result of CFD calculations and found that the FBG pressure sensor effectively measured multipoint pressure on the surface of the model ship during resistance tests.

The bridge-based and the piezoelectric type sensors are most commonly used as pressure transducers because of their simple structure and excellent durability. Thus, they are comparatively low cost and well suited for a multi-channel system. Generally, the foil strain gauge is used with high pressure (up to 700 MPa) application. The electric capacity type and the piezoelectric type pressure transducer are generally stable and linear; however, when compared with other pressure sensors, the setup is complicated and can be easily subject to the influence of heat. The piezoelectric type sensor is excellent when the response to pressure change is measured. It is therefore well suited for pressure measurement of fast phenomena, such as explosion problems.

7.1.5 Acceleration measurement

Accelerometers are used to measure the acceleration (velocity change rate) of an object. Accelerometers are classified in Table 8.

Table 8: Acceleration measurement methods.

Method	Frequency	Max. Acceleration (G)	Sensitivity	Principle/Characteristic
Piezoelectric type	~10 kHz	50,000	+/-1~2 %	The piezoelectric acceleration sensor is measuring acceleration using the piezo-electric effect.
Servo type	DC ~ 300 Hz	10	+/-1 %	Since small and high-accuracy measurement is possible, it is used in broad fields such as vibration measurement and seismic observation
Strain gauge type	DC ~ kHz level	1,000	+/-1 %	There are metal type and semiconductor type which use the strain gauge for the relative-displacement detection sensor.
Semiconductor-type	Hz~10 kHz level	20,000	+/-1 %	These use MEMS (Micro Electro Mechanical Systems) technology. • Capacitance type • Piezoresistance type • Thermal detection type

Table 9: Comparison between Optical Sensing Technologies (distances are approximate).

Technologies	Topology	Range	Temperature	Strain	Pressure	Vibration
OTDR	Distributed	< 70 m	Yes	Yes	No	No
ROTDR	Distributed	< 20 km	Yes	No	No	No
BOTDR	Distributed	< 50 km	Yes	Yes	No	No
FBG	Multi-Point	< 50 km	Yes	Yes	Yes	Yes
Fabry-Perot	Single-Point	< 10 km	Yes	Yes	Yes	Yes

7.1.6 Multi-variable measurements

(1) Fibre Optic

The fibre optic sensor has an optical fibre connected to a light source to allow for detection in tight spaces. The fibre optic sensor is available for measuring most physical data such as temperature, strain, pressure, vibration, etc. Since the sensor assembly is constituted from glass, the optical fibre sensor does not require electric supply, shows excellent explosion-proof performance and resistance to thunderbolt and electromagnetic induction noise. A particular feature

of fibre optic sensors is its ability to connect multipoint sensors using one optical fibre. Some typical optical fibre sensors are listed below and summarized in Table 9.

- OTDR (Optical Time Domain reflectometer). The fracture location and bending point of an optical fibre are detectable. Example: Maintenance of fibre optic cable, Falling-stone detection, Watergate opening-and-closing detection.
- ROTDR (Raman Optical Time Domain Reflectometer). The temperature distribution along optical fibre is measured. Example: Temperature monitoring of a power cable, fire detection in a tunnel.
- BOTOR (Brillouin Optical Time Domain Reflectometry). The strain and temperature distribution along optical fibre are measured. Example: Measurement of strain distribution of bridge / large structures, slope failure detection.
- FBG (Fibre Bragg Grating). Distortion, temperature, pressure, etc. are measured using the reflected light of the diffraction grating formed in optical fibre. Application: strain, vibration, displacement, temperature, pressure measurement of the structure.
- Interferometric sensor (Fabry-Perot optical fibre). The interference phenomenon by composition of two waves is extracted. Application: strain, vibration, temperature, pressure, shock strain measurement of the structure, sonar.

(2) *Digital Image Correlation*
Digital Image Correlation (DIC) is a full-field image analysis method based on grey-scale digital images that can determine the contour and displacement field of an object in three dimensions under load. The accuracy of the Digital Image Correlation system with high-speed digital cameras was thoroughly investigated in both field and laboratory conditions by Schmidt *et al.* (2005a). Rigid body panel translation results, conducted in-situ on a test range, matched a calibrated micrometer within 1.09% for 0.1-inch increments from 0.1 to 1.0 inches with greater accuracy for most increments. The dynamic displacements from a bend and release laboratory test closely matched those from a laser interferometer, and strains from the same test matched both strain gauges and calculated values. The worst-case error for dynamic displacement was 1.27 %. The technique is broadly applicable for air blast deformation measurements, crash testing, high strain rate testing, and other dynamic phenomena. Catalanotti (2010) applied the DIC method to measure the crack resistance curves in CT and CC test specimens manufactured using cross-ply CFRP composite laminates. The measurement fields are the basis for the rigorous determination of the surface crack or kink-band tip (in the absence of delamination) location, and for the automatic computation of the J-integral. The comparison between the R-curves obtained in CT specimens using the FE-based post-processing and the DIC-based method indicates that the results are virtually the same and that the DIC method proposed is a valid alternative to measure R-curves associated with longitudinal tensile failure mechanisms in composite materials.

7.2 Novel measurement Techniques

This section concerns the most significant advances made in sensor technology to address sensor size, network configuration and power consumption challenges. More specifically, microelectromechanical systems have reduced sensor size significantly, wireless sensor networks have expanded the scope of sensor applications, and energy harvesting devices on-board sensor systems now support remote sensing capabilities. The following sections provide a summary of microelectromechanical systems, wireless sensor networks and energy harvesting devices.

7.2.1 MEMS

Microelectromechanical systems (MEMS) are sensor systems micro-machined into silicon, glass, ceramics, polymers, titanium or tungsten. MEMS are commonly micro-machined out of silicon due to its affordability and the availability of micro-machining infrastructure within the electronic integrated circuit industry (Maluf *et al.*, 2004)). MEMS machined shape and design

are customized for a particular application to utilize piezoresistive, piezoelectric and thermoelectric effects. Examples of MEMS pressure, accelerometer and angular rate sensors are also reported in Maluf *et al.* (2004). The pressure sensor in Figure 7 utilizes piezoresistors on the N-type (negatively charged silicon) layer to convert the stress in the N-type layer (produced by pressure on the layer) to voltage. The sensitivity of the pressure sensor can be adjusted by the N-type layer thickness and piezoresistor positioning in the areas of highest stress concentration with identical resistance (Maluf *et al.*, 2004). Piezoresistors without identical resistance will result in zero offset and affect the quality of the sensor measurement. The accelerometer shown in Figure 8 also utilizes piezoresistors to convert the acceleration of the MEMS inertial mass to voltage. Acceleration of the MEMS sensor causes the inertial mass to rotate about the hinge, displacing the piezoresistors.

The size and relatively inexpensive cost of MEMS sensors make them an attractive alternative to conventional sensors. Calibration and accuracy of the MEMS sensors is one challenge that may result in poor sensor system performance. The following sections present methods and challenges of MEMS calibration as well as some examples of MEMS application.

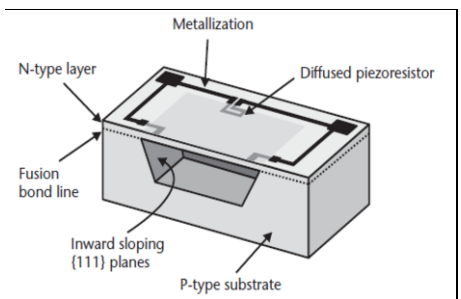

Figure 7: Piezoresistive pressure sensor (400 µm x 800 µm x 150 µm) converting stress in N-type layer to voltage (from Maluf *et al.,* 2004).

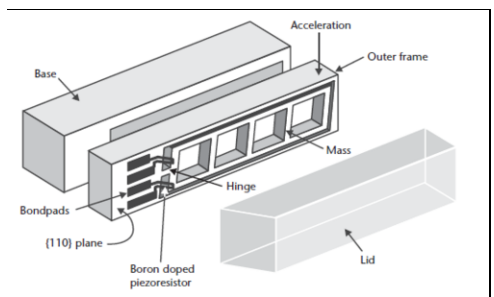

Figure 8: Piezoresistive accelerometer converting inertial mass displacement to voltage through piezoresistors (from Maluf *et al.,* 2004).

(1) *MEMS Sensor Error and Calibration*

One particular application of MEMS sensors is within a navigation aid inertia measurement unit (IMU). An IMU consists of accelerometers and gyroscopes (angular-rate sensors) to measure the position of an object in six degrees of freedom. The accuracy of the IMU gyroscope and accelerometer is important when considering the amount of drift that develops from an accelerometer or gyroscope with bias offset or noise. As such, it is important to verify the MEMS-based IMU is sufficiently accurate for its application. To quantify the accuracy of an IMU, a grade scheme is proposed in (Barbour, 2010) (shown in Table 10) as a function of the MEMS bias stability (bias rate).

Table 10: Navigation IMU grade levels (reproduced from Barbour, 2010).

Application Grade	Commercial	Tactical	Navigation	Strategic	
Gyroscope	> 1 deg/s	~ 1 deg/h	0.01 deg/h	~0.001 deg/h	
Accelerometer	> 50 mg	~ 1 mg	25 µg	~1 µg	

Generally, MEMS inertial sensors are calibrated within the laboratory before deployment into the field. Unfortunately, the installed environmental conditions, age of the sensor and run-to-run biases and thermal drifts are dynamic in nature and require infield calibration (Barbour, 2010). This is especially accurate for low-cost MEMS-based inertial sensors which suffer from large errors due to temperature dependence (Barbour, 2010). The review paper by Barbour (2010) provides an extensive summary of inertial sensor errors and calibration techniques in the laboratory and field.

MEMS-based inertial sensors are subject to deterministic and random classes of errors. Deterministic errors are a result of the system properties or manufacturing defects and removed through calibration (Barbour, 2010). Deterministic errors include:

- Bias: A nonzero output when no load input is applied. Bias is divided into static (offset), dynamic time varying (bias drift) and dynamic temperature varying (temperature drift).
- Scale Factor Error: When the ratio between the rate of change of output to the rate of change of input in is not consistent.
- Non-orthogonality Misalignment Error: The misalignment of the sensor sensitive axis with the platform axis.

Unlike deterministic errors, random errors cannot be corrected through calibration algorithms. Random errors require a stochastic modelling approximation in order to minimize their effect on the system reading. The calibration techniques reviewed in Barbour (2010) are generally categorized as:

- Calibration with High-Precision Equipment: Installing the IMU onto a levelled turntable (single or multi-axial) coupled with specific techniques, Kalman filtering and optimization algorithms to determine the precise inertial sensor error coefficients
- Calibration without Equipment Multiposition-based: Utilizes the Earth's gravity and rotation rate during infield calibration to determine the error coefficient
- Calibration without Equipment Kalman Filter-based: Utilizes Kalman filtering techniques to estimate the navigation state as well as the calibration error coefficient
- Camera-IMU Self-Calibration: IMU self-calibration via joint camera utilizing object shape and motion to estimate calibration parameters

Some of the concluding remarks indicate additional work is required to incorporate nonlinear scale factors, magnetic disturbances and g-dependent bias in the calibration algorithms. When reviewing the different calibration methods within (Barbour, 2010) it is important to consider that the paper focuses on low-cost MEMS. Different grades of IMUs will have different sensitivities and calibration requirements. The following section on MEMS applications highlights several comparisons between conventional and MEMS-based sensor systems. Once the sensor systems were compared they were used on a normal and abnormal motor to detect the associated faults using a wireless sensor system. Test results indicated that low-cost MEMS-based sensors are sufficiently accurate to replace conventional sensors.

(2) *MEMS application examples*

An example of a MEMS application in a harsh environment is the early work of Stauffer (2006). In this paper, the MEMS accelerometer is subject to 10,000 successive shocks of 1,000 g (sensor mounted onto a M16 gun) and remains within the required specification, unfortunately not further clarified. In addition to the extreme shock loads, the MEMS products were demonstrated to fully function from -120ºC to 180ºC. The grade of the MEMS sensors or the specification tolerances are not provided; however, this is a promising example of MEMS applications in harsh environments.

A comparison of MEMS-based accelerometers and current sensors was reported in Son *et al.* (2016) for machinery fault diagnosis applications. Conventional and MEMS-based accelerometers were subject to periodic and impulsive excitation using a calibration exciter and modal

impact hammer, respectively. The MEMS-based accelerometer was consistent with the conventional accelerometer for the frequency excitation; however, some variation was observed in the impulsive test amplitude and wave form. Variations observed in the impulsive excitation were likely a result of difference in mass between the two accelerometers. The paper also evaluated the performance of a MEMS-based current sensor with two conventional current sensors using different magnitudes of 60Hz AC electricity. Test results showed that the MEMS-based sensor had higher noise levels and showed more sensitivity at lower frequencies.

The works by Bryne *et al.* (2016) evaluated two low-cost MEMS IMUs using nonlinear observer (NLO) theory for attitude estimation and virtual vertical reference (VVR) measurement in heave estimation. Performance of the MEMS-based IMUs were compared to measurements by proven sensor systems for marine surface vessels. In the works of Bryne *et al.* (2016) they acknowledge that MEMS sensor errors include: bias, noise (internal and external), nonlinearity, scale factors, cross-coupling and g-sensitivity. It was assumed that the nonlinearity, scale factors, cross-coupling and g-sensitivity sensor error were accounted for by the IMU manufacturer and neglected in this study. An offshore supply vessel operating in the North Sea with a Rolls-Royce Marine dynamic positioning (DP) system was used to evaluate one STIM300 and ADIS16485 MEMS IMU. The MEMS IMUs (and NLO theories) were compared using station keeping with the DP system and manoeuvring over two hours. The study found that the choice of NLO theory has a greater influence on the sensor performance than the IMU. The results of the manoeuvring study found that the attitude estimation of the MEMS IMU was within acceptable limits; however, the heave estimate was 'marginally acceptable'.

7.2.2 WSN

The advent of wireless sensor networks (WSNs) has provided a solution for sensor networks in environments too harsh for or without access to a consistent power source. A WSN consists of sensor nodes to measure, store, process and transmit data wirelessly to a base station(s) which receives, compiles, stores and transmits the sensor data to a server network. Generally, the base station and server network have access to a constant power source with the sensor node relying on its own power source to perform its duty. Some application examples include:

- Railway condition monitoring (Hodge *et al.*, 2015): WSN utilizing fixed MEMS sensors with energy harvesting and mobile base station on the locomotive.
- Animal tracking (Zebranet) (Puccinelli and Haenggi, 2005): WSN using mobile low-power global positioning system with peer-to-peer data swaps for improved database reliability.
- Smart power grid (Fadel *et al.*, 2015): Groups of WSNs to monitor power generation, transmission and consumption.
- Building response to seismic events (Torfs *et al.*, 2013): WSN using MEMS accelerometers and strain gauges with line-of-site linkage with base station.
- Self-healing mine field (Rolader *et al.*, 2004): WSN which uses RF to autonomously reposition mines in an anti-tank mine field.
- Sniper locator (Maroti *et al.*, 2004): WSN utilizing hundreds of sensors to self-localize and use acoustic principals to locate a sniper in an urban multi-path environment.

The performance of the WSN is highly dependent on the capability and reliability of the sensor nodes ability to measure, process, store and transmit data to the base station. The following sections will focus on the sensor to base station layout, protocols, challenges and potential solutions of WSN.

(1) *Sensor Node*
The sensor node is required to perform its specific measurement function as well as process and store the data until it is transmitted to the base station while using a remote power supply. According to Rawat *et al.* (2014), a sensor node consists of:

- Sensor suited for its application,
- Energy source and storage,
- Processor/microcontroller for data manipulation,
- System protocols,
- Memory for data storage, and
- Transceiver to transmit data to the base station.

Some available sensor node examples are IRIS (Memsic (2017a)) and MICAz (Memsic, 2017b), both used in large scale networks (over 1000 nodes) for building monitoring/security to measure high speed acoustic, video and vibration data, IMote2 (Crossbow, 2017), used for condition health, vibration and seismic monitoring and analysis as well as digital image processing, Waspmote (Libelium, 2017), highly customizable sensor node with 120 different sensor applications and 16 different wireless communication interfaces, and WiSMote (WiSMote, 2017), used for measuring temperature, luminosity and acceleration (3-axis). For each sensor node component listed above there are layouts, specialized components and protocols developed to optimize the node and network capability and reliability.

(2) *Sensors*
The low power requirements of WSNs mean MEMS sensors are well suited; however, many applications include traditional sensor devices. A detailed review of sensor types is listed in Section 7.1.

Table 11: Energy consumption of common sensor node platforms (from Shaikh and Zeadally, 2016).

	IRIS	MicaZ	IMote2	Waspmote	WiSMote
Radio Standard	802.15.4/ ZigBee	802.15.4/ZigBee	802.15.4	802.15.4/ZigBee	802.15.4/ZigBee/6LoWPAN
Microcontroller	Atmega1281	ATMEGA128	Marvell PXA271	Atmel Atmega 1281	MSP430F5437
Sleep	8µA	15µA	390µA	55µA	12µA
Processing	8mA	8mA	31-53mA	15mA	2.2mA
Receive	16mA	19.7mA	44mA	30mA	18.5mA
Transmit	15mA	17.4mA	44mA	30 mA	18.5mA
Idle	-	-	-	-	1.6mA
Supply	2.7-3.3V (2x AA Battery)	2.7V (2x AA Battery)	3.2V (3x AAA Battery)	3.4-4.2 V (battery)	2.2-3.6V (2x AA battery)
Average	-	2.8mW	12mW	-	-

(3) *Energy Source/Storage*
Sensor nodes require a remote source of power from either battery, USB or energy harvesting device. Sensor nodes equipped with energy harvesting capability need a converter to convert the energy and store it in a supercapacitor or recharge a battery (Shaikh and Zeadally, 2016). The power requirements of currently available sensor node platforms are listed in Table 11.

Each sensor platform is customizable to the project measurement and transmission requirements. The sample and transmission rates will increase the power requirements of the unit. Therefore, assume the listed power requirements are a minimum for the listed platforms.

(4) *Microcontroller*

Sensor nodes are generally equipped with a microcontroller or processer to manage/compute the data processing as well as store and send data to the base station. The sensor node instructions (sampling, transmission and storage rate and range), updates and protocols are managed by the microcontroller. Sensor node data processing includes data validation (Hodge *et al.*, 2015) by analysing sensor and data status to determine the presence of sensor faults, data noise or null values and minimize communication errors.

Table 12: Summary of WSN standards and technical details (from Rawat *et al.*, 2014).

	Frequency (ISM)	Max Data Rate	Range	Battery Life	Network Topology	Power Consumption	Target Market/Application
IEEE 802.15.4 (ZigBee)	868/915 MHz: 2.4 GHz	250 kbps	100 m	Days-years	Star, P2P, Mesh	Low	Smart-meter, Smart grid devices
UWB IEEE 802.15.4a	3.1-10.6 GHz	110 Mbps	10 m	Multi-year		Low	Real-time monitor and track location (Indoor)
Blue-tooth	2.4 GHz	3 Mbps	10-100 m		P2P	Low	Consumer electronics
BLE	2.4 GHz	1 Mbps	200 m	Months - Years	P2P	Ultra-low	Health fitness, Smart devices
Z-wave	sub - 1 GHz	40 kbps	30 m	Multi-year	Mesh	Low	Home automation, security, consumer electronics
ANT	2.4 GHz	1 Mbps		Year	Star, P2P, Tree, Mesh	Ultra-low	Health Fitness, Heart-rate monitor, Speed sensors
Wavenis	868, 915, 433 MHz	100 kbps	1-4 km	Multi-year	P2P	Ultra-low	M2M, smart meter, Telemetry, Home automation
Dash7	433 MHz	200 kbps	2 km	Multi-year		Low	Mobile payments, Smart meter, Supply chain
EnOcean	868; 315 MHz	125 kbps	300 m	Battery-less		Ultra-low	Building, Industrial automation self-powered sensors, switches.

(5) *Protocols*

The data transmission component of the WSN consumes the most power (Magno *et al.*, 2013). It is therefore important to set the sensor node protocols to minimize data transmission and extend battery life. Protocols are the procedures the WSN follows to optimize the battery life of the sensor nodes and meet the requirements of the application. The following protocol examples from an open system interconnection model (Hodge *et al.*, 2015) consisting of five layers in the protocol stack with data transmission planes:

- Physical layer: Manages how data is transmitted to the network from the sensors.
- Data link layer: Manages the network topology (tree, mesh, etc.)
- Network layer: Manages how the data is transmitted through the data (in data packets for example).

- Transport layer: Manages sending and receiving of data.
- Application layer: Manages software data access.
- Power management plane: Manages sensor node power consumption.
- Mobility management plane: Manages the location of the sensor nodes (especially important in mobile WSNs).
- Task management plane: Manages node groups to ensure power and data generation levels are in line.

(6) *Memory and data transmission*
Data storage volume on board the sensor node is customizable to the application sample rate, data processing and transmission rate. The sensor node may be required to store and process/prepare large volumes of data before the transceiver is able to transmit the data to the base station. Data transmission between the sensor node and the base station is generally transmitted via wireless communication standards such as IEEE 802.11 (WiFi) and IEEE 802.15.4 (short range, low power and low data rate wireless sensor communication) (Rawat *et al.*, 2014). IEEE 802.15.4 specifies the physical and medium access control (MAC) lower layers of the protocol stack. The upper layers of the protocol stack are defined by 6LoWPAN (Montenegro *et al.*, 2007), Zigbee, ISA1001.11a and WirelessHART (Kim *et al.*, 2008). Some examples of emerging wireless technologies include; Bluetooth low energy, ZigBee green power, Wi-Fi direct and EnOcean (Rawat *et al.*, 2014). A technical summary of the WSN standards/technologies are provided in Table 12.

7.2.3 Energy Harvesting Devices

There are many energy harvesting devices that can be used in sensor nodes to support power requirements. Available energy sources include radio frequency (RF), solar, thermal, fluid flow-based, wind, microbial fuel cell (using microorganisms to convert chemical energy to electrical energy) and mechanical-based energy (vibrations, pressure and stress-strain) which utilize electromagnetic, electrostatic and piezoelectric methods to convert the energy to electricity. Each energy source can be harvested and used to charge a battery or supercapacitor or directly power the sensor node (assuming the energy source is constant and regular).

RF-based energy harvesting converts radio waves from a radar or antenna to DC power through a conditioning phase (Kausar *et al.*, 2014). The type of condition and efficiency is dependent on input power range (distance between source and receiver), application requirements, source power and antenna gain. The RF source may be the base station in a WSN, data mule or dedicated source in positions throughout the sensor field when a reliable external power source is available. As the distance between the source and sensor node increases, the converted power decreases. In order to boost the power, the sensor node conditioning phase can include: Multistage Villard Voltage Multiplier circuit, Multistage Dickson Charge Pump, or Multistage Cockcroft-Walton Multiplier (Shaikh and Zeadally, 2016). Examples of RF-based energy harvester are passive radio frequency identification tags used to track animals or near field communications between smartphones.

Solar energy harvesters utilize the photovoltaic effect to convert solar rays to DC power through silicon-based cells. The most effective way of utilizing a solar harvester is by storing the energy in a supercapacitor or battery and using the energy when required (Shaikh and Zeadally, 2016). Similar to the customization of WSN for a particular application, the solar panel size, cell composition and efficiency are also customizable for off-the-shelf sensor nodes. Some challenges with respect to photovoltaic cells are the variability of sunlight and cleaning frequency (Hodge *et al.*, 2015).

Thermal energy harvesters utilize the Seebeck effect to convert the temperature differential across a thermoelectric generator (TEG) to power (Shaikh and Zeadally, 2016). The usability

of thermal harvesters is a balance of the TEG characteristically low efficiency and high reliability. Some examples of thermoelectric harvesters include wearable TEG used in wireless area body networks to monitor physiological parameters. Wearable TEGs use the temperature differential between the room and body to produce approximately 0.026 mW for 36ºC/30ºC temperature differential (Shaikh and Zeadally, 2016).

A comparison between different energy harvesting sources and associated power density are listed in Table 13. By comparing the power density in Table 13 with the average power requirement of the MicaZ node platform in Table 12, one can compute the proportion of the node power supplied by an individual or series of energy harvesters for a particular application.

Table 13: Energy harvesting methods used for WSNs (reproduced from Kausar *et al.*, 2014).

Energy Source	Classification	Power Density	Weakness	Strengths
Solar power	Radiant Energy	100 mW/cm^3	Require exposure to light, low efficiency for indoor devices	Limitless use
RF waves	Radiant Energy	0.02 μW/cm^2 at 5km	Low efficiency for indoor	Limitless use
RF energy	Radiant Energy	40 μW/cm^2 at 10m	Low efficiency for out of line of sight	Limitless use
Body heat	Thermal Energy	60 μW/cm^2 at 5ºC	Available only for high temperature differences	Easy to build using thermocouple
External heat	Thermal Energy	135 μW/cm^2 at 10ºC	Available only for high temperature differences	Easy to build using thermocouple
Body motion	Mechanical Energy	800 μW/cm^3	Dependent on motion	High power density
Blood flow	Mechanical Energy	0.93 W at 100 mmHg	Energy conversion efficiency is low	High power density
Air flow	Mechanical Energy	177 μW/cm^3	Low efficiency for indoor	High power density
Vibration	Mechanical Energy	4 μW/cm^3		High power density
Piezoelectric	Mechanical Energy	50 μJ/N		High power density

7.3 Big-data analysis

The reduction in sensor size, sensor application variability, sample rate and network means that the collected data from experimental tests of health monitoring has the potential to get to Big Data levels. Examples of Big Data volume, veracity, variety and visualization in the literature with respect to marine and offshore structures is limited. The available literature consists of news articles and marketing material for different companies and class societies offering their services in the Big Data space (*e.g.*, Antuit, 2016). The initial goal of this section is to capture the technical details of Big Data applications to marine and offshore structures. Unfortunately, the bulk of the literature pertains to data collection, sorting, storage and retrieval on an electrical or network system level (*e.g.*, Pantelimon *et al.*, 2016; Perner, 2015; Spaho *et al.*, 2015; Simms, 2015; Tan *et al.*, 2016); outside the scope of ISSC. Alternatively, a high-level review of Big Data and its role in the maritime industry is provided.

7.3.1 Values of Big Data as a Technology

Today, Big Data (technology) is considered valuable to address the following challenges in and of data (DNV-GL, 2014; IBM, 2014; Huang *et al.*, 2014; Kambatla *et al.*, 2014; Koga, 2015; Lovoll and Kadal, 2014; Tableau, 2017; Wang, 2017) – Volume, Velocity, Variety, Veracity and Visualization.

- *Volume*
  Volume is the value of Big Data that most believe (Lu *et al.*, 2015). The reality is that most of our maritime data is remotely comparable in size with those in the financial or pharmaceutical industry.

- *Velocity*
  Velocity of data in motion makes data bigger. With the current costs of satellite communication, it is not feasible to "stream" data from a remote offshore rig every single second. Usually, a ship exchanges data onshore via satellites once every two to three hours or a few minutes. This pragmatism slows down the move of the maritime data, and consequentially, prevents our data from becoming "big".
- *Variety*
  It characterizes the daily routines of the brave souls offshore. Sailors steering a powered ship in rough seas rely on a variety of information or data, such as forecast of weather and seas, route and location, vessel speed, fuel consumption, emission, machine health and efficiency, cargo delivery and so on.
- *Veracity*
  Veracity of data is a challenge. Maritime data is inherently associated with uncertainties and flaws. Like all other industries, it is a lasting challenge to deal with data quality (Hazen *et al.*, 2014; Kwon *et al.*, 2014; Lin *et al.*, 2015).
- *Visualization*
  This is an opportunity being explored. Charts, diagrams and dashboards are proven marvels for visualizing insights gained from data analysis. If delivered in a secured cyber space, the modern visualizations would enable faster decision-making that leads to better operational efficiency.

The maritime industry is busy harnessing the technological advantages in Variety, Veracity and Visualization, while keeping an eye on the rising opportunities in Volume and Velocity.

7.3.2 Recent Activities in the Maritime Industry

Activities in development and adoption of Big Data are seen in classification societies, OEMs, in addition to technology start-up companies.

(*i*) *Classification societies*
Classification societies see the importance in data and have identified data as a strategically important area for future shipping industry and class services. The American Bureau of Shipping (ABS) views Big Data as one of the key technologies that support future classification services (ABS, 2015; Howard, 2016). They conducted a Proof of Concept project (Wang and Hu, 2016a) to investigate the feasibility of Big Data for maritime use and the gap in adoption of Big Data technologies. DNV-GL (2017) has launched a new industry data platform – "Veracity" – to help the maritime industry improve its profitability and explore new business models through digitalization. This data platform is designed to help companies improve data quality and manage the ownership, security, sharing and use of data. Lloyd's Register (2014,a,b) describes the importance of Big Data in shipping and offshore oil and gas industries, and listed data management and data analytics as key technologies that the industries will invest in now and in the near future (LR, 2016). Class NK (2015, 2016) established a Ship Data Center with partners of IT companies and Japan's shipping companies. The intent is to collect shipping related data.

(*ii*) *OEMs*
OEMs intend to build technology-driven services for maintenance of equipment and systems. With more and more "smart" products sold, OEMs are trying to capitalize the large volume of data from sensors that are built into their machinery products. Predictive analytics are used more and more to support condition-based maintenance (CBM) and alike to rationalize the maintenance scheme that has been largely age or calendar-based. Big Data as a technology is increasingly integrated into CBM to:

- Extract, move, store data related to machinery condition
- Assess the machine's health and efficiency
- Predict the future condition
- Optimize the maintenance program
- Report for regulatory compliance

A notable example is GE Predix (GE, 2015; Dittrick, 2016), an industrial IoT platform, which is specifically designed for the unique and complex challenges of industrial data. Predix is developed to drive the digital transformation of GE's own businesses across 10 industries. This unique and flexible platform is built with some Big Data technology for managing the entire flow of data.

(*iii*) *Start-ups*

Big Data has been favoured by companies building new services. Some have shown tangible promises. AIS data service deals with vessel tracking data (or AIS data) in a similar way to GPS data and has become free and available to the general public. Some companies have gone one step further - generating operational profiles from many vessel's AIS data (Armstrong, 2013; Mathews, 2016). This leap forward was made possible with Big Data, where AIS data (with inherent uncertainties) are collected and processed at scale and speed. The insights gained from analysis would tell how a vessel is most likely operated, which is a key input to optimization of ship operations and designs. Another example is provided by performance benchmarking. As more organizations adopt performance evaluation schemes in guiding designs and operations, how to quickly gather data from a large pool of vessels is identified as a challenge. Big Data offers tools that meet the required agility in data extracting, transformation and processing. Industrial projects and start-up companies have demonstrated the great potential of Big Data as a cost-effective, agile tool for gathering and aggregating data in different formats from various sources (Tan *et al.*, 2015; Wang and Hu, 2016).

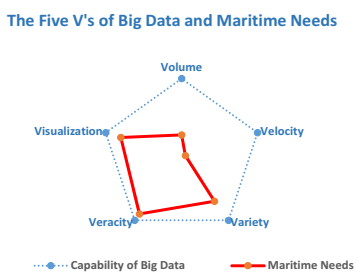

Figure. 9: The power (5 V's) of Big Data to the maritime industry versus its full potential as a technology (Wang, 2017).

7.3.3 Status of Maritime Application of Big Data

Big Data as an IT has advanced to a great level of maturity as Gartner's Hyper Cycle claimed over the last few years (Gartner, 2017). At briefly explained in the last sub-section, the maritime industry is now mostly exploring Big Data with growing expectation (Dugan *et al.*, 2014), and has not yet reached the stage when our industry enjoys the fruits that Big Data as a technology can bring to us (Wang, 2016b).

7.3.4 Future Potentials of R&D

As the industry is increasingly digitized, Big Data and technologies that support data will continue to be a focal point of R&D (Wang *et al.*, 2015; Wang, 2016b). As the maritime industry is still exploring the vast possibilities that Big Data may offer, we can foresee continued interest in research and product development. As always, some areas are promising, and some are yet to prove the values. Expectedly, opportunities of Big Data come from at least the following areas

- Near term potentials are in AIS data, predictive analytics, and performance evaluation.
- Long term potentials are in data management (Hadoop, data lake, data mart, etc.), cybersecurity (ABS, 2016), IoT (Le *et al.*, 2015), autonomous shipping, and alternative inspections.

Worth noting the challenges of Big Data adoption. They come from a variety of angles, from resistance to data sharing, costs of emerging technologies, knowledge and skill gaps, to reluctance to investing in R&D during the current economy with prolonged low oil prices.

7.3.5 Conclusions

Big Data has been a buzz word in the maritime industry for some time. Many have come to realize that the technology will greatly improve how we manage data at scale and how we use data. The industry is undergoing a tremendous change towards digitalization (Aspera, 2017). Emerging technologies such as Big Data will lead to transformation of the maritime industry.

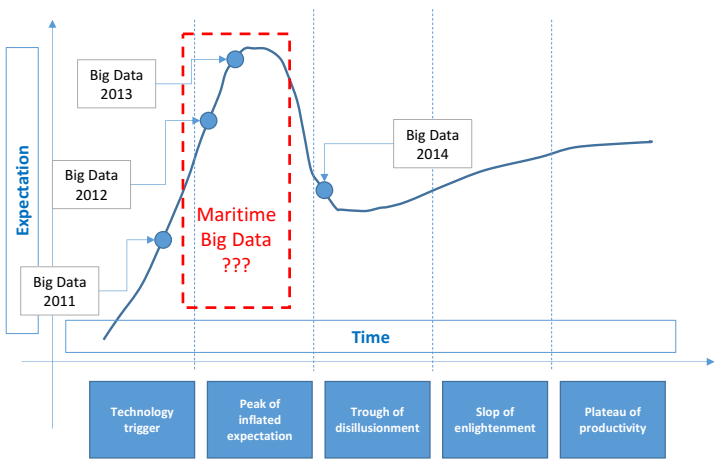

Figure. 10: Big Data as an IT has matured to the stage of "slop of enlightenment", while the maritime industry still views it with great expectations (Wang, 2016).

8. CONCLUSIONS AND RECOMMENDATIONS FOR FUTURE WORK

Following the path set by the mandate, this report has presented in a systematic and orderly manner basic concepts and recent advancements in structural testing related to ship and offshore structures.

Most of the techniques for 'dry' testing of structures at a specimen or component level share a common background with mechanical or civil engineering, and for this reason benefit of well-established approaches coded by standards over time. Notwithstanding these similarities, the importance of accurate experimental investigations supporting design and maintenance of ship and offshore structures is the reason for further improvements of techniques for material testing. As attention moves to 'large scale' (here the expression denotes also the scaled representations

of full-scale structures) or the sea environment becomes part of the experimentation, the peculiarity of the naval constructions emerges, and experimentation must find its own way to address specific issues and needs (welded structures, likely presence of defects, corrosion, testing under water and ice environmental conditions, etc.). Challenges in structural scaling are still ahead and improvements in scaling laws may add more value to certain type of tests in the future.

Miniaturization of sensors as well as the decrease in equipment cost invite us to plan experiments with sensor arrays instead of using just few sensors. As the number of sensor increases, efficient transmission of information becomes critical, and each sensor as a source of data becomes the node of a network. Each node may even provide multiple outputs, integrated or not in the same sensor, or even more complex information as in the case of the fatigue damage sensor (FDS). This concept is at the foundation of the wireless sensor networks, where the concern for cabling issues is reduced to a minimum. Aiming to increase the spatial resolution or to cover a larger domain, field measurements like digital image correlation (DIC) provide a contactless approach to the measurement of deformations and crack propagation. Extending the DIC capability to track dynamical problems and to sense multiple domains (*e.g.*, solid & fluid) is probably the next step but calibration and accuracy requirements of DIC are still a concern. The huge amount of data made available by complex measurement systems, especially if sparse and heterogeneous, fall typically into the 'Big Data' problem. Applications in the maritime field seem promising (monitoring of climate and metocean conditions by means of the ship-buoy concept, optimal routing, SHM of fleets) but data sharing and assessment of data quality are issues requiring further assessment also in ship and offshore engineering.

Another valuable trend is provided by the integration of experiments and numerical simulations. Traditionally, the link has been 'one-way', with data flowing from experiments to the validation of numerical simulations. In the opposite sense, also experimentation often benefits of numerical simulations for the design of experimental setups and for performing a sensitivity analysis to estimate the propagation of experimental uncertainties. Also for Structural Health systems, the cross-flow of experimental, monitoring and design data is essential. Hybrid methods instead pave the way for bi-directional 'coupling' between experimentation and simulations. In this perspective, virtual sensors can be defined expanding numerically the measurement datasets, different sources of information (data fusion) can be mixed, missing physics can be inserted into the experiment by driving dedicated hardware (*e.g.*, as in the hardware-in the-loop approach).

A committee's growing perception has been that full-coverage of the topics related to structural experimentation cannot be achieved without continuing the committee activity; as a leading example, composite materials testing, neglected in this report due to lack of space and specific expertise, call for being prioritized in the next committee mandate. Moreover, selected benchmarks – addressing for instance scaling, test reproducibility, miniaturization and integration of sensors along with new emerging techniques - will undoubtedly provide the opportunity to get a qualified insight into challenging experimental problems and techniques in a more critical way.

REFERENCES

Aalberts P., van der Cammen J., Kaminski M. (2010). The Monitas system for the Glas Dowr FPSO, 2010 Offshore Technology Conference, Houston, TX.

ABS (2003). Guide for surveys using risk-based inspection for the offshore industry, American Bureau of Shipping

ABS (2014). Guide for Fatigue Assessment of Offshore Structures, American Bureau of Shipping.

ABS (2015). Data Analytics: Setting the Foundation for a Data-driven Business http://www.abs-group.com/Knowledge-Center/Insights/Data-Analytics-Setting-the-Foundation-for-a-Datadriven-Business/, American Bureau of Shipping.

ABS (2016). Guidance Notes on Structural Monitoring Using Acoustic Emissions, American Bureau of Shipping.

Achtarides, T. (1979). Wave excited two-node vertical resonant vibration (springing) of flexible ships, Marine Tech.79: Ocean Energy, Marine Tech. Soc.Annual Conf., New Orleans, LA.

Adedipe O., Brennan F., Kolios A. (2015). Corrosion fatigue load frequency sensitivity analysis, Marine Structures, 42, 115-136.

Adedipe O., Brennan F., Kolios A. (2016). Review of corrosion fatigue in offshore structures: present status and challenges in the offshore wind sector, Renewable and Sustainable Energy Reviews, 61, 141-154.

Aggelis D., Kordatos E., Matikas T. (2011). Monitoring of Metal Fatigue Damage using Acoustic Emission and Thermography, Journal of Acoustic Emission, 29, 29-113.

Akai A., Inaba K., Shiozawa D., Sakagami T. (2015). Estimation of fatigue crack initiation location based on dissipated energy measurement, Journal of the Society of Materials Science, 64(8), 668-674.

Aldous L., Smith T., Bucknall R., Thompson P. (2015). Uncertainty analysis in ship performance monitoring, Ocean Engineering, 110, 29-38.

Alsos H. S. (2008). Analysis of Ship Grounding – Assessment of ship damage, fracture and hull girder behaviour, Doctoral Thesis, Norwegian University of Science and Technology.

Alsos H. S., Amdahl J. (2009). On the resistance to penetration of stiffened plates – Part I: Experiment, International Journal of Impact Engineering, 36 (6), 799-807.

Andrieu A., Pineau A., Besson J., Ryckelynck D., Bouziz O. (2012). Beremin model: Methodology and application to the prediction of the Euro toughness data set, Engineering Fracture Mechanics, 95, 102-117.

Antuit (2016). Datalytyx and Antuit to Launch Offshore Big Data Delivery Centre. http://www.antuit.com/about-us/news/datalytyx-and-antuit-to-launch-offshore-big-data-delivery-centre/.

API (2016a). API RP 580, Risk Based Inspection. American Petroleum Institute.

API (2016b). API RP 581, Risk-Based Inspection Technology, American Petroleum Institute.

Armstrong V. (2013). Vessel Optimisation for Low Carbon Shipping, Ocean Engineering, 73, 195-207.

ASTM E1820-17 (2017). Standard Test Method for Measurement of Fracture Toughness.

ASTM E1921-17 (2017). Standard Test Method for Determination of Reference Temperature, T0, for Ferritic Steels in the Transition Range.

ASTM E208-06 (2012). Standard Test Method for Conducting Drop-Weight Test to Determine Nil-Ductility Transition Temperature of Ferritic Steels.

ASTM E23-16b (2016). Standard Test Methods for Notched Bar Impact Testing of Metallic Materials.

ASTM E399-17 (2017). Standard Test Method for Linear-Elastic Plane-Stain Fracture Toughness KIc of Metallic Materials.

ASTM E739-10 (2015). Standard Practice for Statistical Analysis of Linear or Linearized Stress-Life (S-N) and Strain-Life (E-N) Fatigue Data 1. Annual Book of ASTM Standards, (Reapproved), 1-7.

ASTM E8/E8M-16a. (2016). Standard Test Methods for Tension Testing of Metallic Materials.

Azcona J., Bouchotrouch F., González M., Garciandia J., Munduate X., Kelberlau F., Nygaard T.A. (2014). Aerodynamic thrust modelling in wave tank tests of offshore floating wind turbines using a ducted fan, Journal of Physics: Conference Series 524 (2014), 012089.

Azcona J., Munduate X., González L., Nygaard T. (2017). Experimental validation of a dynamic mooring lines code with tension and motion measurements of a submerged chain, Ocean Engineering, 129, 415-427.

Badino A., Borelli, D., Gaggero, T., Rizzuto, E., Schenone, E., (2012). Normative framework for ship noise: present situation and future trends, Noise Control Engineering Journal, 60(6), 740-762.

Banabic D. (2000). Forming limits of sheet metal, Formability of Metallic Materials, D. Banabic, Ed., Springer, Berlin, 173-214.

Barbour N. M. (2010). Inertial Navigation Sensors, NATO report No. RTO-EN-SET-116, Charles Stark Draper Laboratory, Cambridge, MA.

Barsoum F., Suleman J., Korcak A., Hill E. (2009). Acoustic emission monitoring and fatigue life prediction in axially loaded notched steel specimens, Journal of Acoustic Emission, 27, 40-63.

Bayarri M. J., Berger J. O., Paulo R., Sacks J., Cafeo J. A., Cavendish J., Lin C. H., Tu J. (2017). A framework for validation of computer models. Technometrics, 49, 138-154.

Bell, S. (2001). Good practice guide no. 11 Issue 2 - A beginner's guide to uncertainty of measurement, Project UNCERT, NPL, UK.

Bennett S., Brooks C., Winden B., Taunton D., Forrester A., Turnock S., Hudson D. (2014). Measurement of ship hydroelastic response using multiple wireless sensor nodes, Ocean Engineering, 79, 67-80.

Bennet S., Phillips A. (2017). Experimental investigation of the influence of floodwater due to ship grounding on motions and global loads, Ocean Engineering, 130, 49-63.

Benzerga A. A., Leblond, J. B. (2010). Ductile Fracture by Void Growth to Coalescence, Advances in Applied Mechanics, 44, 169-305.

Blekkenhorst R., Ferrari G. M., Van der Wekken C. J., Ijsseling, F.P. (1986). Development of high strength low alloy steels for marine applications, British Corrosion Journal, 21, 163.

Borelli D., GaggeroT., Rizzuto E., Schenone C. (2015). Analysis of noise on board a ship during navigation and manoeuvres, Ocean Engineering 105, 256-269.

Bracco G., Giorcelli E., Mattiazzo G., Orlando V., Raffero M. (2015). Hardware-In-the-Loop test rig for the ISWEC wave energy system, Mechatronics, 25, 11-17.

Brennan F., de Leeuw B. (2008). The use of inspection and monitoring reliability information in criticality and defect assessments of ship and offshore structures, 27th International Conference on Offshore Mechanics and Arctic Engineering, Estoril, Portugal.

Bristow J. W., Irving P. E. (2007). Safety factors in civil aircraft design requirements, Engineering Failure Analysis, 14(3), 459-470.

Bryne T., Rogne R., Fossen T., Johansen T. (2016). Attitude and heave estimation for ships using mems-based inertial measurements, IFAC Conference Paper Archive, 49(23), 568-575.

BS 7448. Fracture mechanics toughness tests, The British Standards Institution.

BS 7910:2013+A1: (2015). Guide to methods for assessing the acceptability of flaws in metallic structures, The British Standards Institution.

BS 8571:2014 (2014). Method of test for determination of fracture toughness in metallic materials using single edge notched tension (SENT) specimens, The British Standards Institution.

Buren K. Van, Reilly J., Neal K., Edwards H., Hemez F. (2017). Guaranteeing robustness of structural condition monitoring to environmental variability. Journal of Sound and Vibration, 386, 134-148.

Calle M., Alves M. (2015). A review-analysis on material failure modeling in ship collision, Ocean Engineering, 106, 20–38.

Calle M., Oshiro R. E., Alves M. (2017a). Ship Collision and Grounding: Scaled Experiments and Numerical Analysis, International Journal of Impact Engineering, 103, 195-210.

Calle M., Verleysen P., Alves M. (2017b). Benchmark study of failure criteria for ship collision modelling using purpose-designed tensile specimen geometries, Marine Structures, 53, 68-85.

Cao Y., Hui H., Wang G., Xuan F. (2011). Inferring the temperature dependence of Beremin cleavage model parameters from the Master Curve, Nuclear Engineering and Design, 241 (1), 39-45.

Cao B. T., Hou B., Li Y. L., Zhao H. (2017). An experimental study on the impact behaviour of multilayer sandwich with corrugated cores, International Journal of Solids and Structures, 109, 35-45.

Carroll, G. P. (2006). Radiated acoustic power of model ship hull sections estimated from scanning laser Doppler vibrometer vibration response measurements, The Journal of the Acoustical Society of America, 119(5).

Catalanotti, C. (2010) Measurement of resistance curves in the longitudinal failure of composites using digital image correlation, Composites Science and Technology, 70, 1986-1993.

CCS (2015). Rules for intelligent ships, China Classification Society.

Cerik B. C., Shin H. K., Cho S. R. (2016). A comparative study on damage assessment of tubular members subjected to mass impact, Marine Structures, 46, 1-29.

Chen Q., Zimmerman T., Deeger D. (1997). Strength and stability testing of stiffened plate components, Ship Structure Committee Report, SSC-339.

Chen Y., Chen F., Zhang W., Du Z. P., Hua H. X. (2016). influence of solid rubber coating on the response of floating structure to underwater shock wave, Journal of Offshore Mechanics and Arctic Engineering, 138(6), 297-307.

Cheng F. (1997). Some results from Lloyd Register's open water model experiments for high speed craft, 4th International Conference on Fast Sea Transportation (FAST97*)*, Sydney, Australia.

Cheng SQ., Chen GJ., Wang SL. (2016). Trial study on dynamic responses of scaled ship model subjected to underwater explosions, Blasting, 32(1), 22-27.

Cho S. R., Song S. U., Park S. H., Shin H. K. (2017). Plastic and fracture damages of double hull structures under lateral collisions, 6th International Conference on Marine Structures, Lisbon, Portugal.

Class NK (2015). Ship Data Center. Nippon Kaiji Kyokai (Japanese Classification Society).

Class NK (2016). ClassNK Awarded Big Data Award at the Lloyd's List Asia Awards, Press Release, Nippon Kaiji Kyokai (Japanese Classification Society).

Choung J., Shim C. S., Song H. C. (2012). Estimation of failure strain of EH36 high strength marine structural steel using average stress triaxiality, Marine Stuctures, 29 (1), 1-21.

Choung J., Nam W., Lee J. Y. (2013). Dynamic hardening behaviours of various marine structural steels considering dependencies on strain rate and temperature, Marine Structures, 32, 49-67.

Coppejans O., Walters C. (2017). determination of parameters for the damage mechanics approach to ductile fracture based on a single fracture mechanics test, 36th International Conference on Ocean, Offshore and Arctic Engineering, Trondheim, Norway.

Coppotelli G., Dessi D., Mariani R., Rimondi M. (2008). Output-only analysis for modal parameters estimation of an elastically scaled ship. Journal of Ship Research, 52(1), 45-56.

Coutinho C.P., Baptista A.J., Rodrigues J.D. (2016). Reduced scale models based on similitude theory: A review up to 2015, Engineering Structures, 119, 81-94.

Crintea A. Moore P. (2016). Ensuring the Strain Capacity in Threaded-End Single Edge Notched Tension (SENT) Specimens, 22nd International Offshore and Polar Engineering Conference, Rhodes, Greece.

Crossbow (2017). Imote2 High-Performance Wireless Sensor Network Node (IPR2400). Document part number: 6020-0117-02 RevA.

Cui P., Zhang A.M., Wang S.P. (2016). Small-charge underwater explosion bubble experiments under various boundary conditions, Physics of fluids, 28(11), 117103.

Decò A., Frangopol D. (2015). Real-time risk of ship structures integrating structural health monitoring data: Application to multi-objective optimal ship routing, Ocean Engineering, 96, 312-329.

Dessi D., Mariani R. (2008). Analysis and prediction of slamming-induced loads of a high-speed monohull in regular waves, Journal of Ship Research, 52(1), 71-86.

Dessi D., De Luca M., Mariani R. (2009). Correlation of model-scale and full-scale analysis of the ship elastic response in waves. International Conference on Hydroelasticity in Marine Technology, Southampton, UK.

Dessi D., Faiella E. (2015). Damping identification of an elastic panel coupled to a fluid: model-scale and full-scale investigations for ships. Conf. on Noise and Vibration Emerging Technologies, Dubrovnik, Croatia.

Dessi D., Faiella E., Geiser J., Alley E., Dukes J. (2016). Design, assessment and testing of a fast catamaran for FSI investigation, 31st Symposium on Naval Hydrodynamics, 11-16 September, Monterey, California.

Dessi D., Faiella E., Geiser J., Alley E., Dukes J. (2017a). Design and structural testing of a physical model for wetdeck slamming analysis, 6th International Conference on Marine Structures, 8-10 May, Lisbon, Portugal.

Dessi D., Faiella E. (2017b). Experimental analysis of the station keeping response of a double-barge float-over system with an elastically scaled physical model, International Ocean and Polar Engineering Conf., San Francisco, CA.

Dittrick, R. (2016) BP, GE launch offshore big-data system starting with Atlantis in gulf, Oil & Gas Journal.

Diznab M., Mohajernassab S., Seif M., Tabeshpour M., Mehdigholi H. (2014). Assessment of offshore structures under extreme wave conditions by Modified Endurance Wave Analysis, Marine Structures, 39, 50-69.

Det Norske Veritas (2010). DNV-OSS-300-3:2010. Risk Based Verification of Offshore Structures. Oslo, Norway.

DNV-GL (2014) Strategic Research and innovation Position Paper 4-2014.

DNV-GL (2015). Fatigue assessment of ship structures, Class Guideline DNVGL-CG-0129.

DNV-GL (2017). Veracity Industry Data Platform.

Dragt R. C., Van den Heuvel W., Gelink E. R. M., Slot H.M. (2015). Testing of full scale composite journal bearings for offshore underwater applications, 34th International Conference on Ocean, Offshore and Arctic Engineering, St. John's, Newfoundland, Canada.

Drummen I., Storhaug G., Moan T. (2008). Experimental and numerical investigation of fatigue damage due to wave-induced vibrations in a containership in head seas, Journal of Marine Science and Technology, 13(4), 428-445.

Dugan P., Zollweg J., Popescu M., Risch D., Glotin H., LeCun Y., Clark. C. (2014). High performance computer acoustic data accelerator: A new system for exploring marine mammal acoustics for big data applications, International Conference on Machine Learning Applications, Bejing, China.

Eaton A., Safdarnejad S., Hedengren J., Moffat K., Hubbell C., Brower D., Brower A. (2015). Post-installed fiber optic pressure sensors on subsea production risers for severe slugging control, 34th International Conference on Ocean, Offshore and Arctic Engineering, St. John's, Newfoundland, Canada.

Ehlers S., Broekhuijsen J., Alsos H. S., Biehl F., Tabri K. (2008). Simulating collision response of ship side structures: a failure criteria benchmark study, International Shipbuilding Progress, 55 (1-2), 127-144.

Ehlers S., Ostby E. (2012a). Increased crashworthiness due to arctic conditions – the influence of sub-zero temperetature, Marine Structures, 28 (1), 86-100.

Ehlers S., Tabri K., Romanoff J., Varsta, P. (2012b). Numerical and experimental investigation on the collision resistance of the X-core structure, Ships and Offshore Structures, 7 (1), 21-29.

Endo H., Yamada Y., Kitamura O., Suzuki K. (2002). Model test on the collapse strength of the buffer bow structures, Marine Structures, 15 (4), 365–81.

Fadel E., Gungor V., Nassef L., Akkari N., Abbas Malik M., Almasri S., Akyildiz I. (2015) A survey on wireless sensor netowrks for smart grid, Computer Communications, 71, 22-33.

Farrar C. R., Warden, K. (2013). Structural health monitoring: a machine learning perspective, Wiley, UK.

Ficquet X., Hossain S., Kingston E. (2013). Residual stresses measurement in various joint welding, 32nd International Conference on Ocean, Offshore and Arctic Engineering, Nantes, France.

Franz von Bock, Polach R. U., Ehlers S., Kujala P. (2013). Model-scale ice — Part A: Experiments, Cold Regions Science and Technology, 94, 74-81

Franz von Bock, Polach R. U., Ehlers S., (2015). on the scalability of model-scale ice experiments, J. Offshore Mech. Arct. Eng., 137(5).

Fras T., Roth C. C., Mohr D. (2017). Fracture of high-strength armor steel under impact loading, International Journal of Impact Engineering, 111, 147-164.

Frazer G., Reagan D., Ruf W., Cheng J. (2011). Top tension riser fatigue monitoring system, 30th International Conference on Ocean, Offshore and Arctic Engineering, Rotterdam, Netherland.

Fricke W., Paetzold H. (2010). Full-scale fatigue tests of ship structures to validate the S–N approaches for fatigue strength assessment, Marine Structures, 23, 115-130.

Gao X., Ruggieri C., Dodds R. H. (1998). Calibration of weibull stress parameter using fracture toughness data, International Journal of Fracture, 92 (2), 175-200.

Gao Y., Fu S., Ma L., Chen Y. (2016). Experimental investigation of the response performance of VIV on a flexible riser with helical strakes, Ships and Offshore Structures, 11(2), 113–128.

Gartner (2017). Hyper Cycle of Emerging Technologies. http://www.gartner.com/technology/research/methodologies/hype-cycle.jsp

GE (2015). Predix – The Premier Industrial Internet Platform Connecting Machines, Intelligence, and People to Drive Operational and Business Outcomes that Matter, https://www.ge.com/digital/predix.

Getter D. J., Kantrales G. C., Consolazio G. R., Eudy S., Fallaha S. (2015). Strain rate sensitive steel constitutive models for finite element analysis of vessel-structure impacts, Marine Structures, 44, 171-202.

Gong Y., Gao Y., Xie D., Liu J. (2015). Deflection and fracture of a clamped plate under lateral indentation by a sphere, Ocean Engineering, 103, 21-30.

Gorbatov Y., Tekgoz M., Guedes Soares C. (2017). Experimental and numerical strength assessment of stiffened plates subjected to severe non-uniform corrosion degradation and compressive load, Ship and Offshore Structures, 12(4), 461-473.

Grell, W. A., Laz, P. J. (2010). Probabilistic fatigue life prediction using AFGROW and accounting for material variability, International Journal of Fatigue, 32(7), 1042-1049.

Gruben G., Solvernes S., Berstad T., Morin D., Hopperstad O. S., Langseth, M. (2017). Low-velocity impact behaviour and failure of stiffened steel plates, Marine Structures, 54, 73-91.

Guan S. (2015). Current and future tendency of monitoring technology for integrity assessment and life extension of the hull structure of floating production, storage and offloading (FPSO) vessel, 34th International Conference on Ocean, Offshore and Arctic Engineering, St. John's, Newfoundland, Canada.

Guzman R. F., Cheng P. W. (2016). Recommendations for load validation of an offshore wind turbine with the use of statistical data: experience from alpha ventus, Journal of Physics: Conference Series 749, 012017.

Haag S., Hoogeland, M. G., Vredeveldt, A.W. (2017). Grounding damage estimate through acceleration measurements, 36th International Conference on Ocean, Offshore and Arctic Engineering, San Francisco, CA.

Hafele J., Hi C., Gebhardt C. G., Rolfes R. (2017). Efficient fatigue limit state design load sets for jacket substructures considering probability distributions of environmental states, 27th International Ocean and Polar Engineering Conference, San Francisco, California, USA.

Halswell P. K., Wilson P. A., Taunton D. J., Austen S. (2016). An experimental investigation into whole body vibration generated during the hydroelastic slamming of a high-speed craft during the hydroelastic slamming of a high speed craft, Ocean Engineering, 126, 115-128.

Hara T., Fujishiro T. (2010). Effect of separation on ductile crack propagation behavior during drop weight tear test, 8th International Pipeline Conference, Calgary, Alberta, Canada.

Hashimoto K., Fujino M., Motora S. (1978). On the wave induced ship-hull vibration springing caused by higher-order exciting force, J. of the Soc. of Naval Arch. of Japan, 144, 183–194. Written in japanese.

Hauge M., Walters C. L., Zanfir C., Maier M., Ostby E., Kordonets S. M., Osvoll H. (2015). Status Update of ISO TC67/SC8/WG5: Materials for Arctic Applications, 25th International Ocean and Polar Engineering Conference, Kona, Big Island, Hawaii, USA.

Hazen B., Boone C., Ezell, J., Jones-Farmer A. (2014). Data quality for data science, predictive analytics, and big data in supply chain management: an introduction to the problem and suggestions for research and applications, International Journal of Production Economics, 154, 72-80.

Hermundstad O., Aarsnes J., Moan T. (1994). Hydroelastic response analysis of high speed monohull, 1st Conference on Hydroelasticity in Marine Tech., NTNU, Trondheim, Norway, 245–259.

Heshmati M., Zamani A. J., Mozafari A. (2017). Experimental and numerical study of isotropic circular plates response to underwater explosive loading, created by conic shock tube, Materialwissenschaft Und Werkstofftechnic, 48, 106-121.

Hessner K., Reichert K., Borge J., Stevens C., Smith M. (2014). High-resolution X-band radar measurement of currents, bathymetry and sea state in highly inhomogeneous coastal areas, Ocean Dynamics, 64(7), 989-998

Hiekata K., Mitsuyuki T., Enomoto M., Okada K., Furukawa Y. (2016). A study of projection mapping on ship plate using 3d laser scanner, Annual Autumn Meeting and Conference of the Japan Society of Naval Architects and Ocean Engineers (JASNAOE), Japan

Hodge V. J., O'Keefe S., Weeks M., Moulds A. (2015). Wireless sensor networks for condition monitoring in the railway industry: A survey, IEEE Transactions on Intelligent Transportation Systems, 16, 3.

Hong S.Y., Kim B.W., Nam B.W. (2011). Experimental study on torsion springing and whipping of large container ship, 21st International Offshore and Polar Engineering Conference, Maui, HI.

Hong S.Y., Kim B.W., Nam B.W. (2012). Experimental study on torsion springing and whipping of large container ship, International Journal of Offshore and Polar Engineering, 22(2), 97-107.

Hong S. Y., Kim B. W. (2014). Experimental investigations of higher-order springing and whipping-WILS project, Intl. J. Nav. Archit. Ocean Eng., 6, 1160-1181.

Hoogeland M. G., Vredeveldt A. W. (2017). Full thickness material tests for impact analysis verification, 6th International Conference on Marine Structures, Lisbon, Portugal.

Hosseinlou F., Mojtahedi A. (2016). Developing a robust simplified method for structural integrity monitoring of offshore jacket-type platform using recorded dynamic responses, Applied Ocean Research, 56, 107-118.

Howard F. (2016). The Maritime 20-20-20, Keynote presentation, International Symposium on Practical Design of Ships and Other Floating Structures (PRADS). Copenhagen, Denmark.

Huang D., Zhao D:, Wei L., Wang Z., Du Y. (2014). Modelling and analysis in marine big data: Advances and challenges. College of Information, Shanghai Ocean University. China.

Hutchison E. K., Moore P. L., Bath W. P. (2015). SENT Stable tearing crack path deviation and its influence on J, ASME 2015 Pressure Vessels & Piping Conference, Boston, MA.

Iafrati A., Grizzi S., Benitez-Montanes L., Siemann M. (2015). High-speed ditching of a flat plate: Experimental data and uncertainty assessment, Journal of Fluids and Structures, 55, 501-525.

Iafrati A. (2016). Experimental investigation of the water entry of a rectangular plate at high horizontal velocity, Journal of Fluid Mechanics, 799, 637-672.

IBM (2014). Big Data. http://www.ibmbigdatahub.com/infographic/extracting-business-value-4-vs-big-data.
IEEE 802.15.4. (2006). Standard for information technology part 15.4: wireless medium access control (MAC) and physical layer (PHY) specifications for low rate wireless personal area networks (LR-WPANs).
Ince S. T., Kumar A., Park D. K., Paik J. K. (2017). An advanced technology for structural crashworthiness analysis of ship colliding with ice ridge: Numerical modelling and experiments, International Journal of Impact Engineering, 110, 112-122.
International Ship and Offshore Structures Congress 2015 III.2.
ISA (2009). ISA-100.11: Wireless systems for industrial automation: process control and related applications, International Society of Automation.
Ioannou A., Angus A., Brennan F. (2017a). Stochastic prediction of offshore wind farm lcoe through an integrated cost model, Energy Procedia, 107, 383-389.
Ioannou A., Wang L., Brennan F. (2017b). Design implications towards inspection reduction of large scale structures, Procedia CIRP, 60, 434-439.
Irkal M., Nallayarasu S., Bhattacharyya S. (2016). CFD approach to roll damping of ship with bilge keel with experimental validation, Applied Ocean Research, 55, 1-17.
Ishikawa T., Inoue T., Funatsu Y., Otani J. (2012). Evaluation method for crack arrestability of steel plates using small-scale fracture test results, 22nd International Offshore and Polar Engineering Conference, Rhodes, Greece.
IMO MSC.337(91) (2012). Resolution MSC.337(91). Adoption of the code on noise levels on board ships.
IMO Res. MSC.337(91), Code on noise on board ships.
ISO 12135:2016 (2016). Metallic materials - Unified method of test for the determination of quasistatic fracture toughness, International Organization for Standardization.
ISO 14556:2015 (2015). Metallic materials – Charpy V-notch pendulum impact test – Instrumented test method, International Organization for Standardization.
ISO 148 (2009) Metallic materials – Charpy pendulum Impact Test – Part 1: Test Method
ISO 2631-1 (1997). Evaluation of human exposure to whole-body vibration -Part 1: General requirements.
ISO 2631-2 (1997). Evaluation of human exposure to whole-body vibration -Part 2: Continuous and shock-induced vibration in buildings (1 to 80 Hz).
ISO 27306:2016 (2016). Metallic materials – method of constraint loss correction of CTOD fracture toughness for fracture assessment of steel components.
ISO 6954 (1984). Mechanical vibration and shock- Guidelines for the overall evaluation of vibration in merchant ships.
ISO 6954 (2000). Mechanical vibration - Guidelines for the measurement, reporting and evaluation of vibration with regard to habitability on passenger and merchant ships.
ISO 8041-1:2017 (2017). Human response to vibration -- Measuring instrumentation -- Part 1: General purpose vibration meters.
ISSC (2015). ISSC Report of the Technical Committee III.2: Ultimate Strength. 19th International Ship and Offshore Structure Congress, Lisbon, Portugal.
Jalonen R., Ruponen P., Weryk M., Naar H., Vaher S. (2017). A study on leakage and collapse of non-watertight ship doors under floodwater pressure, Marine Structures, 51, 188-201.
Jang B.S., Ito H., Kim K.S., Suh Y.S., Jeon H.T., Ha Y.S. (2010). A study of fatigue crack propagation at a web stiffener on a longitudinal stiffener, Journal of Marine Science and Technology, 15, 176-189.
JCGM 106:2012 (2012). Evaluation of measurement data - The role of measurement uncertainty in conformity assessment, Joint Committee for Guides in Metrology.
Jiang M., Ren B., Wang G., Wang Y. (2014). Laboratory investigation of the hydroelastic effect on liquid sloshing in rectangular tanks, Journal of Hydrodynamics, 26(5), 751-761.

Jiao J., Ren H., Adenya C. A. (2015). Experimental and numerical analysis of hull girder vibrations and bow impact of a large ship sailing in waves, Shock and Vibration, 2015(3), 1-10.

Jensen A.E., Havsg G.B., Pran K., Wang G., Vohra S. T., Davis M. A., Dandridge A. (2000). Wet deck slamming experiments with a FRP sandwich panel using a network of 16 fibre optic Bragg grating strain sensors, Composites / Part B, 31, 187-198.

Jullumstrø E., Aarsnes J. (1993). Hull loads and response on high speed craft. RINA International Conference on High Speed Passenger Craft, London, UK.

Kambatla K., Kollias G.., Vand K., Grama A. (2014). Trends in big data analytics. Journal of Parallel Distribution Computation.74, 2561-2573.

Kandasamy R., Cuia F., Townsend N., Foo C., Guo J., Shenoi A., Xiong Y. (2016). A review of vibration control methods for marine offshore structures, Ocean Engineering, 127, 279-297.

Kandil F. A. (2000a). Glossary of definitions and symbols. Project UNCERT, (1), National Physical Laboratory, UK.

Kandil F. A. (2000b). Introduction to the evaluation of uncertainty. Project UNCERT, (1) National Physical Laboratory, UK.

Kaufer D., Cheng P.W. (2014). Validation of an integrated simulation method with high-resolution load measurements of the offshore wind turbine Repower 5M at Alpha Ventus. Journal of Ocean and Wind Energy, 1, 30-40.

Kausar Z. A. W., Reza M. U., Saleh H., Ramiah (2014). Energizing wireless sensor networks by energy harvesting systems: Scopes, challenges and approaches, Renewable and Sustainable Energy Reviews, 38, 973-989.

Kellner T. (2015). Deep Machine Learning: GE and BP will connect thousands of subsea oil wells to the industrial internet, GE report (http://www.ge.com/reports/post/123572457345 /deep-machine-learning-ge-and-bp-will-connect).

Kim A., Hekland F., Petersen S., Doyle P. (2008). When HART goes wireless: understanding and implementing the WirelessHART standard, IEEE International Conference on Emerging Technologies and Factory Automation, Hamburg, Germany.

Kim K. J., Lee J. H., Park D. K., Jung B. G., Han X., Paik J. K. (2016a). An experimental and numerical study on non-linear impact responses of steel-plated structures in an Arctic environment, International Journal of Impact Engineering, 93, 99-115.

Kim J. FL, Chau-Dinh, T., Zi, G., Lee, W. W., Kong, J. S. (2016b). Probabilistic fatigue integrity assessment in multiple crack growth analysis associated with equivalent initial flaw and material variability, Engineering Fracture Mechanics, 156, 182-196.

Kim Y., Park S-G, Kim B-H, Ahn I-G (2016c). Operational modal analysis on the hydroelastic response of a segmented container carrier model under oblique waves, Ocean Engineering, 127, 357-367.

Kim N.W., Nam, B.W., Kwon, Y.J., Cho, S.K., Park, I.B., Sung, H.G. (2017). Experimental investigation on mating operation during float-over installation of a large topside in waves, International Ocean and Polar Engineering Conference, San Francisco, CA, USA, June 25-30, 1162-1167.

Kitamura O. (1997). Comparative study on collision resistance of side structure, Marine Technology, 34 (4), 293-308.

Kleiman J., Kudryavtev Y. (2012). Residual stress management in welding: residual stress measurement and improvement treatments, 31st International Conference on Ocean, Offshore and Arctic Engineering, Rio de Janeiro, Brazil.

Kleiman J., Kudryavtev Y., Smilenko V. (2013). Non-destructive measurement of residual stresses by an ultrasonic method, 32nd International Conference on Ocean, Offshore and Arctic Engineering, Nantes, France.

Kobayashi T., Takaoka Y., Nihei K., Osawa N., De Gracia L., Ichihashi D. (2016). Improvement of prediction accuracy of hull fatigue life by a fatigue damage sensor under a storm model

loading, Journal of the Japan Society of Naval Architects and Ocean Engineers, 23, 153-157.

Kong X., Li X., Zheng C., Liu F., Wu W-G. (2017). Similarity considerations for scale-down model versus prototype on impact response of plates under blast loads, International Journal of Impact Engineering, 101, 32-41.

Koga, S. (2015). major challenges and solutions for utilizing big data in the maritime industry, World Maritime University Dissertations Paper 490.

Koo J. B., Jang K.B., Suh Y.S., Kim Y.S., Kim M.S., Yu H., Tai J.S.C. (2011). fatigue damage assessment based on full scale measurement data for a large container ship, 21st International Offshore and Polar Engineering Conference, Maui, HI.

Körgesaar M., Tabri K., Naar H., Reinhold E. (2014). Ship collision simulations using different fracture criteria and mesh size, 33rd International Conference on Ocean, Offshore and Arctic Engineering, San Francisco, CA.

Kostenko K. V., Kryukov Y. S. (2016). Technique for detecting a direct signal pulse from an underwater explosive source in a waveguide, Acoustical Physics, 62(1), 112-116.

Kyyro K., Hakala M.H. (1997). Determination of structural dimensioning loads of a fast catamaran, using rigid backbone segmented model testing techniques, 4th International Conference on Fast Sea Transportation (FAST97), Sydney, Australia.

Kubiczek J.M., Burchard K.S., Ehlers S., Schöttelndreyer M. (2017). Material relationship identification for finite element analysis at intermediate strain rates using optimal measurements, 6th International Conference on Marine Structures, Lisbon, Portugal.

Kubo A., Yajima H., Aihara S., Yoshinari H., Hirota K., Toyoda M., Kiyosue T., Inoue T., Handa T., Kawabata T., Tani T., Yamaguchi T. (2012). Experimental study on brittle crack propagation behavior with large scale structural component model tests - Brittle crack arrest design for large container ships, 22nd International Offshore and Polar Engineering Conference, Rhodes, Greece.

Kvåle K., Øiseth O. (2017). Structural monitoring of an end-supported pontoon bridge, Marine Structures, 52, 188-207.

Kwon Y. W., Priest E.M., Gordis J.H. (2013). Investigation of vibrational characteristics of composite beams with fluid-structure interaction, Composite Structures, 105, 269-278.

Kwon, O., N. Lee and B. Shin (2014). Data quality management, data usage experience and acquisition intention of big data analytics, International Journal of Information Management, 34, 387-394.

Kwon Y.J., Nam B.W., Kim N. W., Kwak H. W., Park I. B., Jung D. H., Sung H.G. (2017). A model test for docking operations of a transportation vessel during float-over installation, 27th International Ocean and Polar Engineering Conference, San Francisco, CA.

Larsen J. M., Jha S. K., Szczepanski C. J., Caton M. J., John R., Rosenberger A. H., Jira, J. R. (2013). Reducing uncertainty in fatigue life limits of turbine engine alloys, International Journal of Fatigue, 57, 103-112.

Lau T., Kelso R. (2016). A scaling law for thrust generating unsteady hydrofoils, Journal of Fluids and Structures, 65, 455-471.

Lavroff J., Davis M., Holloway D., Thomas G. (2007). The whipping vibratory response of a hydroelastic segmented catamaran model, 9th International Conference on Fast Sea Transportation (FAST2007), Shanghai, China.

Le Gall, F., Vallet Chevillard S., Gluhak A., Walravens N., Xueli Z., Hadji H.B. (2015). Benchmarking internet of things deployment: Frameworks, best practices and experiences, Modeling And Processing For Next-Generation Big-Data Technologies, Springer, 473-496.

Ledezma D., Amer A., Abdellatif F., Outa A., Trigui H., Patel S., Roba, B. (2015). A market survey of offshore underwater robotic inspection technologies for the oil and gas industry, SPE Saudi Arabia Section Annual Technical Symposium and Exhibition, Al-Khobar, Saudi Arabia.

Lee K., Cho S., Kim K., Kim J., Lee P. (2015a). Hydroelastic analysis of floating structures with liquid tanks and comparison with experimental tests, Applied Ocean Research, 52, 167-187.
Lee G. J. (2015b). Dynamic orifice flow model and compartment models for flooding simulation of a damaged ship, Ocean Engineering, 109, 635-653.
Lee P.S. (2017). Underwater explosion experiments using pentolite, Explosives & Blasting, 35(3), 21-30. (In Korean)
Lehmann E., Pschmann J. (2002). Energy absorption by the steel structure of ships in the event of collisions, Marine Structures, 15 (4), 491-441.
Li X., Li Y., Zheng Y. (2014). Effects of stress wave effects on the damage behavior of marine low carbon steel based on the low-speed Taylor rod experiment, Ship Mechanics,12, 1495-1504.
Li Y., Wang Y., Wu W., Du Z., Li X., Zhang W. (2015a). Dynamic mechanical properties and constitutive relations of marine 907+A steel, Journal of Harbin Engineering University, 127-129. (In Chinese)
Li S., Zhang A. M., Yao X. L. (2015b). Experimental and numerical study on the dynamic pressure caused by the bubble jet, Journal of Physics, COnf. Series, 656(1), 12-25.
Li S., Zhang A. M., Han R., Liu Y. (2017). Experimental and numerical study on bubble-sphere interaction near a rigid wall, Physics of Fluids, 29(9), 092-102.
Lin J-C., Leu F-Y., Chen Y. (2015). ReHRS: A hybrid redundant system for improving MapReduce reliability and availability, Modeling and Processing for Next-Generation Big-Data Technologies, 4, Springer.
Libelium (2017). Waspmote Technical Guide. Libelium Comunicaciones Distribuidas S.L. v7.4. Zaragoza, Spain.
Liu K., Wang Z., Tang W., Zhang Y., Wang G. (2015a). Experimental and numerical analysis of laterally impacted stiffened plates considering the effect of strain rate, Ocean Engineering, 99, 44-54.
Liu B., Villacencio R., Guedes Soares V. (2015b). Simplified method for quasi-static collision assessment of a damaged tanker side panel, Marine Structures, 40, 267-288.
Liu F., Li H., Lu H. (2016). Weak-mode identification and time-series reconstruction from high-level noisy measured data of offshore structures, Applied Ocean Research, 56, 92-106.
Liu N. N., Wu W. B., Zhang A. M., Liu Y. L., Liu N. N., Wu W. B. (2017). Experimental and numerical investigation on bubble dynamics near a free surface and a circular opening of plate, Physics of Fluids, 29(10), 107-102.
LR (2010). Guidance Notes for Risk Based Inspection for Hull Structures, Lloyd's Register.
Lloyds Register Energy (2014a). Asset Management: From Data to Decision. Lloyd's Register Group Limited.
Lloyd's Register Foundation (2014b). Foresight Review of Big Data. Lloyd's Register Foundation Report Series: No. 2014.2.
LR (2016). Global Marine Technology Trends 2030, Lloyd's Register.
LMS (2015). FPSO JIP on Life Cycle Management Hull, http://www.fpsoforum.com/jips/completed-jips/.
Lovoll G., Kadal J.C. (2014). Big Data - the new data reality and industry impact, DNV-GL.
Lu, P., Zhang L., Liu X., Yao J., Zhu Z. (2015). Highly efficient data migration and backup for big data applications, in elastic optical inter-data-center networks, IEEE Network, 29(5), 36-42.
Lupton R.C., Langley R.S. (2017). Scaling of slow-drift motion with platform size and its importance for floating wind turbines, Renevable Energy, 101, 1013-1020.
Lugni C., Bardazzi A., Faltinsen O. M., Graziani G. (2014). Hydroelastic slamming response in the evolution of a flip-thourgh event during shallow-liquid sloshing, Physics of fluids, 26.
Lugni C., Greco M., Faltinsen O. (2015). Influence of yaw-roll coupling on the behavior of a FPSO: An experimental and numerical investigation, Applied Ocean Research, 51, 25-37.

Magno M., Jackson N., Mathewson A., Benini L., Popovici E. (2013). Combination of hybrid energy harvesters with MEMS piezoelectric and nano-Watt radio wake up to extend lifetime of system for wireless sensor nodes, Architecture of Computing Systems, 26th International Conference. Prague, Czeck Republic.

Maljaars J. Pijpers R., Slot H., (2015). Load sequence effects in fatigue crack growth of thick-walled welded C-Mn steel members, International Journal of Fatigue, 79, 10-24.

Maluf N., Williams K. (2004). An Introduction to microelectromechanical systems engineering, Second Edition, Artech House, Inc. Norwood, MA.

Mariani R., Dessi D. (2012). Analysis of the global bending modes of a floating structure using the proper orthogonal decomposition, Journal of fluids and structures, 28, 115-134.

Maron A., Kapsenberg G. (2014). Design of a ship model for hydro-elastic experiments in waves, International Journal of Naval Architecture and Ocean Engineering, 6, 1130-1147.

Maroti M., Simon G., Ledeczi A., Sztipanovits J. (2004). Shooter localization in urban terrain. Computer, IEEE Journal, 37(8), 60-61.

Matsuo K., Fujimoto S., Shiraishi K. (2015). Introduction of AR technologies to ship building works, National Maritime Research Institute (NMRI), Technical Report 14, Japan.

Mc Goldrick R., Russo V. (1956). Hull vibration investigation on SS-Gopher Mariner, Technical Report, Report No. 1060, David Taylor Model Basin.

Memsic Inc. (2017a). IRIS Wireless Measurement System (XM2110CA), www.aceinna.com.

Memsic Inc. (2017b). MICAz Wireless Measurement System (MPR2400CB), www.aceinna.com.

Minami F., Takashima Y., Ohata M., Yamashita Y. (2013). Constraint-based assessment of fracture in welded components, Welding in the World, 57, 707-718.

Ming F.R., Zhang A.M., Xue Y.Z., Wang S.P. (2016). Damage characteristics of ship structures subjected to shockwaves of underwater contact explosions, Ocean Engineering, 117, 359–382.

Minorsky V. U. (1959). An analysis of ship collisions with reference to protection of nuclear plants, Journal of Ship research, 1-4.

Moan T., Amdahl J, Ersdal G. (2017). Assessment of ship impact risk to offshore structures – New NORSOK N-003 guidelines, Marine Structures, in press, https://doi.org/10.1016/j.marstruc.2017.05.003.

Mohr D., Marcadet S. J. (2015). Micromechanically-motivated phenomenological Hosford-Coulomb model for predicting ductile fracture initiation at low stress triaxialities, International Journal of Solids and Structures, 67-68, 40-55.

Mondoro A., Soliman M., Frangopol D. (2016). Prediction of structural response of naval vessels based on available structural health monitoring data, Ocean Engineering, 125, 295-307.

Montenegro G., Kushalnagar N., Hui J., Culler D. (2007). Transmission of IPv6 packets over IEEE 802.15.4.

Moon S. J., Kwon J. I., Park J. W., Chung J. H. (2017). Assessment on shock pressure acquisition from underwater explosion using uncertainty of measurement, International Journal of Naval Architecture and Ocean Engineering, 9, 589-597.

Moore P., Hutchison E. (2016). Comparison of J equations for SENT Specimens, 1st European Conference on Fracture, Catania, Italy.

Nematbakhsh A., Michailides C., Gao Z., Moan T. (2015). comparison of experimental data of a moored multibody wave energy device with a hybrid cfd and biem numerical analysis framework, 34th International Conference on Ocean, Offshore and Arctic Engineering, St. John's, Newfoundland, Canada.

Niklas K., Kozak J. (2016). Experimental investigation of Steel–Concrete–Polymercomposite barrier for the ship internal tank construction, Ocean Engineering, 111, 449-460.

Osawa N., Nakamura T., Yamamoto N., and Sawamura J. (2013). Development of a new fatigue testing machine for high frequency fatigue damage assessment, 32nd International

Oshiro R., Calle M., Mazzariol L., Alves, M. (2017). Experimental study of collision in scaled naval structures, International Journal of Impact Engineering, 110, 1-13.

Otani J., Works O., Funatsu Y., Inoue T., Shirarata H. (2011). Improvement of arrestability for brittle crack for welded joint: development of higher toughness YP47 (460N/mm2) Class steel plate for large container ships-3, 21st International Offshore and Polar Engineering Conference, Maui, HI, USA.

Ouyang D. H., Zhang Q. T., Wang, F. (2016). Experimental and numerical investigation of effects of charge density on the bubble characteristics originating from the combustion of pyrotechnic mixtures, Flow Turbulence & Combustion, 97(3), 1-10.

Paik J. K., Thayamballi A. K. (2003). An experimental investigation on the dynamic ultimate compressive strength of ship plating, International Journal of Impact Engineering, 28 (7), 803-811.

Paik J. K., Kim K.J., Lee J.H., Jung B.J., Kim S.J. (2017). Test database of the mechanical properties of mild, high-tensile and stainless steel and aluminium alloy associated with cold temperatures and strain rates, Ships and Offshore Structures, 12, 230-256.

Pan J., Farag, N., Lin T., Juniper, R. (2002). Propeller induced structural vibration through the thrust bearing, Annual Conference of the Australian Acoustical Society, Adelaide, Australia.

Panapakidis I., Michailides C., Angelides D. (2016). Missing wind speed data: clustering techniques for completion and computational intelligence models for forecasting, 26th International Offshore and Polar Engineering Conference, Rhodes, Greece.

Panapakidis I., Michailides C., Angelides D. (2017). Clustering techniques for data analysis and completion of monitored structural responses of a floating structure, 27th International Offshore and Polar Engineering Conference, San Francisco, CA.

Park J. Y, Jo E., Kim M. S , Lee S. J, Lee Y. H. (2016). Dynamic behavior of a steel plate subjected to blast loading, Transactions Of The Canadian Society For Mechanical Engineering, 40, 575-583.

Park D. K., Kim K. J., Lee J. H., Jung B. G., Han X., Kim B. J., Seo J. K., Ha Y. C., Paik J. K., Matsumoto T., Byeon S. H., Kim M. S. (2015). Collision tests on steel plated structures in low temperatures, 34th International Conference on Ocean, Offshore and Arctic Engineering, St. John's New Foundland, Canada.

Pasquier R., Berthon C.F. (2012). Model-scale test vs. full-scale measurement: findings from the full-scale measurement sloshing project. 22nd International Offshore and Polar Engineering Conference, Rhodes, Greece, 17-22 June.

Pedersen P.T., Zhang, S. (2000). Effect of ship structure and size on grounding and collision damage distributions, Ocean Engineering, 27, 1161-1179.

Pedersen C., Deshpande V., Fleck N. (2006). Compressive response of Y-shaped sandwich core, European Journal of Mechanics-A/Solids, 25, 125-141.

Perner, P. (2015). Decision tree induction methods and their application to Big-Data, Modeling and Processing for Next-Generation Big-Data Technologies, 4, Springer.

Popescu P., Slusanschi E., Iancu V., Pop F. (2016). A new upper bound for Shannon entropy. A novel approach in modeling of Big Data applications. Concurrency and computation: Practice and Experience, 28, 351-359.

Puccinelli D., Haenggi M. (2005). Wireless sensor networks: applications and challenges of ubiquitous sensing, IEEE Circuits and Systems Magazine, 5(3), 19-31.

Pussegoda L., Tiku S., Tyson W., Park D-Y., Gianetto J., Shen G., Pisarki H. (2013). Comparison of resistance curves from multi-specimen and single-specimen SEN(T) Tests, 23rd International Offshore and Polar Engineering, Anchorage, Alaska.

Puzak P. P., Babecki A. J. (1959). Normalization procedures for nrl drop-weight test, Welding Journal, 38, 209-.

Qian G., González-Albuixech V., Niffenegger M. (2015). Calibration of Beremin model with the Master Curve, Engineering Fracture Mechanics, 136, 15-25.

Quinton B. W. T., Daley C. G., Colbourne B. B., Cagnon R. E. (2017). Experimental investigation of accidental sliding loads on the response of hull plating, 6th International Conference on Marine Structures, Lisbon, Portugal.

Qiu X., Zhu L., Yan M., Liu B. (2017). Structural response and energy absorption of the simplified ship side under the impact of rigid indenters with different shapes, 6th International Conference on Marine Structures, Lisbon, Portugal.

Rawat P., Singh K., Chaouchi H., Bonnin J. M. (2014). Wireless sensor networks: a survey on recent developments and potential synergies. The Journal of Supercomputing, 68(1). 1-48.

Ren P., Zhou J., Tian A., Zhang W., Huang W. (2017). Experimental and numerical investigation of the dynamic behavior of clamped thin panel subjected to underwater impulsive loading, Latin American Journal of Solids and Structures, 14(6), 978-999.

Rodd J. L. (1996). Observations on conventional and advanced double hull grounding experiments, International Conference on Designs and Methodologies for Collision and Grounding protection of Ships, San Francisco, CA.

Roessle M. L., Fatemi A. (2000). Strain-controlled fatigue properties of steels and some simple approximations, International Journal of Fatigue, 22(6), 495-511.

Rolader G.E., Rogers J., Batteh J. (2004). Self-healing minefield. SPIE Proceedings 5441, Battlespace Digitization and Network-Centric Systems IV, Defense and Security, Orlando, FL.

Roth C. C., Gary G., Mohr D. (2015). Compact SHPB system for intermediate and high strain rate plasticity and fracture testing of sheet metal, Experimental Mechanics, 55(9), 1803-1811.

Roth C. C., Mohr D. (2016). Ductile fracture experiments with locally proportional loading histories, International Journal of Plasticity, 79, 328-354.

Roubos A., Groenewegen L., Peters D. J. (2017). Berthing velocity of large seagoing vessels in the port of Rotterdam, Marine Structures, 51, 202-219.

Rubino V., Deshpande V. S., Fleck N. A. (2008a). The dynamics response of end-clamped sandwich beams with Y-shaped or corrugated core, International Journal of Impact Engineering, 35, 829-844.

Rubino V., Deshpande V. S., Fleck N. A. (2008b). The collapse response of sandwich beams with Y-frame core subjected to distributed and local loading, International Journal of Mechanical Sciences, 50, 233-246.

Rubino V., Deshpande V. S., Fleck N. A. (2009). The dynamic response of clamped Y-frame and corrugated core sandwich plates, European Journal of Mechanics-A/Solids, 28, 14-24.

Rubino V., Deshpande V. S., Fleck N. A. (2010). The three-point bending of Y-frame and corrugated core sandwich beams, International Journal of Mechanical Sciences, 52, 485-494.

Ruponen P., Kurvinen P., Saisto I., Harras J. (2013). Air compression in a flooded tank of a damaged ship, Ocean Engineering, 57, 64-71.

Saad-Eldeen S., Garbatov Y., GuedesS oares C. (2016a). Experimental strength assessment of thin steel plates with a central elongated circular opening, Journal of Constructional Steel Research, 118, 135-144.

Saad-Eldeen S., Garbatov Y., Guedes Soares C. (2016b). Experimental strength analysis of steel plates with a large circular opening accounting for corrosion degradation and cracks subjected to compressive load along the short edges, Marine Structures, 48, 52-67.

Saad-Eldeen S., Garbatov Y., Guedes Soares C. (2017). Experimental compressive strength analyses of high tensile steel thin-walled stiffened panels with a large lightening opening, Thin-Walled Structures, 113, 61-68.

Salah B., Slimane Z., Zoheir M., Jurgen, B. (2015). Uncertainty estimation of mechanical testing properties using sensitivity analysis and stochastic modelling, Measurement, 62, 149-154.

Sankararaman S., Ling, Y., Mahadevan, S. (2011). Uncertainty quantification and model validation of fatigue crack growth prediction, Engineering Fracture Mechanics, 78(7), 1487-1504.

Sarzosa D., Souza R., Ruggieri C. (2015). J-CTOD relations in clamped SE(T) fracture specimens including 3-D stationary and growth analysis, Engineering Fracture Mechanics 147, 331-354.

Sauder T., Chabaud V., Thys M., Bachynski E.E., Sæther L.O. (2016). real-time hybrid model testing of a braceless semi-submersible wind turbine. Part I: The Hybrid Approach, 35th International Conference on Ocean, Offshore and Arctic Engineering, Busan, South Korea.

Scheu M.N., Kolios A., Fischer T., Brennan F. (2017). Influence of statistical uncertainty of component reliability estimations on offshore wind farm availability, Reliability Engineering and System Safety, 168 28-39.

Schiere M., Bosman T., Derbanne Q., Stambaugh K., Drummen I. (2017). Sectional load effects derived from strain measurements using the modal approach, Marine Structures 54, 188-209.

Schmidt T., Tyson J., Revilock D., Padula S., Pereira J., Melis M., Lyle K. (2005). performance verification of 3d image correlation using digital high-speed cameras, 2005 SEM Annual Conference and Exposition, Portland.

Schmidt T. Tyson J., Galanulis K., Revilock D., Melis M. (2005). Full-field dynamic deformation and strain measurements using high-speed digital cameras, Proc. of SPIE, 5580, 175-.

Schöttelndreyer M., Tautz I., Kubiczek. J. M., Fricke W., Lehmann E. (2011). Influence of Bulbous bow structures on their collision behavior, Analysis and Design of Marine Structures, Hamburg.

Schöttelndreyer M., Tautz I., Fricke W., Werner B., Daske C., Heyer H., Sander M. (2013). Experimental and numerical investigations of an alternative stiffening system for ship side structures to increase collision safety, Analysis and Design of Marine Structures, Espoo.

Shaikh F., Zeadally S. (2016). Energy harvesting in wireless sensor networks: A comprehensive review, Renewable and Sustainable Energy Reviews, 55, 1041-1054.

Shi X. H., Zhang J., Guedes Soares, C. (2017). Experimental study on collapse of cracked stiffened plate with initial imperfections under compression, Thin-Walled Structures, 114, 39-51.

Shibahara, M. (2012). Measurement of Welding Deformation Based on Stereo Imaging Technique, 22nd International Offshore and Polar Engineering Conference, Rhodes, Greece.

Shinoda T., Nagata Y. (2015). Trend of 3D Measurement Technology and Its Application, Komatsu Technical Report Vol.61, No168, Japan. (in Japanese).

SILENV (2012). Ships oriented innovative solutions to reduce noise and vibrations, FP7. http://www.silenv.eu/.

Simms D. (2015). Big Data, Unstructured Data, and the Cloud: Perspectives on Internal Controls, Modelling and Processing for Next-Generation Big-Data Technologies, 4.

Son J-D., Ahn B-H, Ha J-M, Choi B-K (2016). An Availability of MEMS-based Accelerometers and Current Sensors in Machinery Fault Diagnosis, Measurement, 94, 680-691.

Sormunen O., Castrén A., Romanoff J., Kujala P. (2016a). Estimating sea bottom shapes for grounding damage calculations, Marine Structures, 45, 85-109.

Sormunen O., Körgesaar M., Tabri K., Heinvee M., Urbel A., Kujala P. (2016b). Comparing rock shape models in grounding damage modelling, Marine Structures, 50, 205-223.

Sormunen O. (2017). Impact of sea bottom shape in rounding damage, suitability of modelling with Gaussian processes, Progress in the Analysis and Design of Marine Structures, International Conference on Marine Structures, Lisbon, Portugal.

Sotoudeh K., Zhang S., Eren S., Kabra S., Milititsky M., Gittos M. (2013). evaluation of residual stresses in steel-to-nickel dissimilar joints, 32nd 3International Conference on Ocean, Offshore and Arctic Engineering, Nantes, France.

Spaho, E., Barolli A., Xhafa F., Barolli L. (2015). P2P Data Replication: Techniques and Applications. Modeling and Processing for Next-Generation Big-Data Technologies, 4, Springer.

Stauffer J-M. (2006). Current capabilities of mems capacitive accelerometers in a harsh environment. IEEE Aerospace and Electronics Systems Magazine, 21(11), 29-32.

Stenius I., Rosén A., Battley M., Allen T. (2003). Experimental hydroelastic characterization of slamming loaded marine panels, Ocean Engineering, 74, 1-15.

Storhaug G., Mathisen, J., Heggelund, S.E. (2009). Model tests and full-scale measurements of whipping on container vessels in the North Atlantic. 28th International Conference on Offshore Mechanics and Arctic Engineering, Honolulu, HI.

Storhaug G., Haraide O. (2013). Assessment of hull monitoring measurements for a large blunt vessel, 32nd International Conference on Ocean, Offshore and Arctic Engineering, Nantes, France.

Storheim M., Amdahl J., Martens I. (2015). On the accuracy of fracture estimation in collision analysis of ship and offshore structures, Marine Structures, 44, 254-287.

St-Pierre L., Deshpande V. S., Fleck N.A. (2015). The low velocity impact response of sandwich beams with corrugated core or a Y-frame, International Journal of Mechanical Sciences, 91, 71-80.

Suàrez J.C., Townsend P., Sanz E., Diez de Ulzrrum I., Pinilla P. (2016). The effect of slamming impact on out-of-autoclave cured prepregs of GFRP composite panels for hulls, Procedia Engineering 167, 252-264.

Sugimoto K., Yajima H., Aihara S., Yoshinari H., Hirota K., Toyoda M., Kiyosue T., Inoue T., Handa T., Kawabata T., Tani T., Usami A. (2012). Thickness effect on the brittle crack arrest toughness value (Kca) - Brittle crack arrest design for large container ships, 22nd International Offshore and Polar Engineering Conference, Rhodes, Greece.

Sun J., Hiekata K. (2014a). Efficient point cloud data processing in shipbuilding: Reformative component extraction method and registration method, J. of Computational and Engineering, 1(3), 202-212.

Sun J., Hiekata K. (2014b). development of curved shell plate's processing plan generation system using 3D measured data and virtual templates, Annual Autumn Meeting and Conference of the Japan Society of Naval Architects and Ocean Engineers (JASNAOE), Japan.

Suominen M., Kujala P., Romanoff J., Remes H. (2017a). The effect of the extension of the instrumentation on the measured ice-induced load on a ship hull, Ocean Engineering 144, 327–339.

Suominen M., Kujala P., Romanoff J., Remes H. (2017b). Influence of load length on short-term ice load statistics in full-scale, Marine Structures 52, 153-172.

Swartz R. A., Zimmerman A. T., Lynch J. P., Rosario J., Brady T., Salvino L., Law K. H. (2012). Hybrid wireless hull monitoring system for naval combat vessels. Structure and Infrastructure Engineering: Maintenance, Management, Life-Cycle Design and Performance, 8(7), 621-638.

Tableau (2017). Top Ten Big Data Trend for 2017. www.tableau.com

Tabri K., Määttänen J., Ranta J. (2008). Model-scale experiments of symmetric ship collisions, Journal of Marine Science and Technology, 13, 71-84.

Tabri K., Matusiak J., Varsta P. (2009). Sloshing interaction in ship collision an experimental and numerical study, Ocean Engineering, 36, 1366–1376.

Tabri K., Varsta P., Matusiak J. (2010). Numerical and experimental motion simulations of non-symmetric ship collisions, Journal of Marine Science and Technology, 15, 87-101.

Tammer M, Kaminski M. (2013). Fatigue oriented risk based inspection and structural health monitoring of FPSOs, 23rd International Offshore and Polar Engineering Conference, Anchorage, AK, USA.

Tammer M., Kaminski M. L., Koopmans M., Tang J. (2014). Current performance and future practices in FPSO hull condition assessments, 24th International Offshore and Polar Engineering Conference, Busan, Korea.

Tan K. H., Zhan Y-Z, Ji G., Ye F., Chang C. (2015). Harvesting big data to enhance supply chain innovation capabilities: An analytic infrastructure based on deduction graph. International Journal of Production Economics, 165, 223-233.

Tanaka Y., Ogawa H., Tatsumi A., Fujikubo M. (2015). Analysis method of ultimate hull girder strength under combined loads. Ships and Offshore Structures, 10(5), 587-598.

Tasai F. (1974). On the calculation methods of wave induced vibrations of ships, Trans. of the West-Japan Soc. of Naval Arch., 48, 163–180. (in japanese).

Tautz I., Schöttelndreyer M., Lehmann E., Fricke W. (2013). Collision tests with rigid and deformable bulbous bows driven against double hull side structures, Collision and Grounding of Ships and Offshore Structures, Trondheim, Norway.

Thomas G., Winkler S., Davis M., Holloway D., Matsubara S., Lavroff J., French B. (2011). Slam events of high-speed catamarans in irregular waves, J Mar Sci Technol, 16(1), 8–21.

Turan O., Helvacioglu I.H., Insel M., Khalid H., Kurt R.E. (2011). Crew noise exposure on board ships and comparative study of applicable standards. Ship and Offshire Strctures, 6(4), 323-338.

Torfs T., Sterken T., Brebels S., Santana J., van der Hoven R., Spiering V., Bertsch N., Trapani D., Zonta D., (2013). Low Power Wireless Sensor Network for Building Monitoring. IEEE Sensors Journal, 13(3), 909-915.

Tveiten B., Wang X., Berge S. (2007). Fatigue assessment of aluminium ship details by hot-spot stress approach, SNAME 2007 Conference, Fort Lauderdale, Florida.

UK HSE (2001). Probabilistic methods: Uses and abuses in structural integrity, Report for the Safety and Health Executive, Bomel Limited, ISBN 0 7176 2238 X.

UKAS (2016). The Expression of Uncertainty in Testing. Edition 2: M 3003, United Kingdom Accredation Service, 1–14.

Van den Bas L, Sanderse B. (2017). Uncertainty quantification for wind energy applications—literature review. Technical Report SC-1701, Centrum Wiskunde & Informatica, Amsterdam.

Von Bock und Polach F. R. U., Ehlers S., (2015). On the scalability of model-scale ice experiments, J. Offshore Mech. Arct. Eng. 137(5).

Voormeeren L., Walters C., Tang L., Vredeveldt A. (2014). estimation of failure parameters for finite element simulations based on a single state of stress and arbitrary stress-strain relation, 33rd Internation Conference on Ocean, Offshore and Arctic Engineering, San Francisco, CA.

Vredeveldt A. W., Wevers L. J. (1992). Full scale ship collision tests, Conference on the Prediction Methodology of Tanker Structural Failure.

Wakahara M., Nakajima M., Fukasawa T. (2008). Development of an affix-type multipoint pressure sensor by use of FBG (1st Report), The Japan Society of Naval Architects and Ocean Engineers, 7, 1-7. (in Japanese).

Wallin K., Karjalainen-Roikonen P., Suikkanen P. (2016). Crack arrest toughness estimation for high strength steels from sub-sized instrumented Charpy-V Tests, 26th International Ocean and Polar Engineering Conference, Rhodes, Greece.

Walters C., van der Weijde G. (2013). Development and validation of a low-cost CTOD procedure, 23rd International Offshore and Polar Engineering, Anchorage, AK.

Walters C., Bruchhausen M., Lapetite J., Duvalois W. (2017) Fracture testing of existing structures without the need for repairs, 36th International Conference on Ocean, Offshore and Arctic Engineering, Trondheim, Norway.

Wang X., Koh C., Zhang J. (2014). Substructural identification of jack-up platform in time and frequency domains, Applied Ocean Research, 44, 53-62.

Wang S., Li Y., Li H. (2015a). Structural model updating of an offshore platform using the cross model cross mode method: An experimental study, Ocean Engineering, 97, 57-64.

Wang Z. X., Gu W. B., Liu J. Q. (2015b). Experimental study on peak pressure of shock waves in quasi-shallow water, Mathematical Problems In Engineering, 1-8.

Wang G., Hu K., (2016a). To establish ship performance assessment scheme in a dynamically changing environment, International Symposium on Practical Design of Ships and Other Floating Structures (PRADS), Copenhagen, Denmark.

Wang G. (2016b). Maritime Big Data – Where are we on the Gartner Hype Cycle? https://www.linkedin.com/pulse/maritime-big-data-where-we-gartner-hype-cycle-ge-george-wilwwwang reinserirla adopo gratner

Wang Z., Liu K., Chunyan J., Chen D., Wang G., Guedes Soares C. (2016c). Experimental and numerical investigations on the T joint of jack-up platform laterally punched by a knife edge indenter, Ocean Engineering, 127, 212-225.

Wang J., Xiang S., Fu S., Cao P., Yang, Y., He J. (2016d). Experimental investigation on the dynamic responses of a free-hanging water intake riser under vessel motion, Marine Structures, 50, 1-19.

Wang G. (2017). What values does Big Data bring to the Maritime Industry? https://www.linkedin.com/pulse/what-values-does-big-data-bring-maritime-industry-ge-george-wang.

Wei Z.J., Faltinsen O.M., Lugni C., Yue Q.J. (2015). Sloshing-induced slamming in screen-equipped rectangular tanks in shallow-water conditions, Physics of Fluids, 27(3).

WES 2815:2014 (2014). Test method for brittle crack arrest toughness, Kca. The Japan Welding Engineering Society, Tokyo, Japan.

Wevers L. J., Vredeveldt A. W. (1999). Full scale ship collision experiments, TNO, report 98-CMC-R1725 Delft, The Netherlands.

WiSMote (2017) WiSMote. www.wismote.com.

Woisin G. (1979). Konstruktion gegen kollisionsauswirkungen – design against collision, Schiff & Hafen, 12, 1059-1069.

Wolf M. (2003). Full-scale collision experiment, X-type Sandwich side hull, EU Sandwich project report, Deliverable TRD448, EU Sandwich project.

Woo J., Kim D., Na W.B. (2015). Damage assessment of a tunnel-type structure to protect submarine power cables during anchor, Marine Structures, 44, 19-42.

Wu W., Wang Y., Tang D., Yue Q., Du Y., Fan Z., Lin Y., Zhang Y. (2016). Design, implementation and analysis of full coupled monitoring system of FPSO with soft yoke mooring system, Ocean Engineering, 113, 255-263.

Xie Y. G., Guo J., Xin-Fei L. I., Cui H. B., Yao X. L. (2015). Analysis of time-frequency characteristics of wall pressure signals of hull structure subjected to underwater explosion, Journal of Dalian University of Technology, 55, 492-497. (In Chinese)

Xie Yaoguo, Cui Hongbin, Li Xinfei, Yao Xiongliang. (2016). Analysis of time-frequency characteristics of free-field pressure under underwater explosion, Chinese Journal of Ship Research, 11 (2), 27-32. (In Chinese)

Xue J., Zhang Z., Ostby E., Nyhus B., Sun D. (2009). Effects of crack depth and specimen size on ductile crack growth of SENT and SENB specimens for fracture mechanics evaluation of pipeline steels, International Journal of Pressure Vessels and Piping, 86, 787-797.

Yamada Y., Endo. H. (2005). Collapse mechanism of the buffer bow structure on axial crushing, International Journal of Offshore and Polar Engineering, 15 (2), 147-154.

Yamada Y. (2006). Bulbous buffer bows: a measure to reduce oil spill in tanker collisions, PhD thesis, Department of Mechanical Engineering, Technical University of Denmark, DTU.

Yamada Y., Endo H. (2007). Experimental and numerical study on the collapse strength of the bulbous bow structure in oblique collision, Marine Technology, 45(1), 42–53.

Yamamoto N., Negayama H., Furukawa N., Mouri M., Yasunaga R., Inami A., Nakamura T., Okada T., Mori T., Tanaka S., Shimanuki H., Sumi Y., Sugimura T., Morikage Y. (2012).

Analytical and experimental study on the thickness effect to fatigue strength, 22nd International Offshore and Polar Engineers, Rhodes, Greece.

Yanuka D., Shafer D., Krasik Y. (2015). Shock wave convergence in water with parabolic wall boundaries, Journal of Applied Physics, 117(16), 632-641.

Yi J-H. (2016). Laboratory tests on local damage detection for jacket-type offshore structures using optical FBG sensors based on statistical approaches, Ocean Engineering, 124, 94-103.

Yue J., Dong Y., Zhou H. (2012). Fatigue analysis on a multi-planer tubular kk joints based on scaled model test, 22nd International Society of Offshore and Polar Engineers, Rhodes, Greece.

Zhang A. M., Cui P., Cui J., Wang Q. X. (2015a). Experimental study on bubble dynamics subject to buoyancy, Journal of Fluid Mechanics, 776, 137-160.

Zhang P., Cheng Y., Liu J., Wang C., Hou H., Li Y. (2015b). Experimental and numerical investigations on laser-welded corrugated-core sandwich panels subjected to blast loading, Marine Structures, 40, 225-246.

Zhang S. H., Quan L., Jin H., Jia, Z. (2015c). Research on positioning method of underwater explosion source, Blasting, 32, 118-121. (In Chinese)

Zhang Z., Wang Y., Zhao H., Qian H., Mou J. (2015d). An experimental study on the dynamic response of a hull girder subjected to near field underwater explosion, Marine Structures, 44, 43-60.

Zhang X., Noel N., Ferrari G., Hoogeland M. (2016), Corrosion behaviour of mooring chain steel in seawater, Eurocorr 2016, Montpellier, France.

Zhang A. M., Wu W. B., Liu Y. L., Wang Q. X. (2017a). Nonlinear interaction between underwater explosion bubble and structure based on fully coupled model, Physics of Fluids, 29(8), 082-111.

Zhang C., Suo T., Tan W., Zhang X., Liu J., Wang C., Li Y. (2017b). An experimental method for determination of dynamic mechanical behavior of materials at high temperatures, International Journal of Impact Engineering, 102, 27-35.

Zhang S., Villavicencio R., Zhu L., Pedersen P. T. (2017c) Impact mechanics of ship collisions and validations with experimental results, Marine Structures, 52, 69-81.

Zhang Y., Huang Y., Wei Y. (2017d). Ultimate strength experiment of hull structural plate with pitting corrosion damage under uniaxial compression, Ocean Engineering, 130, 103-114.

Zhao W., Yang J., Hu Z., Tao L. (2014). Prediction of hydrodynamic performance of an FLNG system in side-by-side offloading operation, Journal of Fluids and Structures, 46, 89-110.

Ziemer G., Evers K. U. (2014). Ice model tests with a compliant cylindrical structure to investigate ice-induced vibrations, 33rd International Conference on Offshore Mechanics and Arctic Engineering, San Francisco, CA.